Technische Universität München

TUM School of Medicine and Health

The role of tumor cell-intrinsic STING signaling in antitumor immunity and immune checkpoint inhibitor therapy responsiveness

Larsen Vornholz

Vollständiger Abdruck der von der TUM School of Medicine and Health der Technischen Universität München zur Erlangung eines

Doktors der Naturwissenschaften (Dr. rer. nat.)

genehmigten Dissertation.

Vorsitz: Prof. Kathrin Schumann, Ph.D.

Prüfer der Dissertation:

1. Prof. Dr. Jürgen Ruland
2. Prof. Dr. Dirk Haller

Die Dissertation wurde am 20.09.2023 bei der Technischen Universität München eingereicht und durch die TUM School of Medicine and Health am 03.01.2024 angenommen.

Teile der vorliegenden Arbeit wurden bereits veröffentlicht unter:

Vornholz, L., Isay E.S., Kurgyis, Z., Strobl, C.S., Loll, P., Mosa M.H., Luecken, M.D., Sterr, M., Lickert, H., Winter, C., Greten, F.R., Farin, H.F., Theis, J.T., Ruland, J. 2023. *Synthetic enforcement of STING signaling in cancer cells appropriates the immune microenvironment for checkpoint inhibitor therapy*. Sci. Adv. 9, eadd8564. 10.1126/sciadv.add8564.

Declaration of co-contribution

The following parts of this thesis were generated independently by collaborators or by co-authors listed in the original publication Vornholz, L. et al. *Sci. Adv.* ***9***, eadd8564 (2023):

1) Library preparation and sequencing of RNA samples (Rupert Öllinger[1])
2) *In vitro* organoid experiments (Mohammed H. Mosa[2,3], Henner F. Farin[2,3])
3) CITE-seq library preparation and sequencing (Michael Sterr[4], Thomas Walzthöni[5])

The following parts of this thesis were done together or with substantial technical help and scientific input of co-authors listed in the original publication Vornholz, L. et al. *Sci. Adv.* ***9***, eadd8564 (2023):

1) Bioinformatic analyses of TCGA COADREAD data (Christof Winter[6])
2) Generation and validation of STING^{N153S}-expressing tumor cells as part of the Master`s thesis: “Tumor cell-intrinsic constitutive activation of STING” (Sophie E. Isay[1,6])
3) Bioinformatic analyses of CITE-seq data (Daniel C. Strobl[5])

Affiliation of these contributors

1) TranslaTUM, Center for Translational Cancer Research, Technical University of Munich, Munich, Germany
2) Institute for Tumor Biology and Experimental Therapy, Georg-Speyer-Haus, Frankfurt/Main, Germany
3) Frankfurt Cancer Institute, Goethe University Frankfurt, Frankfurt/Main, Germany
4) Institute for Diabetes and Regeneration Research, Helmholtz Center Munich, Neuherberg, Germany
5) Institute for Computational Biology, Department of Computational Health, Helmholtz Center Munich, Neuherberg, Germany
6) Institute of Clinical Chemistry and Pathobiochemistry, School of Medicine, Technical University of Munich, Munich, Germany

Table of Content

Abstract

Immune checkpoint inhibitors (ICI) have revolutionized cancer immunotherapy. In particular, patients with mismatch repair-deficient (dMMR) colorectal cancer (CRC) exhibit better responsiveness to ICI therapy than patients with MMR-proficient (pMMR) CRC (Le et al., 2017, 2015; Mandal et al., 2019). To be clinically effective, ICI need immunologically “hot” niches in the tumor microenvironment (TME) that provide the initial cues for tumor antigen presentation and lymphocyte recruitment. These niches are typically shaped by the mutational landscape of cancer cells. However, how tumor cell-intrinsic mechanisms couple to antitumor immunity remains poorly defined. Studies suggested that the therapy-responsive fraction of tumor mutational burden (TMB)-high tumors is due to an enrichment of neoantigens in the tumor tissue, which arise from the dMMR-driven hypermutator phenotype (Germano et al., 2017). However, the prevalence of mutation-generated immunogenic neoantigens is insufficient to recruit the necessary immune cells into the TME that mediate the antitumor immune response (Spranger et al., 2016), suggesting that additional mechanisms govern ICI sensitivity. By using human and murine CRC models, we found that the superior antitumor immune response of dMMR tumors is mediated by tumor cell-intrinsic cGAS-STING activation, which is triggered by aberrant cytosolic DNA. Furthermore, tumor cell-intrinsic STING activation controls the immunogenicity of dMMR CRC by promoting inflammatory cues that are indispensable for recruiting cytotoxic CD8+ T cells and unleashing their tumoricidal activity *in vivo*. Based on this observation, we subsequently equipped pMMR human and murine tumor cells with a constitutively active STING^{N153S} variant. Even in the absence of a genomic instability-driven ligand, the expression of constitutively active STING^{N153S} in pMMR tumor cells was sufficient to induce tumor cell-intrinsic interferon signaling, enhance antitumor immune responses, and create “hot” TMEs, which sensitized the previously ICI-resistant “cold” tumors to ICI therapy. Beyond CRC, we show that the expression of STING^{N153S} also enhances the ICI therapy responsiveness in melanoma. Thus, our findings propose a novel strategy to sensitize resistant tumors to ICI therapy by modulating tumor cell-intrinsic signals through synthetic STING enforcement.

Zusammenfassung

Immun-Checkpoint-Inhibitoren (ICI) haben die Krebs-Immuntherapie revolutioniert. Vor allem Patienten mit Mismatch-Reparatur-defizientem (dMMR) Kolorektalkrebs (KRK) sprechen deutlich besser auf die ICI Therapie an als Patienten mit MMR-kompetentem (pMMR) KRK (Le et al., 2017, 2015; Mandal et al., 2019). Für die klinische Wirksamkeit von ICI ist das Vorhandensein von immunologisch „heißen" Nischen in der Tumormikroumgebung (TMU), welche die initialen Signale für die Tumorantigenpräsentation und die Lymphozyten-Rekrutierung enthalten, notwendig. Dabei werden diese Nischen maßgeblich durch die Mutationslandschaft der Tumore geschaffen. Nach wie vor ist jedoch unklar, wie diese Tumorzell-intrinsischen Mechanismen mit der Antitumor-Immunität zusammenhängen. Aus Studien geht hervor, dass die Anreicherung von Neoantigenen im Tumorgewebe, welche durch den dMMR-getriebenen Hypermutatorphänotyp entstehen, für das Therapieansprechen der Tumore mit hoher Tumormutationslast (TMB) verantwortlich sind (Germano et al., 2017). Das Vorhandensein von immunogenen Neoantigenen, welche durch Mutationen hervorgerufenen werden, ist jedoch nicht ausreichend, um die notwendigen Immunzellen, welche die Antitumor-Immunantwort ausüben, in die TMU zu rekrutieren (Spranger et al., 2016). Dies impliziert, dass weitere Mechanismen die ICI Sensitivität bestimmen. Anhand humaner und muriner KRK-Modelle konnten wir zeigen, dass die bessere Antitumor-Immunantwort von dMMR KRK durch eine Tumorzell-intrinsische Aktivierung des cGAS-STING Signalweges entsteht. Dieser Signalweg wird durch aberrante zytosolische DNA augelöst. Des Weiteren kontrolliert die Tumorzell-intrinsische STING Aktivierung die Immunogenität von dMMR KRK *in vivo* durch die Steigerung von inflammatorischen Signalen, welche für die Rekrutierung von zytotoxischen CD8+ T Zellen und die Auslösung deren Antitumor-Aktivität unverzichtbar sind. Basierend auf diesen Beobachtungen haben wir in einem nächsten Schritt humane und murine pMMR Tumorzellen mit einer konstitutiv-aktiven $STING^{N153S}$-Variante ausgestattet. Die Expression von konstitutiv-aktivem $STING^{N153S}$ in pMMR Tumoren war ausreichend, um Tumorzell-intrinsische Interferonsignale auszulösen, die Antitumor-Immunantwort zu verstärken und eine immunologisch „heiße" TMU zu generieren, was dazu führte, dass die bisher ICI-resistenten „kalten" Tumore für die ICI Therapie empfindlicher wurden. Über den KRK hinaus zeigen wir, dass die Expression von $STING^{N153S}$ auch das ICI Therapieansprechen im Melanom

verbessert. Damit stellen unsere Resultate eine neue Strategie für die Modulation von Krebszell-intrinsischen Programmen durch synthetische STING-Signalverstärkung dar, um bisher resistente Tumore auf ICI ansprechbar zu machen.

Glossary

Agonist	ligand to a receptor that produces a biological response
ANOVA	analysis of variance
Aneuploidy	abnormal number of chromosomes in a cell
APCs	antigen-presenting cell
AU	arbitrary units
Bioavailability	fraction of an administered drug that reaches the systemic circulation
Bp	base pairs
CCL	C-C motif chemokine ligand
CD	cluster of differentiation
cGAMP	cyclic guanosine monophosphate-adenosine monophosphate
cGAS	cyclic guanosine monophosphate-adenosine monophosphate synthase
CITE-seq	cellular indexing of transcriptomes and epitopes by sequencing
CRC	colorectal cancer
CRISPR/Cas9	clustered regularly interspaced short palindromic repeats/ CRISPR-associated protein 9
CT26	chemically induced BALB/c-derived colon carcinoma cell line
CTL	cytotoxic T lymphocyte
CTLA-4	cytotoxic T lymphocyte associated antigen 4
CXCL	C-X-C motif chemokine ligand
DAMP	damage-associated molecular pattern
DC	dendritic cell
dLN	draining lymph nodes
DMEM	Dulbecco`s Modified Eagle Medium
dMMR	mismatch repair deficiency
DNA	deoxyribonucleic acid
dsDNA	double-stranded DNA
ELISA	enzyme-linked immunosorbent assay

Exome	protein-coding regions of genes in the genome
FACS	fluorescence-activated cell sorting
Fc	fragment crystallizable
FCS	fetal calf serum
FITC	fluorescein isothiocyanate
Gain-of-function	alteration that enhances biological functions
GSEA	gene set enrichment analysis
GZMB	granzyme b
Haplotype	group of genes within an organism that was inherited from a single parent
ICB	immune checkpoint blockade
ICI	immune checkpoint inhibitor
IFN	Interferon
IFNAR1	Interferon-alpha/beta receptor 1
Ig	immunoglobulin
IL-	interleukin-
Iono	ionomycin
IRF	IFN regulatory factor
ISGs	IFN stimulated genes
ISG15	IFN-stimulated gene 15
kDa	kilodalton
KO	knockout
MC38	chemically induced C57BL/6-derived colorectal cancer cell line
MHC	major histocompatibility complex
MLH1	MutL homolog 1
MMR	Mismatch repair
MSH2	MutS homolog 2
MSH6	MutS homolog 6
MSI	microsatellite instability
MSI-H	microsatellite instability, high-grade
MSS	microsatellite stable
mtDNA	mitochondrial DNA
Mutation	genetic alteration

Neoantigen	new peptide that arises from mutations in the DNA
NES	normalized enrichment score
NF-κB	nuclear factor κB
NK cell	natural killer cell
Off-target effect	effect of a drug on an unintended target
Organoids	3D multicellular *in vitro* tissue construct that mimics its corresponding *in vivo* organ
PAMP	pathogen-associated molecular pattern
PBS	phosphate-buffered saline
PD-1	programmed cell death protein 1
PD-L1	programmed death ligand 1
PMA	phorbol 12-myristate 13-acetate
pMMR	mismatch repair proficiency
PMS2	PMS1 homolog 2
POLD	DNA polymerase delta
POLE	DNA polymerase epsilon
PRF1	perforin 1
PRR	pattern recognition receptor
qPCR	quantitative real-time polymerase chain reaction
Reactome	open-source and peer-reviewed pathway database
RNA	ribonucleic acid
RNA-seq	RNA sequencing
SAVI	STING-associated vasculopathy with onset in infancy
scRNA-seq	single-cell RNA sequencing
ssDNA	single-stranded DNA
STAT	signal transducer and activator of transcription
STING	stimulator of IFN genes
t-SNE	t-distribution stochastic neighbor embedding
TBK1	TANK-binding kinase 1
TCGA	The Cancer Genome Atlas
TCR	T cell receptor
TMB	tumor mutational burden
TME	tumor microenvironment
TNF	tumor necrosis factor

Transgene	a gene that has been transferred naturally or through genetic engineering techniques
T reg	regulatory T cell
SD	standard deviation
SEM	standard error of the mean
UMAP	uniform manifold approximation and projection
WB	western blot
WES	whole-exome sequencing
WT	wild-type

1 Introduction

1.1 Immune checkpoint inhibitor (ICI) therapy

1.1.1 Immune checkpoints

To be properly activated, naïve T cells require three stimulatory signals from antigen-presenting cells (APCs). Namely, the interaction of the T cell receptor (TCR) with an antigen presented on the major histocompatibility complex (MHC), co-stimulatory signals that come from interactions of the B7 proteins CD80/CD86 on APCs with the co-receptor protein CD28 on T cells, and inflammatory cytokines which guide differentiation and effector capacities (Arasanz et al., 2017). T cell activation is accompanied by the upregulation of inhibitory receptors such as programmed cell death protein 1 (PD-1) and cytotoxic T lymphocyte associated protein 4 (CTLA-4) to balance the immune response. These so-called immune checkpoints are members of immunoglobulin-related receptors expressed on immune cells such as T cells to regulate T cell functionality (Greenwald et al., 2005; Sharpe and Pauken, 2018). PD-1 signaling is triggered upon binding to its ligands, programmed death ligand 1 (PD-L1) or PD-L2, which are expressed on tumor, stromal, and myeloid cells and inhibit T cell activity by reducing effector functions (cytotoxicity and cytokine production) and diminishing the responsiveness towards further stimuli (Patsoukis et al., 2020). CTLA-4 executes its inhibitory function by disrupting the T cell stimulatory CD28-CD80/CD86 signal since it binds to CD80/CD86 with higher affinity than CD28 (Rowshanravan et al., 2018). Furthermore, it is suggested that CTLA-4 controls CD80/CD86 availability by physically capturing and removing these proteins from APCs, a process known as trans-endocytosis (Qureshi et al., 2011).

Physiologically, these mechanisms are critical to promote immune tolerance and thereby prevent autoimmune disorders. Perturbations of these regulatory “checkpoint” pathways profoundly affect host immunity. For example, whereas malfunctioning of the PD-1 pathway predisposes mice to autoimmune disorders (Nishimura et al., 1999), sustained expression of PD-1 at high levels is commonly observed during chronic infections and cancer (Sharpe and Pauken, 2018). In cancer particularly, the activation of the PD-1 pathway leads to tumor immunosuppression by inhibiting T cell effector functions, promoting T cell exhaustion, and conferring peripheral immune tolerance (Pauken and Wherry, 2015). Based on the observation that tumors hijack the inhibitory

capacities of immune checkpoint signals to shut down T cell responses, the concept of inhibiting these immune checkpoint signals with blocking antibodies was soon translated to the clinics and enjoyed great success (Robert, 2020).

1.1.2 ICI therapy in cancer

With the era of immunotherapeutic approaches, therapies targeting immune checkpoints have revolutionized cancer immunotherapy (Chen and Han, 2015; Robert, 2020). In 2011, the United States Food and Drug Administration (FDA) approved the first immune checkpoint inhibitor (ICI) therapy using CTLA-4-blocking antibodies (ipilimumab) for melanoma (Hodi et al., 2010; Hoos et al., 2010; Wolchok et al., 2013). Soon after that, antibodies targeting PD-1 (pembrolizumab and nivolumab) (Herbst et al., 2016; Overman et al., 2017; Robert et al., 2015a, 2015b) and PD-L1 (atezolizumab and durvalumab) (Herbst et al., 2020; Horn et al., 2018; Mathieu et al., 2021; Ning et al., 2017; Paz-Ares et al., 2019) were also authorized for use in cancer patients. However, response rates substantially vary between the individual checkpoint classes. Whereas the clinical success of CTLA-4 inhibition as monotherapy is limited to metastatic melanoma, where its inhibition achieves a response rate of 20% (Hodi et al., 2010), targeting the PD-1/PD-L1 axis showed clinical activity in nearly 20 different cancers (Zhao et al., 2020; P. Zhao et al., 2019). More specifically, response rates vary from 10-30% in solid tumors such as liver, bladder, and kidney cancers to 40-50% in melanoma, microsatellite instability-high (MSI-H)/mismatch repair-deficient (dMMR) cancers (e.g., colorectal cancer (CRC)), and PD-L1-high non-small-cell lung cancers (NSCLCs), and even up to 65-75% in Hodgkin lymphoma (Zhao et al., 2020; P. Zhao et al., 2019). Combining these ICI therapies increased responsiveness and displayed synergistic potential in some cancer settings. For example, adding anti-CTLA-4 to the anti-PD-1 treatment regimen increased the response rate in metastatic melanoma from 43% (nivolumab alone) to 59% (Larkin et al., 2019) and in renal cell carcinoma (RCC) from ca. 25% (nivolumab alone) to 40% (Motzer et al., 2018). Moreover, this combination is also approved for patients with hepatocellular carcinoma and NSCLC (Wong et al., 2021). With the aim to refine the therapeutic regimen and improve therapy success, the development of immuno-oncology drug pipelines is massively expanding, which is represented by more than 3,000 active clinical trials (2/3 of all immuno-

oncology trials) that are testing T cell-targeting immunomodulators as mono- or combination therapy (Xin Yu et al., 2019).

1.1.3 Biomarkers for ICI therapy

Currently, some potentially predictive markers inform the stratification of patients that might be susceptible to ICI therapy, such as the presence and activation status of effector T cells (immunoscore), PD-L1 expression levels (Meng et al., 2015) and genetically driven factors such as tumor mutational burden (TMB) and MMR status (Le et al., 2017; Lyu et al., 2018). The immunoscore is a measure of the presence of CD3+ and CD8+ T cells in the tumor (Blank et al., 2016; Pagès et al., 2018). Interestingly, MSI-H/dMMR CRC patients with tumors with higher numbers of tumor-infiltrating lymphocytes (TILs) had better survival outcomes than patients with tumors with lower TIL numbers (Prall et al., 2004). Also, the baseline level of intratumoral TILs was linked to better therapy responsiveness in MSI-dMMR CRC (Le et al., 2015). This is in line with the clinical manifestation that immunologically active “hot” tumors, which are considered immune-inflamed, are associated with better ICI therapy responsiveness (Galon and Bruni, 2019; Liu and Sun, 2021). Moreover, TILs also demonstrated clinical relevance in MSS CRC patients, which suggests that intratumoral TILs might indicate CRC prognosis beyond the MSI status (Pagès et al., 2018).

The expression of PD-L1 appears to be an obvious marker since it is the ligand for PD-1. In NSCLC patients, for example, PD-L1 expression serves as a diagnostic parameter (Gibney et al., 2016; Topalian et al., 2016). However, clinical survival data in other cancer entities did not show significant relationships (Droeser et al., 2013; Mlecnik et al., 2011; Yarchoan et al., 2019; Yu et al., 2019). Particularly in CRC, the potential as a global predictor is limited since no trend between PD-L1 expression and drug efficacy was observed in MMR-proficient (pMMR) CRC (Le et al., 2015; Overman et al., 2017). Moreover, an analysis of a selected subgroup of PD-L1-high MSI-H/dMMR tumors did not predict better survival outcomes in patients with PD-L1-high tumors (Le et al., 2015; Overman et al., 2017).

The level of TMB (ratio of non-synonymous somatic mutations per megabase) has been observed to correlate with ICI responsiveness in melanoma, NSCLC, and CRC

(Le et al., 2015; Ready et al., 2019; Snyder et al., 2014). Tumors with high TMB, driven by genomic instability, which can be caused by endogenous defects in DNA homeostasis (e.g., MMR defects) or exogenous insults (e.g., smoking), are suggested to produce novel tumor-specific antigens, called neoantigens (Schumacher et al., 2019), and thereby enhance the ICI therapy responsiveness (Germano et al., 2017). Although a meta-analysis of 27 cancer types showed that the response rates generally correlated with TMB (Yarchoan et al., 2017), there are some clinical studies (Hanna et al., 2018; Miao et al., 2018; Riaz et al., 2017) in which TMB alone was not able to clearly distinguish responders from non-responders which indicates that additional mechanisms contribute to ICI therapy responsiveness.

1.2 Colorectal cancer (CRC)

1.2.1 CRC risk factors

CRC is the second most common cause of death from cancer (Safiri et al., 2019; Siegel et al., 2020). CRC develops as a multistep process whereby a series of genetic and environmental triggers disturb the homeostatic cellular balance by deregulating processes involved in genome integrity, cell cycle, and apoptosis, which collectively allow cancerous cells to survive, proliferate and disseminate (Hanahan and Weinberg, 2011, 2000). Through the initiation of oncogenic signals, the sustained promotion of neoplastic transformations gives rise to cancerous progression and cancer cell outgrowth. The cause for developing CRC comprises risk factors that can be of environmental origin, such as dietary habits, lifestyle, and the microbiome, or due to genetic alterations such as deficiencies in the MMR machinery or facilitated by the genetic predisposition to diseases such as inflammatory bowel disease (IBD) (Mármol et al., 2017; Sawicki et al., 2021). Genetically, CRC can be classified as sporadic (70% of CRC), familial (25% of CRC), or inherited (5% of CRC). Being the majority of CRC cases, sporadic cancerous conditions develop due to somatic mutations without evidence of inheritance, family history of CRC, or IBD. Familial CRC is considered to be caused by inherited mutations. Although patients with familial CRC have a family history of CRC, there is an absence of genetic variants that are associated with hereditary syndromes. Inherited CRC is evoked by germline mutations that have a high penetrance. The two most common forms of inherited CRC are the autosomal dominant hereditary nonpolyposis colorectal cancer (HNPCC) with mutations in MMR

genes (e.g., *MLH1, MSH2, MSH6, PMS1, PMS2*), clinically described as Lynch syndrome, and the autosomal dominant familial adenomatous polyposis (FAP) which arises from defects in the DNA replication and cell division regulating oncogene adenomatous polyposis coli (APC) (Mármol et al., 2017; Sawicki et al., 2021).

1.2.2 Molecular pathways of CRC development

Genetic instability is a critical feature underlying CRC. From a pathological point of view, there are three key mechanisms: chromosomal instability (CIN), CpG island methylator phenotype (CIMP), and microsatellite instability (MSI) (Alzahrani et al., 2021; Mármol et al., 2017). With 70-85% of CRC cases, CIN is the most frequent malignant driver, whereby imbalances in the number of chromosomes lead to loss of heterozygosity and aneuploidy (Grady and Carethers, 2008; Pino and Chung, 2010). These genetic alterations deregulate tumor suppressor genes (e.g., APC, TP53) and oncogenes (e.g., KRAS, PI3K), which are critically involved in the tightly controlled maintenance of cellular functions. For example, inactivation of the oncogene APC promotes β-catenin-driven cell division, hyperactivation of KRAS and PI3K promotes MAP kinase-dependent cell proliferation, and TP53 loss of function causes uncontrolled cell cycle entry, ultimately promoting tumorigenesis (Grady and Carethers, 2008; Pino and Chung, 2010). In the context of CIMP, which is characterized by epigenetic instability, promoter hypermethylation leads to gene silencing and loss of protein expression of tumor suppressors (Lao and Grady, 2011). Finally, MSI develops as a consequence of impaired DNA repair mechanisms (e.g., MLH1 deficiency) (Boland and Goel, 2010). Microsatellites are replication error-prone short DNA tandem repeats (1-6 base pairs (bp)) in coding or non-coding regions throughout the genome. If errors in the microsatellite DNA regions are left unrepaired, mutations accumulate continuously. Consequently, tumors may develop when these mutations hit protein-coding regions or when reading frames of oncogenes or tumor suppressor genes are altered (Boland and Goel, 2010).

1.2.3 Conventional and targeted therapies for CRC

To define the optimal choice of treatment for CRC patients, tumor-related characteristics and patient-related factors are considered (Mármol et al., 2017). Generally, surgery and chemotherapy are the first-line treatment options for CRC

patients. In the case of unresectable tumors, radiotherapy and mono- or multi-agent chemotherapy are the leading strategies. Although chemotherapy has evolved as the backbone of CRC treatment, limitations such as systemic toxicity or acquired resistance dampen its therapeutic success. In particular, resistance to methylating (e.g., temozolomide (TMZ)), alkylating (e.g., busulfan), or platinum-based (e.g., cisplatin) chemotherapeutics were observed in dMMR tumor cells (Alex et al., 2017; Fink et al., 1998). Interestingly, the use of these genotoxic agents can even lead to MMR inactivation in human cancer and thereby drive therapeutic resistance (Bardelli et al., 2001; Li, 2008).

The development of targeted therapies and immunotherapeutic approaches has substantially prolonged patient survival (Xie et al., 2020). Numerous agents are designed to aim at intracellular targets (e.g., with small molecules) or at extracellular targets (e.g., with antibodies) to counteract tumor growth and enhance immune surveillance. Small molecules can enter tumor cells and inactivate enzymes with roles in proliferation, differentiation, and migration (e.g., Wnt/β-catenin, NOTCH, PI3K/AKT), eventually triggering apoptosis (Xie et al., 2020). Monoclonal antibodies (e.g., cetuximab, bevacizumab) against targets on the surface can bind receptors (e.g., EGFR) or membrane-bound complexes (e.g., VEGF-A) on tumor cells to slow down tumor growth (Xie et al., 2020). Moreover, targeting inhibitory receptors on immune cells (e.g., PD-1) restores antitumor immune responses and thus holds promising potential for CRC, especially for dMMR CRC (Le et al., 2015).

1.2.4 ICI therapy in CRC

Clinically, 5-10% of CRC are dMMR (Mármol et al., 2017). These tumors usually respond poorly to standard chemotherapy regimens (Alatise et al., 2021; Alex et al., 2017; Cercek et al., 2020). In 2017, pembrolizumab (anti-PD-1) was first in line to be approved by the FDA for the treatment of metastatic CRC due to its good efficacy in dMMR CRC. Interestingly, this was the first time that FDA approval was given for a molecular feature (MSI-H/dMMR) and not a tumor entity (Lemery et al., 2017), considering the therapy success also in non-CRC MSI-H/dMMR tumor patients. The study (KEYNOTE-016) reported a response rate of 40-50% with progression-free survival (PFS) of 78% (at 20 weeks) in dMMR patients, whereas pMMR patients did

not respond (Le et al., 2017, 2015). This finding was confirmed by an independent study using pembrolizumab in MSI-H CRC (O'Neil et al., 2017). In another study (KEYNOTE-164), pembrolizumab achieved an objective response rate of 33% as second-line treatment in MSI-H metastatic CRC (Le et al., 2020, 2018). The second PD-1-blocking antibody, nivolumab, also gained FDA approval for dMMR and MSI-H metastatic CRC in 2017 in light of the CheckMate-142 trial, which reported a response rate of ca. 31% and PFS of ca. 50% (at 12 months), regardless of PD-L1 expression levels (Overman et al., 2017). Further studies reported superior clinical activity of combining ipilimumab with nivolumab compared to single-agent treatment (Lenz et al., 2018; Morse et al., 2019; Overman et al., 2018). In 2018, the doublet regimen, including nivolumab and ipilimumab, gained FDA approval for patients with metastatic dMMR/MSI-H CRC (Sahin et al., 2019). Furthermore, a recent phase 2 study testing dostarlimab (anti-PD-1 monoclonal antibody) as neoadjuvant treatment in dMMR stage II or III rectal adenocarcinoma showed that all patients (12 out of 12) who received the nine cycles of dostarlimab had a clinical complete response (Cercek et al., 2022). How long this effect will last and whether these patients will remain in complete remission is to be observed. Notably, another study with single anti-PD-1 treatment in metastatic dMMR tumors showed that the durability of the objective response in responsive patients exceeded 75% after 30 months (Marabelle et al., 2020). Taken together, immunotherapy with immune checkpoint-blocking antibodies displays outstanding clinical efficacy for CRC patients with defects in the MMR pathway, holding great promise for being a curative treatment.

1.3 Mismatch repair (MMR)

1.3.1 DNA damage and repair

In mammalian cells, DNA has evolved to be physiologically restricted to mitochondria and the nucleus, where it serves as a genetic blueprint for a living organism. While mutagenesis is essential for evolution and species fitness, preserving the genomic sequence information is integral for a prosperous organism. DNA is continuously exposed to harmful agents from various sources. Environmentally, physical factors (e.g., asbestos), radiation (e.g., UV, ionizing radiation), and chemical triggers (e.g., crosslinking and alkylating agents, dietary and therapeutic compounds) cause DNA damage by aberrantly modifying the DNA constituents (e.g., base oxidation, base

methylation, single-strand/double-strand breaks) (Chatterjee and Walker, 2017). Endogenously, DNA damage occurs during normal DNA metabolism and processing reactions such as DNA replication, recombination, and repair (Chatterjee and Walker, 2017). Since genetic instability can cause cellular dysfunction, ultimately leading to disease (e.g., cancer), cells are equipped with sophisticated systems such as DNA repair mechanisms that collectively function to robustly counteract the consequences of deleterious damages to the DNA and maintain genome integrity.

DNA damage repair is a spatiotemporally regulated multistep process that includes lesion-specific sensor proteins that allow the recognition of errors and damages, followed by the sequentially coordinated recruitment of factors that together build the DNA damage repair complex (Chatterjee and Walker, 2017). Due to the variable nature of damages inflicted on DNA, mammalian cells have evolved distinct repair mechanisms to respond accordingly. In principle, DNA damage repair functionally comprises the repair of DNA breaks (single-strand, double-strand, telomeres), the repair of base DNA damages, and the repair of multiple and bulky base damages (Chatterjee and Walker, 2017). The importance of DNA damage repair (DDR) is reflected by the fact that mutations in the DDR network cause numerous cancer predisposition syndromes (Li et al., 2021).

1.3.2 The MMR pathway

In eukaryotes, DNA replication is mainly carried out by the DNA polymerases (Pol) Polδ and Polε (Hsieh and Zhang, 2017). These high-fidelity DNA polymerases yield a very low spontaneous mutation rate (10^{-10} mutations per bp per generation). Although being equipped with a 3`-endonuclease activity that fulfills proofreading functions, wrongly incorporated nucleotides may escape the proofreading, resulting in roughly one insertion error in every 10^4-10^5 nucleotide incorporations (Hsieh and Zhang, 2017). The postreplicative MMR mechanism corrects replication errors on the newly synthesized strand, which, if left unrepaired, could contribute to the spontaneous generation of somatic and germline mutations and ultimately predispose to diseases such as cancer (Li, 2008). Although proteins of the MMR machinery also affect mitotic and meiotic recombination, DNA damage signaling, apoptosis, and cell-type-specific processes such as triplet-repeat expansion, somatic hypermutation, and class-switch

recombination, the main job of the DNA MMR system is to correct base-base mispairings and insertion-deletion loops (indels) (Jiricny, 2006). Base-base mismatches are errors in the DNA sequence produced by DNA polymerases. Indels are heteroduplex DNA molecules with extrahelical partnerless nucleotides, which form during DNA synthesis when primer and template strands occasionally dissociate and incorrectly re-anneal (Jiricny, 2006).

The DNA mismatch repair system is evolutionarily highly conserved among various organisms, ranging from bacteria to humans (Jiricny, 2013). The MMR pathway has been studied biochemically and genetically most extensively in *Escherichia coli (E.coli)*, which serves as a prototypical model for understanding the MMR pathways in mammalian cells. In humans, eight genes encode the *E. coli* MutS homologs (hMSH2, hMSH3, hMSH5, and hMSH6) and MutL homologs (hMLH1, hPMS1 (also called hMLH2), hMLH3, hPMS2 (also called hMLH4)). These MMR components function as heterodimers whereby different dimer combinations fulfill distinct tasks (Jiricny, 2006; Li, 2008; Pećina-Šlaus et al., 2020). Within the MutS homologs, MSH2 builds dimers with MSH3 and MSH6. MSH2-MSH6 (also referred to as MutSα) is the most abundant mismatch-binding factor. It recognizes base mismatches and mono- or dinucleotide indels, whereas MSH2-MSH3 (also referred to as MutSβ) recognizes large indels (roughly 13 nucleotides). Within the MutL homologs, MLH1 forms distinct heterodimers with PMS2, MLH2 (PMS1) and MLH3. Whereas the role of MLH1-PMS1 (also referred to as MutLβ) is still ill-defined, the MLH1-PMS2 (also referred to as MutLα) is recruited to the MMR complex following mismatch detection by MutSα. MLH1-MLH3 (also referred to as MutLγ) compensates when MutLα is lacking but has a more dominant role in meiosis. Beyond the MutS and MutL mismatch repair proteins, the MMR complex involves further components such as the exonuclease 1 (EXO1), single-strand DNA-binding protein replication protein A (RPA), replication factor C (RFC), proliferating cell nuclear antigen (PCNA), DNA polymerase Polδ, and DNA ligase I (LIG1) which are essential in the repair process (Li, 2008).

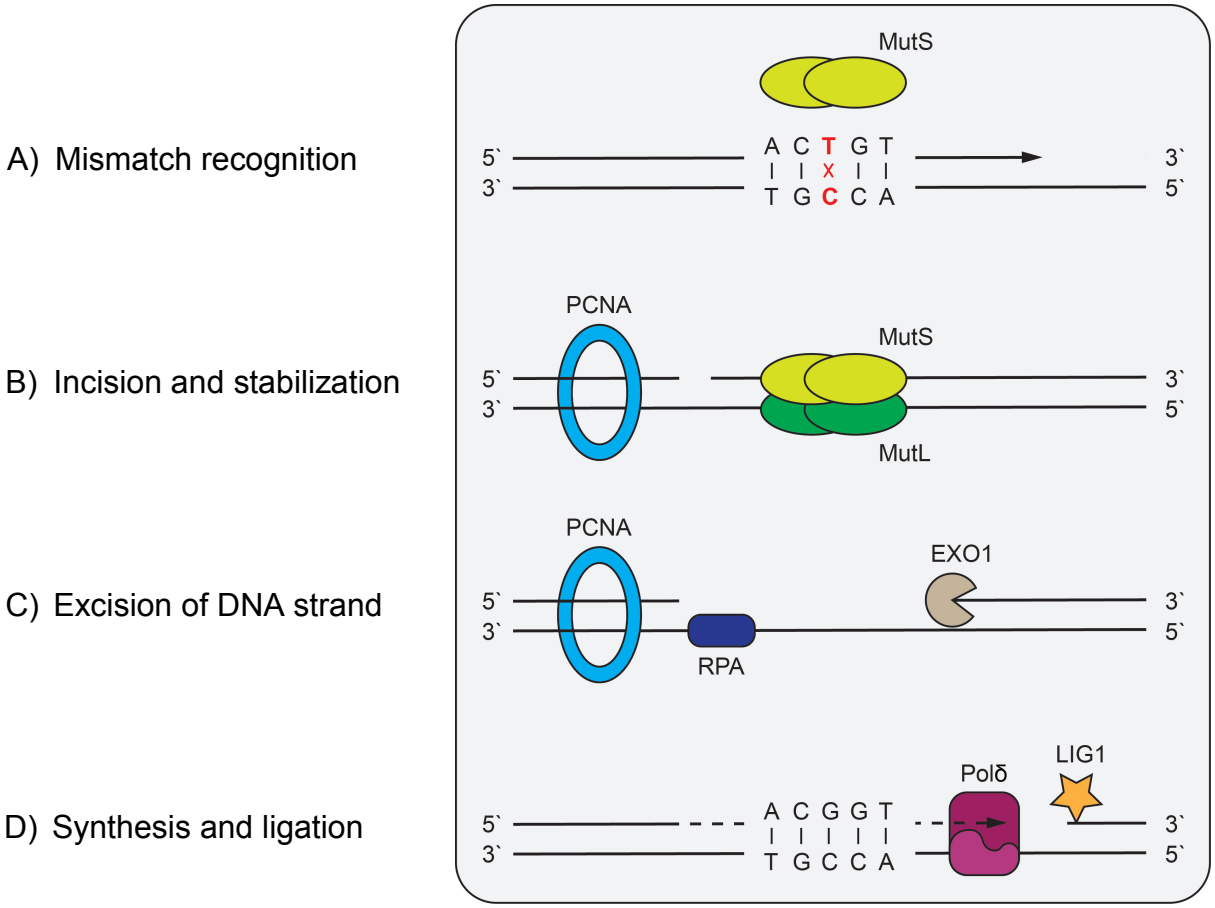

Fig. 1. The MMR pathway.

(A) MutS recognizes the mismatch, and (B) recruits MutL, which incises the erroneous DNA strand in the presence of PCNA. (C) Recruited EXO1 then excises the erroneous DNA strand. (D) To finish the repair process, Polδ re-synthesizes the gap, which is subsequently ligated by the DNA ligase.

Although the mismatch repair pathway in eukaryotes is still incompletely understood, it generally requires the sequential execution of mismatch recognition, repair initiation, lesion excision, and DNA resynthesis (Huang and Li, 2018; Liu et al., 2017). The first line MMR dimers MutSα or MutSβ initiate the DNA repair by recognizing and binding to the detected mismatches (**Fig. 1A**). After DNA lesion recognition, MutL dimers are recruited to the mismatch-bound complex whereby the MutLα dimer MLH1-PMS2 plays the major role in MMR. In the presence of PCNA, MutL incises the unmethylated DNA strand to create a nick near the base mismatch (**Fig. 1B**). Lesion recognition, MutS-MutL recruitment, and strand incision are ATP dependent processes and defects in the ATP activity lead to defects in the MMR. EXO1, a 5`-> 3` exonuclease, then uses

this MutL-created single-strand break to access the erroneous DNA strand and excises the wrongly paired bases (**Fig. 1C**). RPA stabilizes the single-strand gap created by this degradation. Subsequently, the polymerase Polδ coordinates the DNA resynthesis to correctly refill the excised gap (**Fig. 1D**). In the end, LIG1 seals the remaining nick, completing the repair process (Jiricny, 2006; Li, 2008). Although EXO1 works in the 5`->3` direction, EXO1 also aids in the excision of 3`nicks.

1.3.3 MMR deficiency in cancer

Genomic instability is a cancer hallmark (Hanahan and Weinberg, 2011, 2000). The MMR pathway plays a vital role in promoting genomic stability. Deregulation of components in this tightly regulated MMR network is associated with genome-wide instability, predisposition to certain types of cancer, and resistance to certain chemotherapeutic agents (Jiricny, 2006; Li, 2008; Pećina-Šlaus et al., 2020). Initial work independently conducted by Vogelstein and Kolodner and their co-workers identified that germline mutations in *MSH2* (Fishel et al., 1993; Leach et al., 1993) and defects in *MLH1* (Bronner et al., 1994; Leach et al., 1993; Nicolaides et al., 1994) represent the majority HNPCC cases and some cases of sporadic CRC. In the following years, genetic variants of other MMR components were also found in cancerous malignancies beyond CRC. Within the MutS homologs, genetic aberrations in *MSH3* are associated with colorectal, urinary bladder, and endometrial cancers (Kawakami et al., 2004; Yamamoto and Imai, 2015), and variants of *MSH6* are associated with colorectal and endometrial cancer (Poulogiannis et al., 2010; Rosenthal et al., 2020). Within the MutL homologs, mutations in *PMS1* alone or together with other MMR gene mutations can cause CRC (Tanakaya, 2019), *PMS2* gene variants are found in CRC (however less frequent than *MLH1* or *MSH2*), Turcot syndrome, and primitive neuroectodermal tumors (Pećina-Šlaus et al., 2020), and *MLH3* alterations are found in various tumors such as CRC, endometrial tumors, and low-grade glioma (Duraturo et al., 2016; Valle et al., 2019). Altogether, mutations in and deregulation of MMR proteins cause several cancer malignancies and are particularly prevalent in CRC.

1.4 The cGAS-STING pathway

1.4.1 Nucleic acid sensing

To protect our body against infectious agents from the outside and the development of malignancies (e.g., cancer) from the inside, the innate immune system serves as the first line of defense. To recognize danger signals and to instruct adaptive immunity, innate immune cells are equipped with pattern recognition receptors (PRRs), which recognize microbe-specific molecules called pathogen-associated molecular patterns (PAMPs) such as microbial metabolites (e.g., bacterial carbohydrates, viral nucleic acids) or endogenous stress signals called danger-associated molecular patterns (DAMPs) (Akira et al., 2006). Nucleic acids (NAs) are ubiquitous danger signals in vertebrates, and the induction of type I interferons (IFNs) upon NA sensing is a hallmark of innate immunity (Schlee and Hartmann, 2016). To distinguish between self and non-self, the structure (e.g., sequence motifs, conformation), availability (e.g., local concentration, shielding), and localization (e.g., cytosol vs. endosome) of the NA ligands play an essential role (Schlee and Hartmann, 2016). Given the various nature of NA species, such as single-stranded (ss) or double-stranded (ds) RNA and DNA or hybrids thereof, distinct RNA or DNA-recognizing receptors for detecting NAs have evolved. Among DNA-recognizing receptors, cGAS is a prominent DNA sensor that promotes type I IFN production via Stimulator of IFN genes (STING) (Schlee and Hartmann, 2016). The cGAS-STING signaling axis has broad functions in host defense, autoinflammatory disorders, and cancer biology.

1.4.2 cGAS signaling

cGAS is a 520 amino acid protein first purified in 2013 and found to function as a cytosolic DNA sensor and to catalyze the synthesis of cGAMP (Sun et al., 2013). Functionally, cGAS recognizes the foreign DNA of a wide range of microbial pathogens, such as bacteria, viruses, and protozoans (Hopfner and Hornung, 2020). In addition to non-self DNA, cGAS can also recognize extracellular self-DNA (upon cell death), mitochondrial DNA (mtDNA) (upon intrinsic apoptosis), or nuclear DNA (due to defective DNA replication, repair, and mitosis) (Hopfner and Hornung, 2020). Although cGAS does not recognize DNA in a sequence-specific manner, its activation requires the binding of DNA with a certain length. Short DNA of roughly 20 bp can bind to cGAS, however, dsDNA longer than 45 bp form more stable cGAS dimers and higher-order

DNA-cGAS complexes and thus generate stronger enzymatic activity (Li et al., 2013; Zhang et al., 2014).

Upon DNA binding, the activation of cGAS requires the assembly into a dimer, which switches the inactive cGAS into a catalytically active state to catalyze the production of cGAMP. The second messenger molecule, cGAMP, then binds to STING for downstream pathway activation. Besides activating STING within the same cell, cGAMP can also be shuttled to neighboring cells by diffusion through gap junctions (Chen et al., 2016; Schadt et al., 2019), being packed into viral capsids (Bridgeman et al., 2015; Gentili et al., 2015), or by transmembrane carriers (e.g., LRCC8, SLC19A1, P2XR7) (Luteijn et al., 2019; C. Zhou et al., 2020; Y. Zhou et al., 2020). Exposed to the extracellular space, cGAMP is, however, readily degraded by the ectonucleotide pyrophosphatase/phosphodiesterase 1 (ENPP1), thereby controlling cGAMP availability (Li et al., 2014).

1.4.3 STING signaling

STING was found in 2008 as a key mediator of DNA sensing and type I IFN signaling and is widely expressed in both non-immune and immune cells (Ishikawa et al., 2009; Ishikawa and Barber, 2008). STING is a ca. 40 kDa membrane protein composed of four transmembrane domains in the N-terminal region, which anchor STING to the endoplasmic reticulum (ER), a connector region, a ligand-binding domain (LBD) that contains a dimerization domain, and a C-terminal tail (CTT), with both LBD and CTT facing the cytosol. In the CTT, STING harbors a highly conserved PLPLRT/SD TANK-binding kinase 1 (TBK1)-binding motif (Zhang et al., 2019; B. Zhao et al., 2019) and in direct proximity to it a pLxIS motif which is essential for interferon regulatory factor 3 (IRF3) recruitment and activation (Liu et al., 2015; Zhao et al., 2016).

Activation of STING initiates various biological effector functions to promote host immunity whereby the TBK1-IRF3 activation-mediated type I IFN transcription is an essential regulator of host immunity (**Fig. 2**). In addition to host cGAMP, STING also binds directly to cyclic dinucleotides produced by bacteria such as cyclic diGMP, cyclic diAMP, and bacterial cGAMP (Burdette et al., 2011; Webster et al., 2017; Woodward et al., 2010). Independent of cyclic dinucleotides, STING was moreover found to be

activated by several other stimuli, such as ER stress or viral liposomes (Holm et al., 2012; Moretti et al., 2017; Petrasek et al., 2013). At steady state, STING is anchored as a dimer to the ER by factors such as the Ca^{2+} sensor stromal interaction molecule 1 (STIM1) (Srikanth et al., 2019). Upon cGAMP binding, STING undergoes a conformational change that promotes the oligomerization of multiple STING dimers (Ergun et al., 2019; Shang et al., 2019) and induces trafficking to the Golgi. This process enables TBK1 to phosphorylate (in *trans*) and activate other TBK1 molecules close by. Activated TBK1 phosphorylates STING at the serine residue (S366) in the pLxIS motif ("p" represents a hydrophilic residue, "x" any residue, and "S" the serine), which serves as a docking site for IRF3 (Liu et al., 2015; Zhang et al., 2019). Upon recruitment, IRF3 gets activated by TBK1-mediated phosphorylation and forms dimers that subsequently translocate to the nucleus to induce type I IFN production (Agalioti et al., 2000; Zhao et al., 2016). Produced IFNs act in an auto- and paracrine manner via IFN-α receptor 1 (IFNAR1) and IFNAR2, which signal through Janus kinase/signal transducer and activator of transcription (JAK/STAT), to induce IFN-stimulated genes (ISGs) (Schneider et al., 2014), the transcripts of which collectively serve to coordinate host immunity (e.g., antiviral defense, antitumor immunity).

Beyond IFN signaling, the cGAS-STING pathway is also implicated in other effector mechanisms such as NF-κB activation, autophagy, and cell death. For example, certain species (e.g., insects) that lack the CTT of STING can still promote NF-κB responses to orchestrate antimicrobial host defense (Goto et al., 2018; Martin et al., 2018). Moreover, in certain fish species (e.g., zebrafish), STING promotes TNF receptor associated factor 6 (TRAF6)-mediated NF-κB signaling by having additional signaling motifs appended to the CTT (de Oliveira Mann et al., 2019). In human cells, the exact regulation of STING triggered NF-κB activation is, however, still incompletely understood. In the context of autophagy, STING-controlled autophagy was reported to have protective roles in the clearance of microbial pathogens (e.g., *Mycobacterium tuberculosis* (Watson et al., 2012), Gram-positive bacteria (Moretti et al., 2017), and Herpes Simplex Virus-1 (HSV-1) (Yamashiro et al., 2020)). Moreover, STING-induced autophagy can also be triggered upon replicative crisis, thereby preventing tumor cell outgrowth (Nassour et al., 2019). Finally, besides triggering IRF3-mediated IFN expression, STING induces the expression of various pro-apoptotic and pro-necroptotic molecules, thereby contributing to the cell death pathways, including

apoptosis and necroptosis. In lymphoid cells such as T cells, for example, STING activation leads to apoptosis by promoting the upregulation of the pro-apoptotic BH3-only proteins Noxa and Puma (Gulen et al., 2017). Interestingly, when apoptosis is inhibited, STING activation also triggers receptor-interacting protein kinase 3 (RIPK3)-mediated necroptosis involving crosstalk of type I IFNs and tumor necrosis factor (TNF) signaling (Brault et al., 2018).

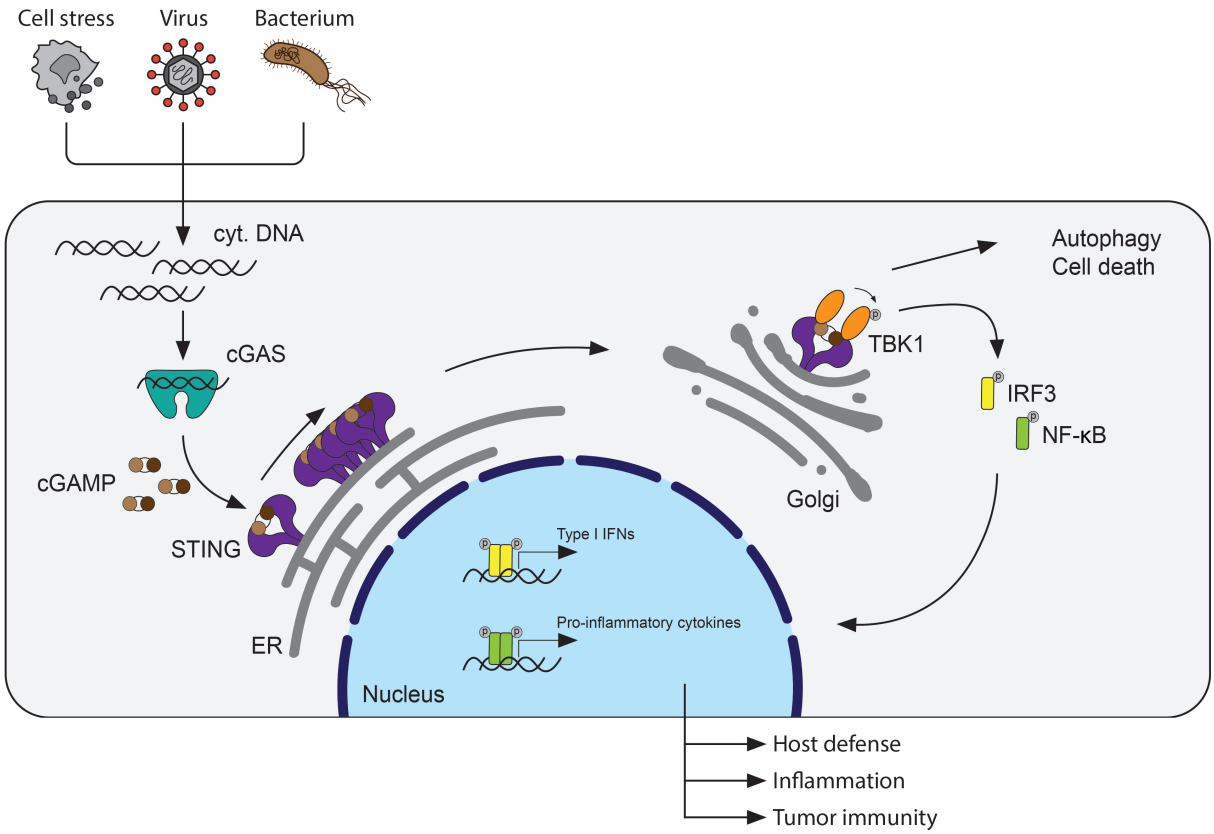

Fig. 2. The cGAS-STING pathway.

DNA from endogenous and exogenous sources is recognized by cGAS, which produces cGAMP for STING activation. Upon activation, STING oligomerizes and translocates from the ER to the Golgi. Engaging the TBK1-IRF3 or NF-κB pathway, STING drives the transcription of genes encoding different effector molecules (e.g., IFN-β, IL-6), which generates an inflammatory immune response to collectively promote host immunity. Moreover, STING plays a role in autophagy and cell death (e.g., apoptosis). Cytosolic DNA (cyt. DNA).

1.4.4 Constitutive STING activity in SAVI disease

The cGAS-STING pathway is of paramount importance in antitumor immunity and host defense against infections. However, aberrant activation, erroneous regulation, or receptor malfunctioning of this signaling pathway can lead to severe inflammatory disorders characterized by elevated IFN levels, which are clinically also called interferonopathies (Uggenti et al., 2019). STING-associated vasculopathy with onset in infancy (SAVI) is such an autoinflammatory disorder whereby genetic variations in STING (e.g., N154S, V155M, and V147L) lead to constitutive STING activation and thus elevated IFN signatures in primary patient cells. These patients are characterized by cytokine dysregulation, recurrent fever, ulcerative skin lesions, vasculitis, interstitial lung disease, and reduced life expectancy (Liu et al., 2014). Murine models of SAVI ($STING^{N153S}$ knock-in mouse) greatly phenocopy the human disease features manifesting upregulated ISGs, hypercytokinemia, lymphocytopenia, and perivascular inflammatory lung disease (Luksch et al., 2019; Warner et al., 2017). Thus, the $STING^{N153S}$ knock-in mouse is a useful model to study the role of constitutive STING activation in this disease. Interestingly, ablation of type I IFN signaling did not protect the mice from developing lung disease, whereas T cell depletion rescued the phenotype (Luksch et al., 2019; Warner et al., 2017). These findings indicate that the SAVI disease develops independently of STING-driven type I IFN signaling but relies on T cells. Considering that STING can drive both IFN-dependent and independent signals in different cell types (e.g., myeloid vs. lymphoid) (Wu et al., 2020), these studies suggest that SAVI-STING drives IFN-independent effects on T cells. The exact molecular mechanism of this SAVI-STING-driven pathology, however, is still part of ongoing research.

1.5 Antitumor immunity

1.5.1 The tumor microenvironment (TME)

Solid tumors are complex tissues composed of various cellular and non-cellular components such as extracellular matrix (ECM), immune cells, blood vessels, and stromal cells, collectively forming a highly dynamic tumor microenvironment (TME). Generally, all types of immune cells can be found in the TME, including T cells, natural killer (NK) cells, dendritic cells (DCs), and macrophages (Belli et al., 2018). Shaped by several factors such as nutrient availability, level of hypoxia, or the inflammatory milieu,

the functionality of the immune cells in the TME can be polarized towards protumoral or antitumoral responses (Belli et al., 2018). For example, the expression of anti-inflammatory cytokines such as transforming growth factor (TGF)-β skews pro-inflammatory macrophages (M1) towards an anti-inflammatory macrophage state (M2), inhibits type 1 T helper (Th1) responses while promoting regulatory T cells (T regs), and suppresses CD8+ T cell and NK cell cytotoxicity (Batlle and Massagué, 2019). In contrast, cytokines such as IFN-γ and interleukin 12 (IL-12) enhance antitumor immune responses by linking innate and adaptive immunity and inducing cytotoxic activities in antitumoral effector cells such as CD8+ T cells (Garris et al., 2018).

Based on their immune landscape, tumors can roughly be categorized into “cold” (immune-excluded or immune-desert) and “hot” (immune-inflamed) tumors (Chen and Mellman, 2017). Whereas immune cells fail to penetrate the tumor tissue in “cold” tumors (Hegde and Chen, 2020), “hot” tumors are characterized by an inflammatory environment, namely by the presence of CD8+ T cells, increased IFN-γ signaling, and high TMB, possibly driven by genomic instability (Hegde et al., 2016). Indeed, the presence of CD8+ T cells is a prognostic factor associated with prolonged cancer patient survival and increased immunotherapy efficacy (Bruni et al., 2020; Corrales et al., 2017). Clinically, “hot” tumors respond better to ICI therapy (Galon and Bruni, 2019; Herbst et al., 2014; Ochoa de Olza et al., 2020; Ribas et al., 2017). Although ICIs restore antitumor immune responses, the infiltration of TILs into the tumor bed, which is coordinated by inflammatory mediators, remains essential to yield therapeutic results (Kubli et al., 2021). Notably, TIL-attracting chemokines such as C-C motif chemokine ligand 5 (CCL5) and C-X-C motif chemokine ligand 10 (CXCL10) recruit antitumor effector cells such as cytotoxic CD8+ T cells and NK cells into the TME (Harlin et al., 2009; Zumwalt et al., 2015).

To mount a powerful antitumor immune response, DC activation is critical for instructing tumor-specific T cell responses and orchestrating adaptive cancer immunity (Chen and Mellman, 2013). In the TME, APCs such as DCs continuously take up dead cell debris alongside tumor antigens and stimulatory DAMPs. Upon activation by these DAMPs, APCs migrate to the draining lymph node (dLN) and cross-present the ingested tumor antigens to lymphoid immune cells for T cell priming and activation.

Through the circulation, these newly educated tumor antigen-specific TILs then migrate to the tumor site, where they infiltrate the tumor tissue and recognize and kill tumor cells by unleashing tumoricidal effector functions. This T cell-mediated cell death amplifies immune stimulatory signals and fuels the continuation of the cancer immunity cycle. The lack of stimulatory signals that elicit inflammatory responses results in impaired induction of DC-dependent tumor-specific cytotoxic CD8+ T cell responses (Chen and Mellman, 2013).

1.5.2 cGAS-STING signals in antitumor immunity

Many PRRs were initially described to promote host immunity in the context of infections (Kawai and Akira, 2010). However, it has become evident that these pathways are also critical regulators of antitumor immunity (Bai et al., 2020). In particular, STING bears great immunomodulatory capacities and is suggested to be a master regulator of the cancer-immunity cycle (Zhu et al., 2019).

In cancer cells, genomic instability or genotoxic stress can lead to the formation of micronuclei, a form of extranuclear encapsulated DNA, which, upon membrane rupture, can be recognized by cGAS and drive cancer cell-intrinsic STING-mediated inflammatory responses (Harding et al., 2017a; Mackenzie et al., 2017). Moreover, mitochondrial stress can lead to mtDNA leakage into the cytosol and activate the cGAS-STING pathway (Kitajima et al., 2019; West et al., 2015). In the TME, tumor-derived self-DNA can be delivered to the cytosol of APCs such as DCs indirectly via extracellular vesicles (e.g., exosomes) or directly via endocytosis where it triggers the activation of the cGAS-STING pathway and subsequent type I IFN expression which promotes antitumor immunity (Deng et al., 2014; Diamond et al., 2018; Woo et al., 2014; Xu et al., 2017). Moreover, tumor-derived cGAMP can be shuttled to neighboring cells, trigger STING activation in immune cells such as DCs in the TME, and promote NK-mediated immunity (Marcus et al., 2018; Schadt et al., 2019). Beyond DCs, it is conceivable that other cell types in the TME also respond to tumor-derived cGAMP, but this requires further investigation.

DCs are professional APCs essential for antitumor immunity by connecting innate to adaptive immunity. In particular, STING-mediated type I IFNs lead to the activation and

maturation of DCs and the enhancement of tumor antigen cross-presentation for CD8+ T cell priming and activation (Corrales et al., 2015; Deng et al., 2014; Woo et al., 2014). Beyond these effects, stimulation of DCs by type I IFNs induces the expression of a plethora of ISGs, like genes encoding cytokines and chemokines, which are essential in shaping productive antitumor immune responses (Ozga et al., 2021). In particular, the chemokines CCL5, CXCL9, CXLC10, and CXCL11 are key mediators of TIL trafficking to the tumor site (Harlin et al., 2009; Zumwalt et al., 2015). Studies with STING- and IFNAR-deficient mice revealed that host STING-induced IFN signaling is critical for the infiltration of CD8+ T cells into the tumor tissue (Demaria et al., 2015).

Arriving in the TME, tumor antigen-specific T cells recognize tumor cells via their TCR and kill the targeted tumor cell by releasing tumoricidal effector molecules such as perforin1 (PRF1), granzyme B (GZMB), or IFN-γ (Weigelin et al., 2021). Studies with STING- and IRF3 knockout (KO) mice revealed that host STING-IRF3-IFN-dependent APCs activation, IFN-β production, and priming of tumor-specific CD8+ T cells are crucial to promoting the antitumor effects of CD8+ T cells (Deng et al., 2014; Woo et al., 2014). Moreover, cGAS-STING-mediated IFN production was shown to enhance the stem cell-like CD8+ T cell differentiation programs, which support T cell-mediated antitumor immune responses (Li et al., 2020). Besides immune cells, the expression of STING in non-immune cells, such as endothelial cells, has also been reported to contribute to IFN-mediated antitumor immune responses (Demaria et al., 2015). In this context, STING expression in endothelial cells was correlated with CD8+ T cell infiltration and prolonged survival in some human cancer types (e.g., colon and breast cancer) (Yang et al., 2019).

1.6 Research objective

MSI-H/dMMR tumors exhibit better responsiveness to ICI therapy than MSS CRCs (Le et al., 2017, 2015; Mandal et al., 2019). It has been suggested that the therapy-responsive fraction of TMB-high tumors is due to an enrichment of neoantigens in the tumor tissue, which arise from the dMMR-driven hypermutator phenotype (Germano et al., 2017). However, the prevalence of mutation-generated immunogenic neoantigens is insufficient to recruit the necessary immune cells into the TME that mediates the effector immune response (Spranger et al., 2016). Moreover, approximately 50% of dMMR tumors do not respond to immune checkpoint blockade, suggesting that additional inflammatory mechanisms and not only the TMB must govern ICI sensitivity. Thus, the aim of this study was:

1) to decipher the molecular mechanisms that determine dMMR ICI therapy responsiveness;

2) to develop strategies to selectively enhance signals that could sensitize immunologically “cold” and ICI-insensitive tumors to immunotherapy such as ICI therapy.

2 Results

2.1 MMR deficiency triggers IFN signaling in CRC

To study the immunostimulatory mechanisms responsible for the superior ICI responsiveness in dMMR CRCs, we accessed genome and RNA sequencing data from 524 colorectal and rectal adenocarcinoma patient samples from The Cancer Genome Atlas (TCGA). We divided the samples based on the mutations in *MLH1, MSH2, POLD1, or POLE,* which are often inactivated in CRC (Mur et al., 2020; Pećina-Šlaus et al., 2020), into two groups: mismatch repair-proficient (pMMR) tumors (n=451) and mismatch repair-deficient (dMMR) tumors (n=73). In line with previous data (Boland and Goel, 2010), the TMB was significantly higher in dMMR than in pMMR cases (**Fig. 3A**). To uncover differences in gene expression signatures, we next performed a pre-ranked gene set enrichment analysis (GSEA) on the differentially expressed genes between dMMR and pMMR tumor groups using the Reactome pathway database. The results revealed that immune and inflammatory processes were among the top differentially regulated pathways in the dMMR group with a strong representation of IFN signaling-related signatures such as “IFN gamma signaling,” “IFN signaling,” and “IFN alpha/beta signaling” (**Fig. 3B**). Thus, dMMR in CRC not only increases the TMB in the tumor tissue but also triggers the activation of IFN signaling.

Because the patient data sets from TCGA were collected from whole tumor tissue, we next planned to selectively investigate inflammatory signals that are intrinsic to cancer cells by using organoids. For this, we collaborated with a research group with access to a primary human CRC organoid biobank (Farin et al., 2023). Similar to the results from the TCGA data, whole-exome sequencing (WES) and RNA-seq revealed that the dMMR organoids exhibited an elevated TMB and a strong enrichment of type I IFN signaling compared to the pMMR samples (Farin et al., 2023; Vornholz et al., 2023). Together, these findings demonstrate that dMMR drives the activation of IFN-related inflammatory signals within the tumor cells.

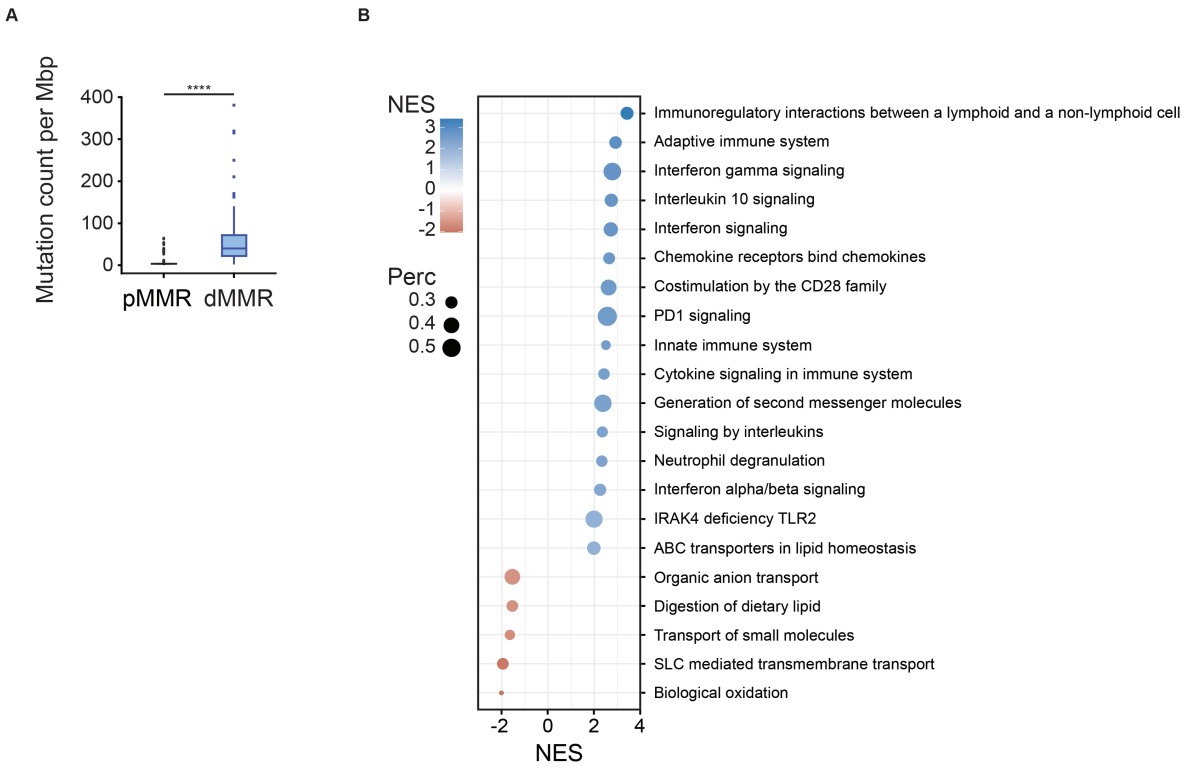

Fig. 3. MMR deficiency triggers IFN signaling in human CRC.

Exome and RNA sequencing data of dMMR and pMMR tumors from 524 colorectal and rectal adenocarcinoma patients. (A) Mutation count per megabase pair (Mbp) of pMMR vs. dMMR tumors. (B) GSEA of differentially expressed gene sets from the Reactome database comparing dMMR vs. pMMR tumors (+ve NES: dMMR). Student`s *t*-test (A) was used to determine significance. Normalized enrichment score (NES), percentage of genes contributing to the enrichment score (Perc).

2.2 Tumor cell-intrinsic STING pathway activation upon MMR deficiency

To mechanistically dissect how defects in MMR drive tumor cell-intrinsic IFN signaling in CRC, we employed CRISPR/Cas9 to genetically edit murine CRC cell lines. First, we generated *Mlh1-/-* MC38 tumor cells. MLH1 deficiency was confirmed by western blotting (**Fig. 4A**). By RNA-seq and GSEA, we found that the MLH1 deficiency leads to a strong induction of IFN signaling, which is represented by the top enriched signatures “IFN signaling” and “IFN alpha/beta signaling” (**Fig. 4B**). Moreover, measuring the expression of the ISG *Isg15* encoding a prototypical marker for productive IFN signaling (Perng and Lenschow, 2018), we confirmed that *Isg15* was

strongly expressed in *Mlh1-/-* tumor cells (**Fig. 4C**). The induction of type I IFNs upon DNA sensing is a hallmark of innate immunity (Schlee and Hartmann, 2016). Thus, we next isolated DNA from the cytosol. Interestingly, we detected an increase in genomic DNA in the cytosol of *Mlh1-/-* tumor cells (**Fig. 4D**), which is released from the nucleus due to genomic instability (Lu et al., 2021; Mackenzie et al., 2017; Talens and Van Vugt, 2019). To validate our finding in another murine adenocarcinoma cell line, we also generated *Mlh1-/-* CT26 tumor cells (**Fig. 4E**). Similar to MC38 cells, the expression of *Isg15* was robustly induced in the *Mlh1-/-* CT26 cells (**Fig. 4F**) confirming that MLH1 deficiency results in tumor cell-driven IFN signaling.

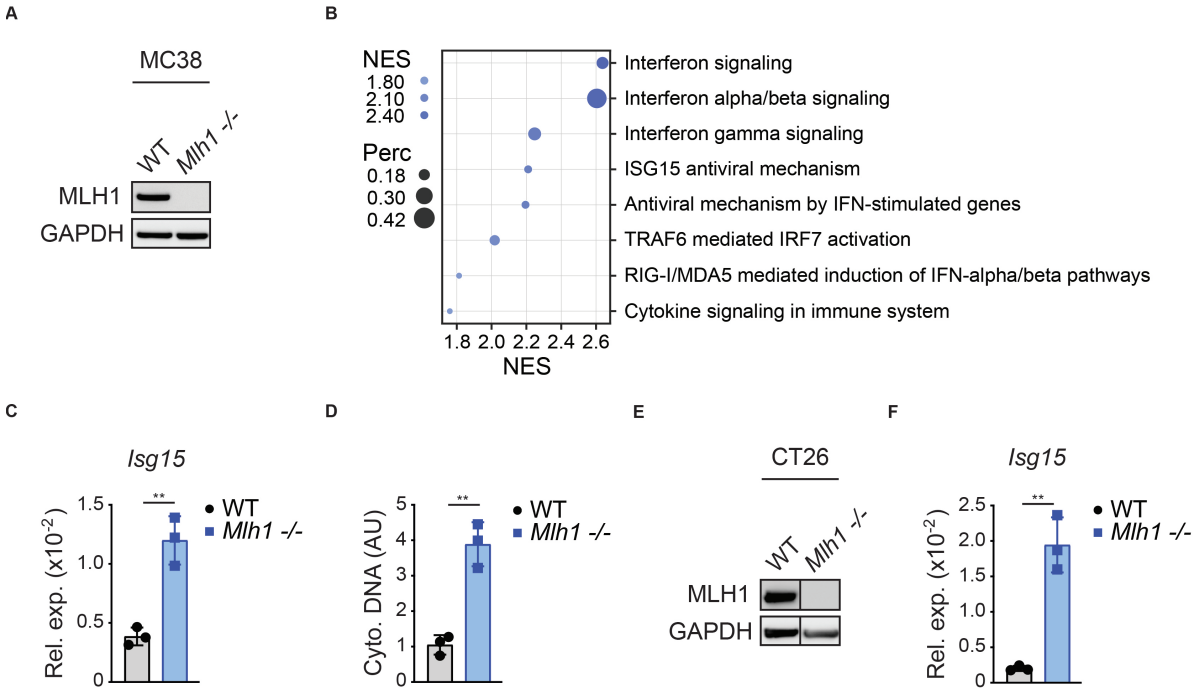

Fig. 4. MMR deficiency drives tumor cell-intrinsic IFN signaling.

(A) MLH1 deficiency in MC38 tumor cells was confirmed by western blotting. (B) GSEA of RNA-seq data to identify differentially expressed gene sets of WT vs. *Mlh1-/-* MC38 tumor cells by using the Reactome database (+ve NES: *Mlh1-/-*). (C) The relative gene expression of *Isg15* in cultured MC38 tumor cells was quantified by qPCR. (D) Cytosolic DNA of MC38 tumor cells was isolated with a commercial kit and quantified by qPCR with primers specific for genomic DNA. (E) MLH1 deficiency in CT26 tumor cells was confirmed by western blotting. (F) The relative gene expression of *Isg15* in CT26 tumor cells was quantified by qPCR. The data represent n=3 independent experiments (C, D, F). Student`s *t*-test was used to determine significance (C, D, F). Normalized enrichment score (NES), percentage of genes contributing to the enrichment score (Perc).

Genomic instability can induce IFN signaling via cGAS upon cytosolic DNA recognition (Mackenzie et al., 2017). Upon activation, cGAS produces the second messenger, cGAMP, which then activates the innate immune adaptor protein STING to induce TBK1-IRF3-mediated type I IFN production (Hopfner and Hornung, 2020). To inspect the signaling pathway that mediated dMMR-triggered IFN signaling, we co-deleted *Cgas* (*Mlh1/Cgas-/-*) or *Sting* (*Mlh1/Sting-/-*) in *Mlh1-/-* MC38 tumor cells (**Fig. 5A**). MLH1 deficiency resulted in an increased cGAMP production which was dependent on the presence of cGAS (**Fig. 5B).** STING expression did not affect the MLH1 deficiency-induced cGAMP production (**Fig. 5B)**. Furthermore, *Mlh1-/-* tumor cells produced higher levels of IFN-β, which was strictly dependent on cGAS-STING (**Fig. 5C)**. Type I IFNs induce STAT1 signaling via IFNAR1 (Schneider et al., 2014). Consistent with the elevated IFN-β production, *Mlh1-/-* tumor cells also displayed increased STAT1 phosphorylation, which was reduced when cGAS-STING was missing (**Fig. 5D)**.

Next, we measured the gene expression of *Isg15* as well as the expression of *Ccl5* and *Cxcl10*, which are important chemoattractants for TILs (Zumwalt et al., 2015). The induction of *Isg15, Ccl5,* and *Cxcl10* in *Mlh1-/-* MC38 cells was strictly dependent on cGAS-STING signaling (**Fig. 5E**). Because IFNAR1 mediates type I IFN-induced signaling, we next tested the effects of autocrine type I IFN signaling in dMMR MC38 tumor cells by using IFNAR1-blocking antibodies. Indeed, blocking IFNAR1 in *Mlh1-/-* tumor cells reduced the gene expression of *Isg15*, *Ccl5*, and *Cxcl10*, which indicates that the transcription of these ISGs is in part driven by autocrine IFNs (**Fig. 5F**). Together, these findings demonstrate that defects in the MMR machinery lead to an accumulation of cytosolic DNA, cGAS-dependent generation of cGAMP, and STING induced transcription of type I IFNs.

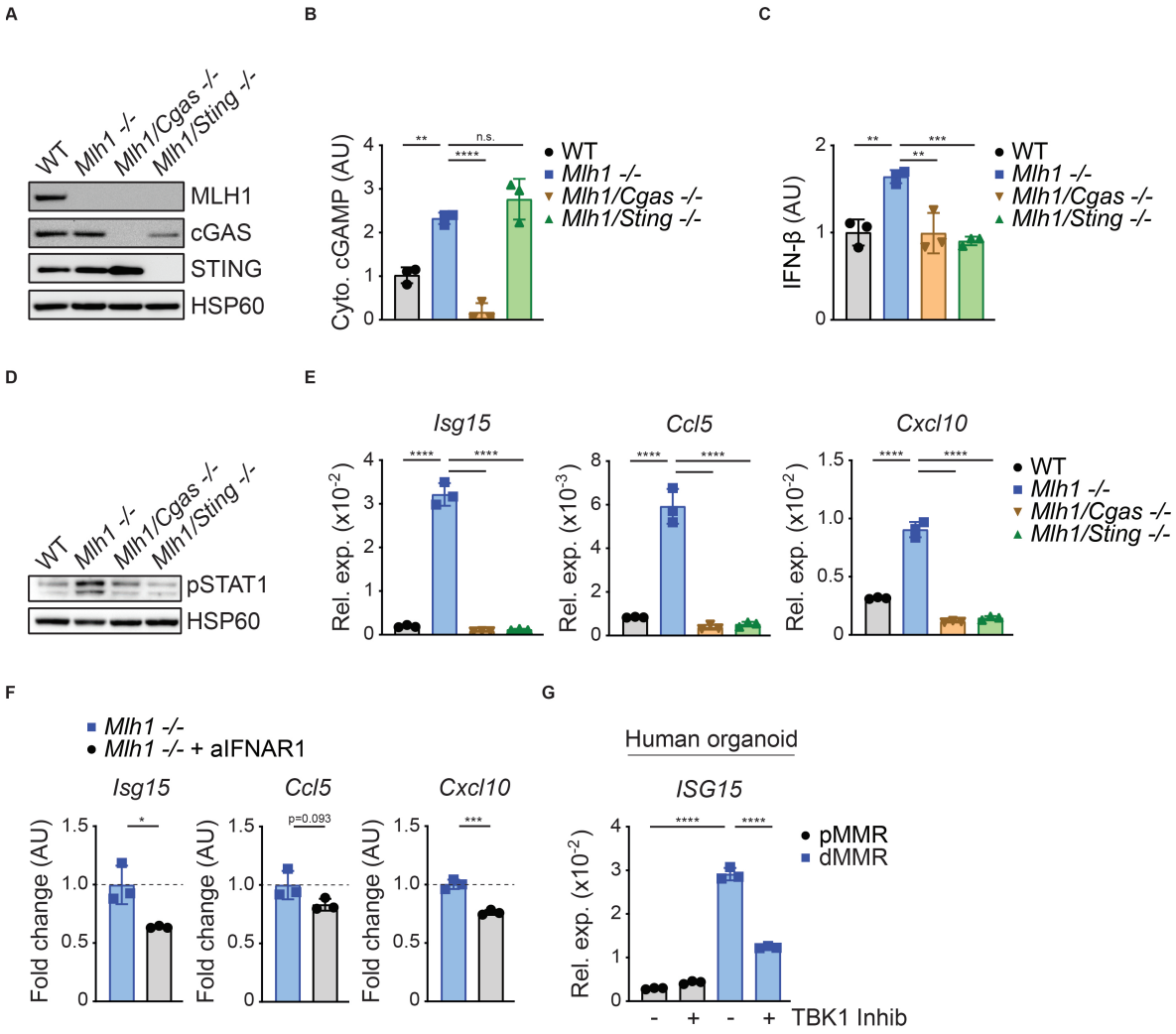

Fig. 5. cGAS-STING mediates IFN signaling in dMMR CRC.

(A) Genetically modified MC38 tumor cells were confirmed by western blotting. (B) Cytosolic cGAMP levels were quantified by ELISA from cell lysates of cultured MC38 tumor cells. (C) IFN-β production from MC38 tumor cells was quantified by ELISA. (D) The phosphorylation of STAT1 in cultured MC38 cells was detected by western blotting. (E) The relative gene expression of *Isg15, Ccl5,* and *Cxcl10* in cultured MC38 tumor cells was quantified by qPCR. (F) *Mlh1-/-* MC38 tumor cells were treated with anti-IFNAR1 blocking antibodies (30 μg/ml) for 24h, and the relative gene expression of *Isg15, Ccl5,* and *Cxcl10* was quantified by qPCR. (G) The relative gene expression of *ISG15* in pMMR vs. dMMR cultured primary organoids was quantified by qPCR 16 h after TBK1 inhibitor treatment. The data represent n=3 independent experiments (B, E), are representative of n=2 independent experiments (C, F), or represent n=3 technical replicates (G). Student`s *t*-test (F) or one-way ANOVA (B, C, E, G) was used to determine significance.

To validate these findings in human CRC, the patient-derived CRC organoids from our collaboration partner were used (Farin et al., 2023). Organoids with defects in MMR displayed increased *ISG15* gene expression compared to their pMMR counterparts (**Fig. 5G)**. This enhanced expression in dMMR organoids was significantly reduced when using pharmacological inhibitors against TBK1, a signaling molecule that mediates STING-induced IFN signaling. Thus, the tumor cell-intrinsic mechanism of MMR deficiency-induced IFN signaling is conserved between mice and humans.

2.3 STING signaling in dMMR CRC mediates immunogenicity

After identifying a role for STING in driving IFN responses in dMMR tumor cells, we next studied how tumor cell-intrinsic STING activation impacts the growth of dMMR cancer cells and how it modulates TMEs *in vivo*. For this, we subcutaneously (sc) transplanted WT, *Mlh1-/-*, and *Mlh1/Sting-/-* MC38 cells into syngeneic C57BL/6 mice. While WT, *Mlh1-/-*, and *Mlh1/Sting-/-* MC38 tumors displayed comparable proliferation rates in *in vitro* cultures (**Fig. 6A**), *Mlh1-/-* cells grew smaller tumors *in vivo* (**Fig. 6B, 6C**). This reduced tumor growth was dependent on STING since the absence of STING enabled *Mlh1-/-* tumor cells to grow comparably to WT tumors.

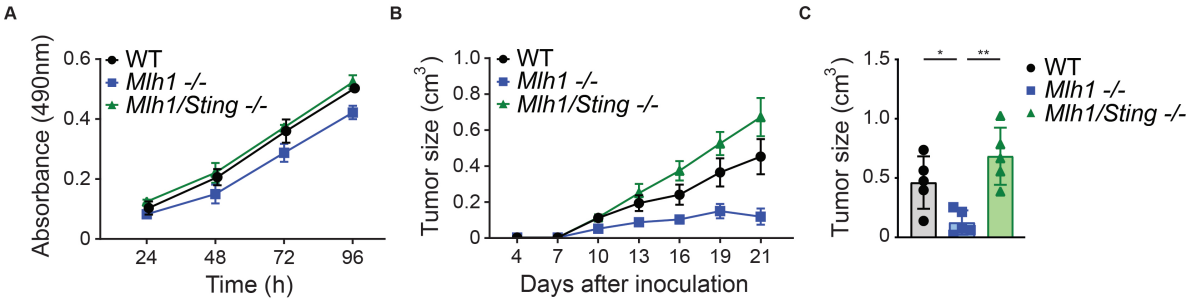

Fig. 6. STING signaling in dMMR CRC controls tumor growth.

(A) *In vitro* proliferation of cultured MC38 tumor cells. (B) Growth of subcutaneously inoculated WT, *Mlh1-/-,* or *Mlh1/Sting-/-* MC38 tumor cells (n=5) in syngeneic WT C57BL/6 mice. (C) Endpoint size of subcutaneously grown tumors. The data represent n=3 independent experiments (A). The data are presented as the mean ± SEM (B). One-way ANOVA (C) was used to determine significance.

To explore the immune microenvironment in these tumor tissues, we analyzed tumor immune infiltrates by flow cytometry and gene expression by qPCR. In the TME of *Mlh1-/-* tumors, we observed an increased gene expression of the chemokines *Ccl5, Cxcl9, Cxcl10, and Cxcl11* which are crucial for recruiting cytotoxic CD8+ T cells and NK cells into tumor tissues (Zumwalt et al., 2015) (**Fig. 7A**). In line with the increased chemokine expression, we detected higher frequencies of CD8+ DCs (CD11c+, CD11b-, CD8+) which are critical APCs in coordinating antitumor immune response by connecting innate to adaptive immunity, and higher frequencies of both cytotoxic T lymphocytes (CTLs) and NK cells which are key tumoricidal effector cells (**Fig. 7B**). The frequencies of CD4+ T cells were unaltered (**Fig. 7B**). Along with the high CTLs and NK cells infiltrates, these cells were characterized by higher IFN-γ production, demonstrating that they are not only recruited to the TME but also functionally active (**Fig. 7C**). In line with the inflamed TME created by the MLH1 deficiency, we also detected an upregulation of the genes encoding the cytotoxic effector molecules *Gzmb, Prf1, Ifng,* and *Tnf* (**Fig. 7D**), which mediate tumor cell killing (Cullen et al., 2010; Du et al., 2021). Importantly, the absence of STING in *Mlh1-/-* tumor cells abolished the dMMR-triggered inflammatory response and TILs recruitment (**Fig. 7A-D**). Thus, tumor cell-intrinsic STING signaling in dMMR tumors is critical to create an inflammatory and immunologically active TME and to induce productive antitumor immunity.

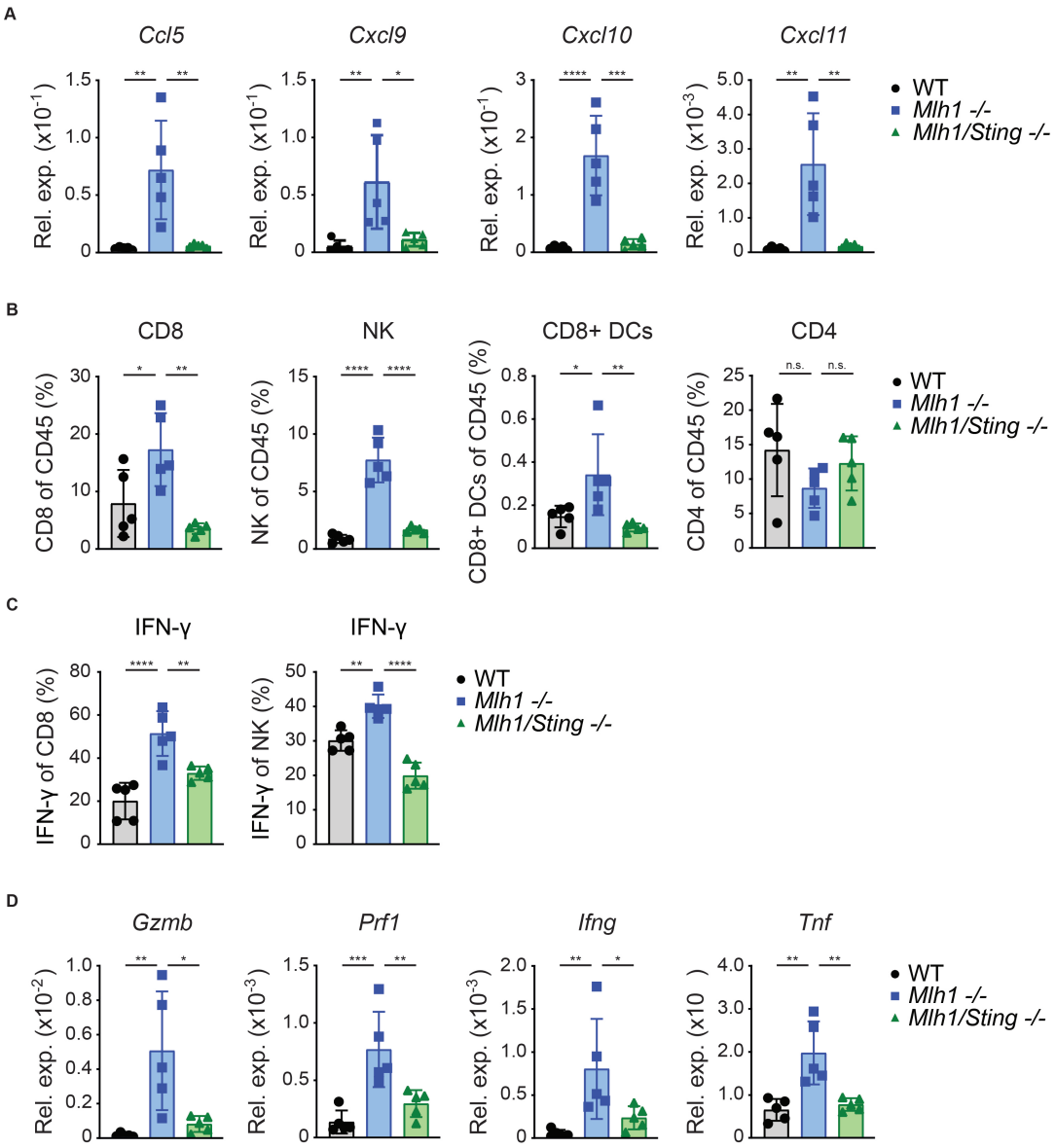

Fig. 7. STING signaling in dMMR CRC promotes antitumor immunity.

At the endpoint (Day 21), subcutaneously grown genetically modified MC38 tumors were explanted for FACS and qPCR analysis. (A) The relative gene expression of chemokines (*Ccl5, Cxcl9, Cxcl10, Cxcl11*) was quantified by qPCR. FACS analyses displaying (B) the percentages (CD8, NK, CD8+ DCs, CD4) of live/CD45+ cells and (C) the percentages (IFN-γ) of CD8+ cells and NK cells. (D) The relative gene expression of cytotoxic effector molecules (*Gzmb, Prf1, Ifng, Tnf*) was quantified by qPCR. One-way ANOVA was used to determine significance.

Given the essential role of type I IFNs in STING signaling, we further assessed the impact of type I IFN signaling in dMMR tumors *in vivo* by treating animals with blocking anti-IFNAR1 antibodies. MMR-deficient tumors that were treated with anti-IFNAR1 grew more aggressively, which highlights the essential role of type I IFN signaling in controlling dMMR tumors *in vivo* (**Fig. 8A**). Because CXCL10, a ligand for the chemokine receptor CXCR3, is an essential chemokine that recruits TILs to the TME (Zumwalt et al., 2015), we treated *Mlh1-/-* tumor-bearing mice with anti-CXCR3 antibodies. Remarkably, the anti-CXCR3 treatment also resulted in a more aggressive tumor growth of *Mlh1-/-* tumors, which indicates that chemotactic signals via CXCL10-CXCR3 are essential to drive antitumor immune responses (**Fig. 8B**). Taken together, these data show that type I IFNs via IFNAR1 and chemokine signals via CXCR3 control the tumor growth of dMMR tumors *in vivo*.

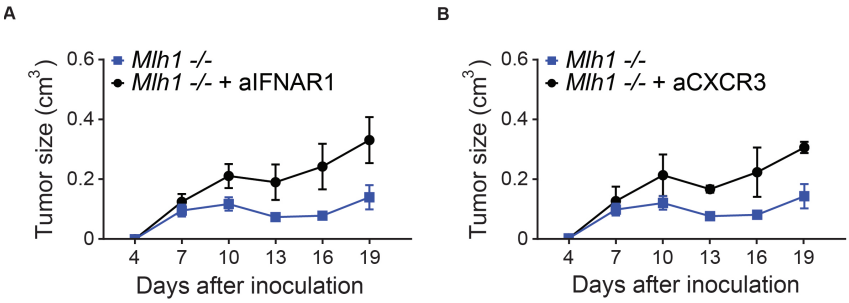

Fig. 8. The dMMR antitumor response requires IFNAR1 and CXCR3 signaling.

Growth of subcutaneously inoculated *Mlh1-/-* MC38 tumor cells in syngeneic WT C57BL/6 mice that were treated without or with (A) anti-IFNAR1 (200 µg/mouse) blocking antibodies or (B) anti-CXCR3 (200 µg/mouse) blocking antibodies every three days starting at Day 0 (n=3-5). The data are presented as the mean ± SEM.

2.4 A strategy to genetically enforce STING signaling in cancer cells

After establishing the importance of tumor cell-intrinsic STING signaling for the immunogenicity of dMMR tumor cells, we examined whether the induction of enforced STING signaling in “cold” pMMR cancer tissues would be sufficient to create a “hot” TME. As a strategy to genetically enforce STING signaling in MC38 tumor cells, we used the constitutively active STING variant ($STING^{N153S}$). This STING variant was originally isolated from patients suffering from the auto-inflammatory disease called SAVI (Liu et al., 2014; Luksch et al., 2019). After cloning the mutant STING sequence into retroviral vectors, we transduced $STING^{N153S}$ into pMMR MC38 cells and confirmed successful insertion by sequencing (**Fig. 9A**). $STING^{N153S}$-expressing pMMR MC38 tumor cells are hereafter termed “$STING^{N153S}$” and parental pMMR MC38 control cells are termed “WT” MC38 cells. To study the effects of $STING^{N153S}$ on gene expression, we performed RNA-seq. GSEA displayed that the introduction of $STING^{N153S}$ into pMMR tumor cells results in a prominent enrichment of IFN signaling signatures as represented by “IFN alpha/beta signaling” and “IFN signaling” (**Fig. 9B**). In line with type I IFN-induced signaling, we observed increased STAT1 phosphorylation when $STING^{N153S}$ is expressed, indicating cell-autonomous constitutive IFN signaling (**Fig. 9C**). STAT1 protein expression was also increased, which is known to be induced by IFN signaling in a feed-forward loop (Schneider et al., 2014). Furthermore, $STING^{N153S}$ induced strong expression of *Isg15*, which was greatly diminished upon pharmacological TBK1 inhibition (**Fig. 9D**). To translate this strategy to human CRC, we again used the organoids from our collaboration partner (Farin et al., 2023) and equipped the patient-derived pMMR CRC organoids with the $STING^{N153S}$ variant. Indeed, $STING^{N153S}$ also induced robust *ISG15* expression in human CRC (**Fig. 9E**). Taken together, the expression of $STING^{N153S}$ is sufficient to activate the IFN pathway in murine and human pMMR tumor cells.

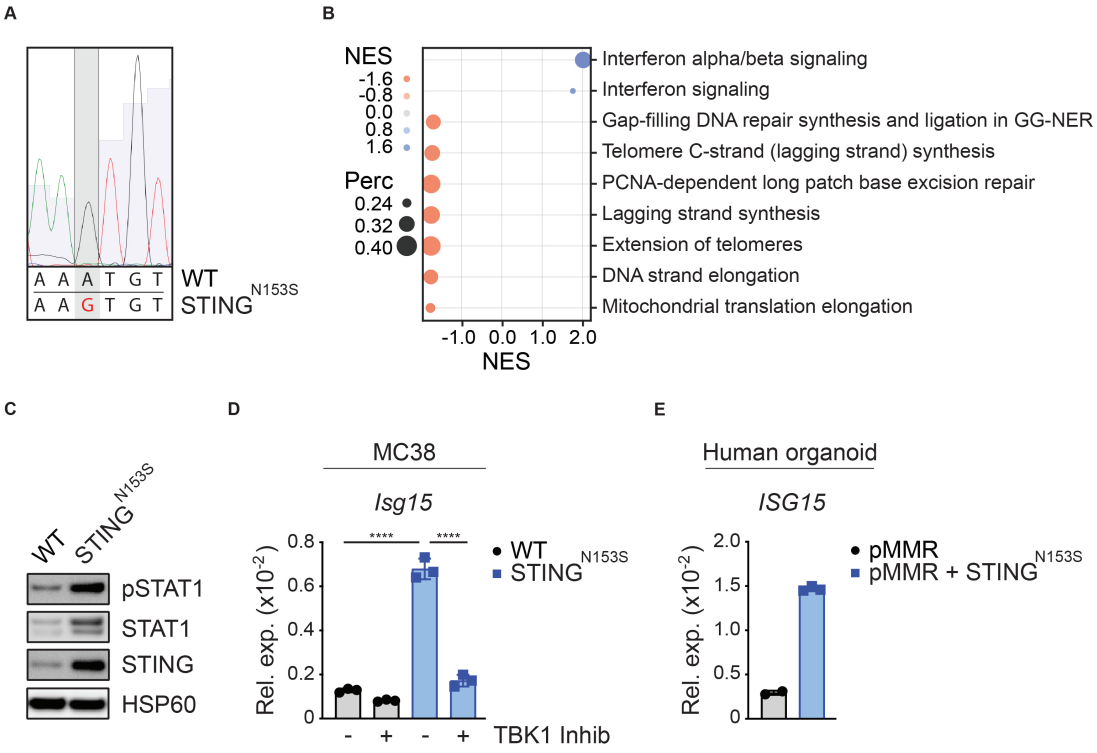

Fig. 9. Constitutively active STING^{N153S} drives IFN signaling in pMMR CRC.

(A) Electropherogram displaying the sequencing result of the PCR-amplified transgene STING^{N153S} from genomic DNA of MC38 tumor cells. (B) GSEA of RNA-seq data to identify differentially expressed gene sets of WT vs. STING^{N153S} MC38 tumor cells by using the Reactome database with a percentage cutoff >0.2 (+ve NES: STING^{N153S}). (C) Phosphorylation of STAT1 in cultured MC38 cells was detected by western blotting. (D) The relative gene expression of *Isg15* in cultured MC38 tumor cells 16 h after TBK1 inhibitor treatment was quantified by qPCR. (E) The relative gene expression of *ISG15* in pMMR and STING^{N153S}-transduced (=pMMR+STING^{N153S}) cultured primary organoids was quantified by qPCR. The data represent n=3 independent experiments (D) or n=2-3 technical replicates (E). One-way ANOVA (D) was used to determine significance. Normalized enrichment score (NES), percentage of genes contributing to the enrichment score (Perc). Validation of successful STING^{N153S} transgene insertion (A) was performed together with Sophie E. Isay as part of her Master`s thesis.

Following activation, STING drives type I IFN gene expression via TBK1 and IRF3. For the execution of this pathway, STING specifically requires serine phosphorylation at position 366 (S365 in mouse STING) (Liu et al., 2015). To test whether the STING^{N153S} mutation specifically triggered the observed IFN signaling effects, we next generated MC38 tumor cells that express the selective IFN-inactive STING mutant S365A in combination with the N153S mutant (STING$^{N153S/S365A}$) or the wild-type (WT) variant

(STING^{WT}). IFN-β production (**Fig. 10A**), STAT1 phosphorylation (**Fig. 10B**), and *Isg15* expression (**Fig. 10C**) triggered by the constitutively active STING^{N153S} mutant were completely abrogated in MC38 tumor cells that expressed the double mutant STING$^{N153S/S365A}$ and were also not induced by the STING^{WT} variant. Thus, STING^{N153S} specifically drives cell-autonomous IFN signaling in MC38 tumor cells.

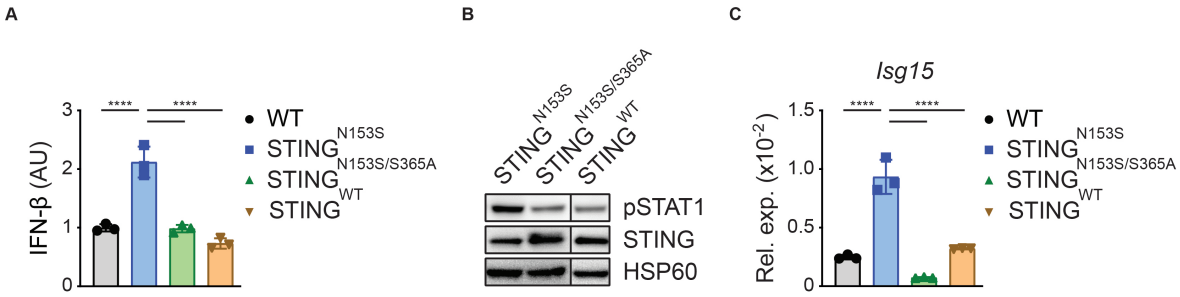

Fig. 10. STING^{N153S} specifically triggers STING-mediated IFN signaling.

(A) IFN-β production from STING-mutant MC38 tumor cells was quantified by ELISA. (B) The phosphorylation of STAT1 in cultured STING-mutant MC38 cells was detected by western blotting. (C) The relative gene expression of *Isg15* in cultured STING-mutant MC38 tumor cells was quantified by qPCR. The data are representative of n=2 independent experiments (A, C). One-way ANOVA (A, C) was used to determine significance.

2.5 Synthetically enforced STING signaling promotes antitumor immunity

After successfully establishing a murine tumor cell model that harbors a constitutively active STING^{N153S} variant, we next investigated the capacity of STING^{N153S} to induce immunogenic TMEs and stimulate antitumor immune responses in previously “cold” tumor tissues. For this, we subcutaneously injected parental WT or STING^{N153S}-expressing MC38 tumor cells into immunocompetent syngeneic C57BL/6 mice and monitored tumor growth. Similar to the effects observed with MMR deficiency (**see Fig. 6B**), enforced STING^{N153S} signaling in MC38 cells significantly reduced tumor growth *in vivo* (**Fig. 11A, 11B**). Notably, the proliferation rates of STING^{N153S}-transduced MC38 cells *in vitro* were similar to their WT counterparts (**Fig. 11C**). To test whether the expression of STING^{N153S} leads to immune-mediated growth inhibition *in vivo*, we next injected STING^{N153S}-transduced MC38 cells into immunocompromised NOD-

SCID mice that lack an intact lymphoid compartment (Hudson et al., 1998). In these animals, the STING^{N153S}-expressing MC38 tumors showed similar growth patterns to the WT MC38 tumors (**Fig. 11D**). This indicates that the control of STING^{N153S}-transduced MC38 cells in WT mice relies on the activation of lymphocytes.

To further inspect the role of STING^{N153S}-triggered IFN signaling in this immune-mediated growth inhibition, we injected STING$^{N153S/S365A}$ and STING^{WT}-transduced MC38 control cells into syngeneic WT C57BL/6 mice. In contrast to STING^{N153S}-expressing tumors, the tumor growth of STING$^{N153S/S365A}$ tumors was comparable to STING^{WT} tumors, which indicates that constitutively active STING^{N153S} signaling is specifically responsible for growth inhibition *in vivo* (**Fig. 11E**). *In vitro*, the different STING-mutant MC38 cells proliferated equally (**Fig. 11F**).

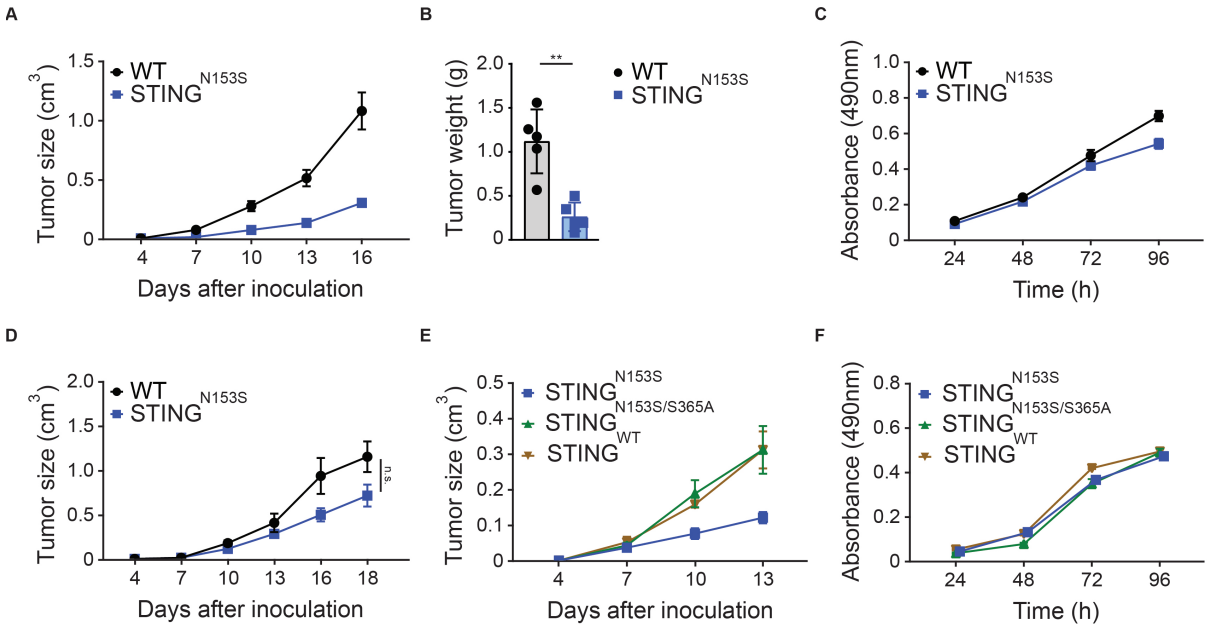

Fig. 11. Synthetically enforced STING^{N153S} signaling controls tumor growth.

(A) Growth of subcutaneously inoculated WT and STING^{N153S} MC38 tumor cells in syngeneic WT C57BL/6 mice (n=5). (B) Endpoint weight of subcutaneously grown tumors (n=5). (C) *In vitro* proliferation of cultured MC38 tumor cells. (D) Growth of subcutaneously inoculated WT and STING^{N153S} MC38 tumor cells in NOD-SCID mice (n=4). (E) Growth of subcutaneously inoculated STING-mutant MC38 tumor cells in syngeneic WT C57BL/6 mice (n=5). (F) *In vitro* proliferation of cultured STING-mutant MC38 tumor cells. The data are presented as the mean ± SEM (A, C-F). Student`s *t*-test was used to determine significance (B, D). Tumor growth experiment (A, B) was performed together with Sophie E. Isay as part of her Master`s thesis.

To further characterize how tumor cell-intrinsic STING^{N153S} modulates the immune-mediated tumor growth control, we next studied the TME of STING^{N153S}-expressing tumors using flow cytometry and gene expression analysis. In line with enforced IFN signaling in STING^{N153S}-transduced MC38 cells *in vitro*, we detected strong induction of the ISG marker gene *Isg15* in the TMEs of STING^{N153S}-transduced tumors *in vivo* (**Fig. 12A**). Moreover, the chemokine genes *Ccl5, Cxcl9, Cxcl10,* and *Cxcl11,* the products of which mediate CTL and NK cell recruitment into the tumor tissue (Bronger et al., 2016; Cao et al., 2021; Zumwalt et al., 2015), were strongly upregulated in the TMEs of STING^{N153S}-expressing tumor cells (**Fig. 12B**). Consistently, STING^{N153S}-expressing tumors contained increased frequencies of CTLs and NK cells (**Fig. 12C**). The frequencies of CD4+ T cells remained unaltered (**Fig. 12C**). Interestingly, these infiltrating CTLs in the TMEs of STING^{N153S}-expressing tumors were characterized by enhanced PD-1 expression and increased IFN-γ production compared to those of tumors formed by WT MC38 cells (**Fig. 12D**). This demonstrates that these CTLs are not only recruited to the TME but also activated in response to tumor cell-intrinsic STING^{N153S} signaling. In line with these findings, we also detected a strongly upregulated expression of the genes encoding the cytotoxic effector molecules *Gzmb, Prf1, Ifng,* and *Tnf* (**Fig. 12E**). Together, genetically enforced STING^{N153S} signaling in MMR-proficient tumor cells is by itself sufficient to shape an immune cell-infiltrated and immunologically active TME that exhibits the key requirements for productive antitumor immunity.

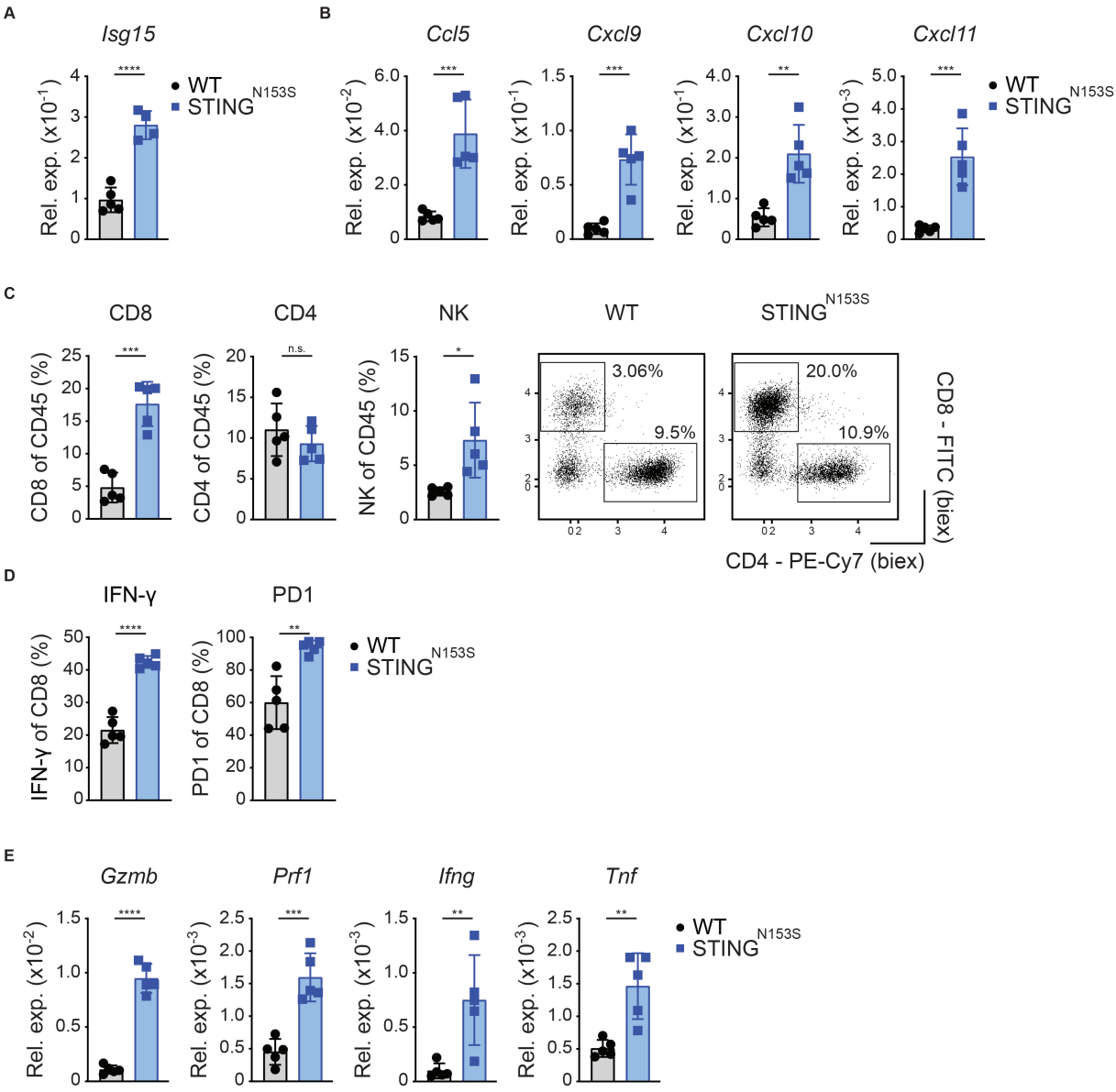

Fig. 12. Synthetically enforced STING^{N153S} signaling promotes antitumor immunity.

At the endpoint (Day 17), subcutaneously grown genetically modified MC38 tumors (n=5) were explanted for FACS and qPCR analysis. The relative gene expression of (A) ISGs (*Isg15*) and (B) chemokines (*Ccl5, Cxcl9, Cxcl10, Cxcl11*) was quantified by qPCR. (C, D) FACS analyses displaying (C) the percentages (CD4, CD8, NK) of live/CD45+ cells and representative dot plots, and (D) the percentages (IFN-γ, PD-1) of CD8+ cells. (D) The relative gene expression of cytotoxic effector molecules (*Gzmb, Prf1, Ifng, Tnf*) was quantified by qPCR. Student`s *t*-test was used to determine significance. Biexponential (biex). Gene expression analysis (A, B, E) was performed together with Sophie E. Isay as part of her Master`s thesis.

2.6 Tumor cell-intrinsic STING enforcement sensitizes to ICI therapy

To investigate whether the expression of STING^{N153S} in a subset of cancer cells is sufficient to sensitize the TME to ICI treatment, we mixed WT and STING^{N153S}-expressing MC38 cells prior to subcutaneous injection. Tumors that contained less than one-third of STING^{N153S}-expressing MC38 cells are hereafter termed "mixSTING^{N153S}", and pure WT MC38 tumors are termed "WT". When treated with isotype control antibodies, mixSTING^{N153S} tumors grew equally compared to WT tumors (**Fig. 13A**). However, upon ICI treatment with anti-PD-1 and anti-CTLA-4 inhibitors, mixSTING^{N153S} tumors exhibited significant tumor regression (**Fig. 13B, 13C**) and improved survival of the animals (**Fig. 13D**).

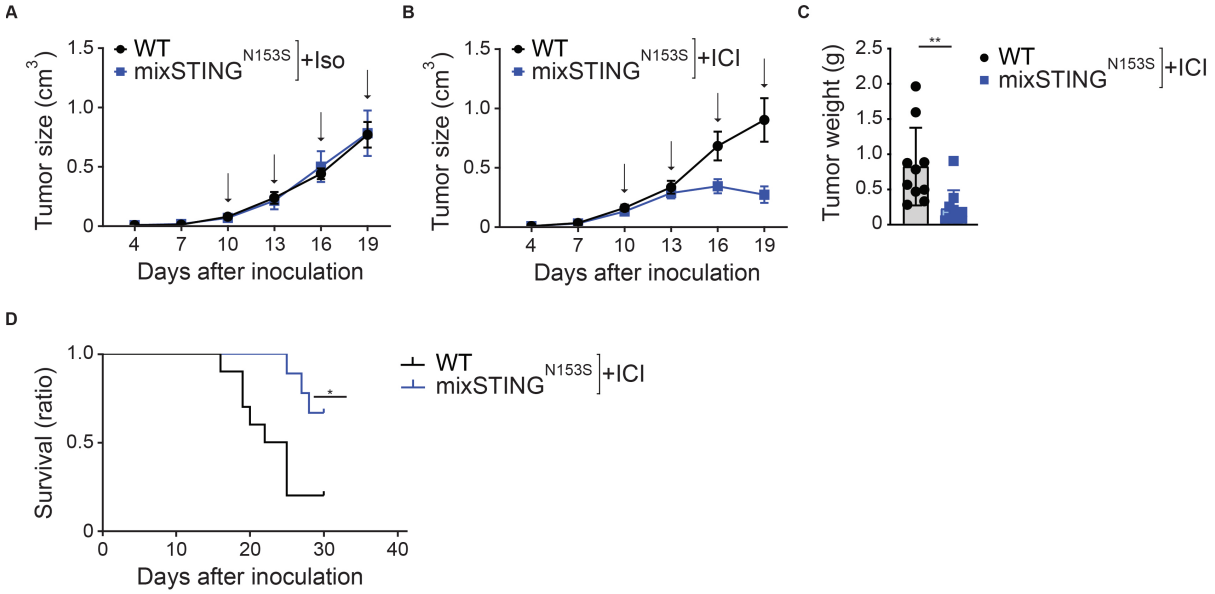

Fig. 13. Tumor cell-intrinsic STING^{N153S} sensitizes to ICI therapy.

Growth of subcutaneously inoculated WT vs. mixSTING^{N153S} MC38 tumors in syngeneic WT C57BL/6 mice (A) treated with isotype control (=iso) (n=4) or (B) treated with anti-PD-1/anti-CTLA-4 (=ICI) (n=8-10) every three days (black arrows). (C) Endpoint weight of subcutaneously grown tumors treated with ICI. (D) Survival of WT vs. mixSTING^{N153S} tumor-bearing mice treated with ICI therapy every three days starting on Day 10 (n=9-10). The data are presented as the mean ± SEM (A, B). Student`s *t*-test (C) or log-rank (Mantel-Cox) test (D) was used to determine significance.

We next studied the TMEs of the responsive mixSTING^{N153S} tumors by using flow cytometry and gene expression analysis (**Fig. 14A**). In these tumor tissues, we detected an enhanced inflammatory state which was characterized by increased expression of the genes encoding the TIL-attracting chemokines *Ccl5, Cxcl9, and Cxcl10* (**Fig. 14B**). Additonally, there was an increase in the frequencies of CD8+ DCs (CD11c+, CD11b-, CD8+), which are critical for tumor antigen cross-presentation and priming of CD8+ T cells against tumor antigens (Fuertes et al., 2011; Noubade et al., 2019) (**Fig. 14C**). Moreover, we observed an increased CTL infiltration, indicative of an enhanced antitumor immune response (**Fig. 14C**). However, there were no discernible differences in CD4+ T cell infiltration (**Fig. 14C**). An increased CTL infiltration was also observed in the dLNs (**Fig. 14D**). Consistent with productive DC and cytotoxic activity, the gene expression of *Il12,* encoding a DC-derived cytokine that shapes antitumor immunity, and *Ifng* was also significantly upregulated in the TME of mixSTING^{N153S} tumors (**Fig. 14E**). Taken together, genetically enforced STING^{N153S} signaling in a subset of tumor cells is sufficient to enhance ICI therapy responsiveness and this enhanced response is characterized by an intensified inflammatory state, increased infiltration of CD8+ DCs and CTLs, and up-regulation of key cytokines that shape the antitumor immunity.

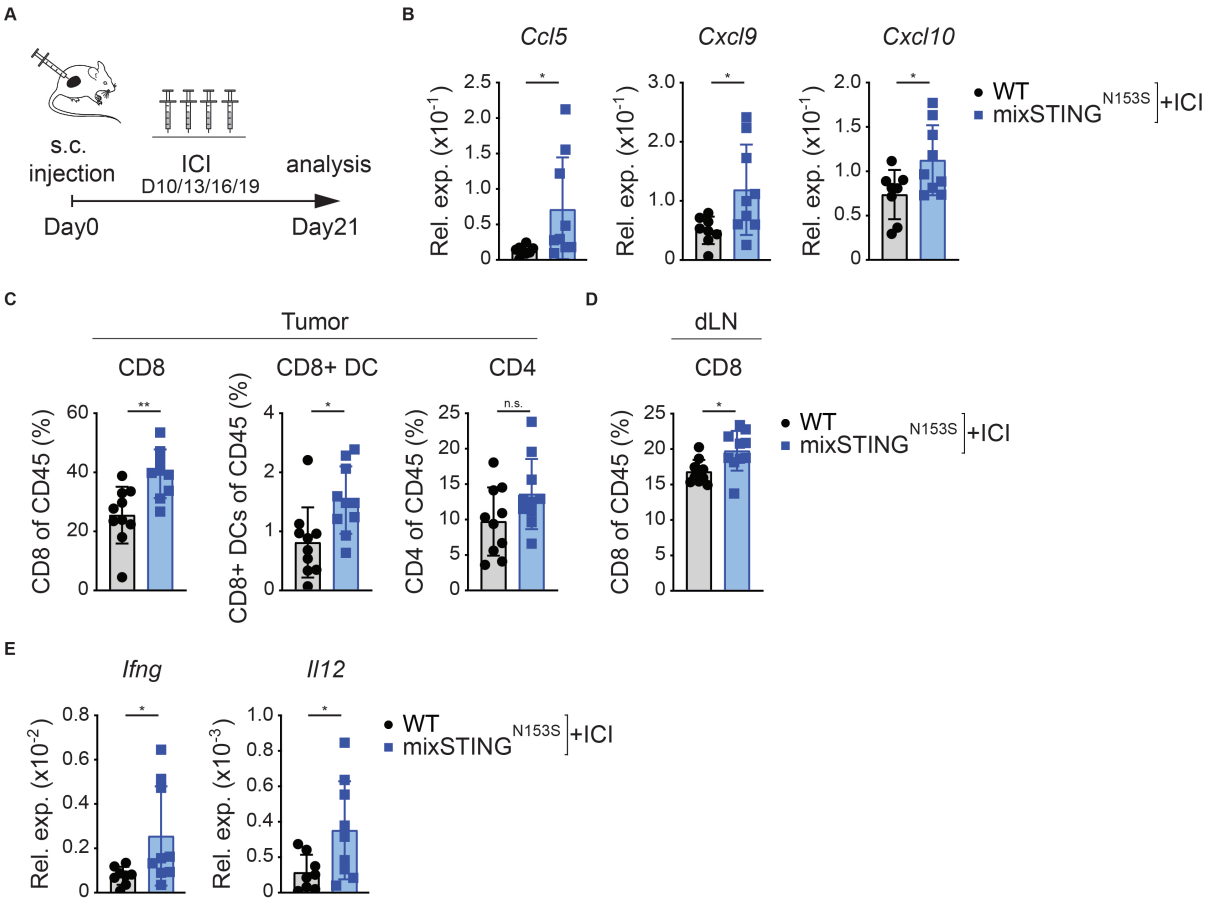

Fig. 14. Tumor cell-intrinsic STING^{N153S} enhances ICI therapy-mediated antitumor immunity.

(A) Schematic representation of the experimental setup *in vivo*. At the endpoint (Day 21), subcutaneously grown MC38 tumors that were treated with ICI therapy were explanted for FACS and qPCR analyses. (B) The relative gene expression of chemokines (*Ccl5, Cxcl9, Cxcl10*) was quantified by qPCR. FACS analyses displaying (C) percentages (CD8, CD8+ DCs, CD4) of live/CD45+ cells in the tumor and (D) percentages (CD8) of live/CD45+ cells in the draining lymph node (dLN). (E) The relative gene expression of cytokines (*Ifng, Il12*) was quantified by qPCR. Student`s *t*-test was used to determine significance.

2.7 Expression of STING^{N153S} in a subset of tumor cells reprograms the TME

To dissect the mechanisms by which synthetically enforced STING^{N153S} signaling sensitizes tumor tissues to ICI treatment, we analyzed the TME of mixSTING^{N153S} and WT MC38 tumors under equal growth conditions (**see Fig. 13A**). For this, we used cellular indexing of transcriptomes and epitopes by sequencing (CITE-seq) (Stoeckius et al., 2017). CITE-seq is a single-cell methodology that enables transcriptomic analysis of individual cells within complex tissues that are pretagged with barcoded antibodies directed against cellular markers. After labeling the cellular suspensions from growing tumors *ex vivo* with a custom-generated antibody panel, we performed an integrated TME analysis on a joint embedding computed by the variational autoencoder TotalVI (Gayoso et al., 2021). By clustering the cells in latent space using modularity maximization, we identified 16 cell population clusters in both TMEs based on gene expression and antibody-derived tag (ADT) abundance (**Fig. 15A, 15B**). Comparing the TMEs of mixSTING^{N153S} to WT tumors, we did not detect differences in the overall composition of either the CD45+ immune or CD45- nonimmune cell populations (**Fig. 15C, 15D**). This observation was further validated by FACS analysis and cellular staining of the TME for CD4 T cells (CD4+), CD8 T cells (CD8+), NK cells (NK1.1+), DCs (CD11c+) or CD8+ DCs (CD11c+, CD11b-, CD8+) (**Fig. 15E**).

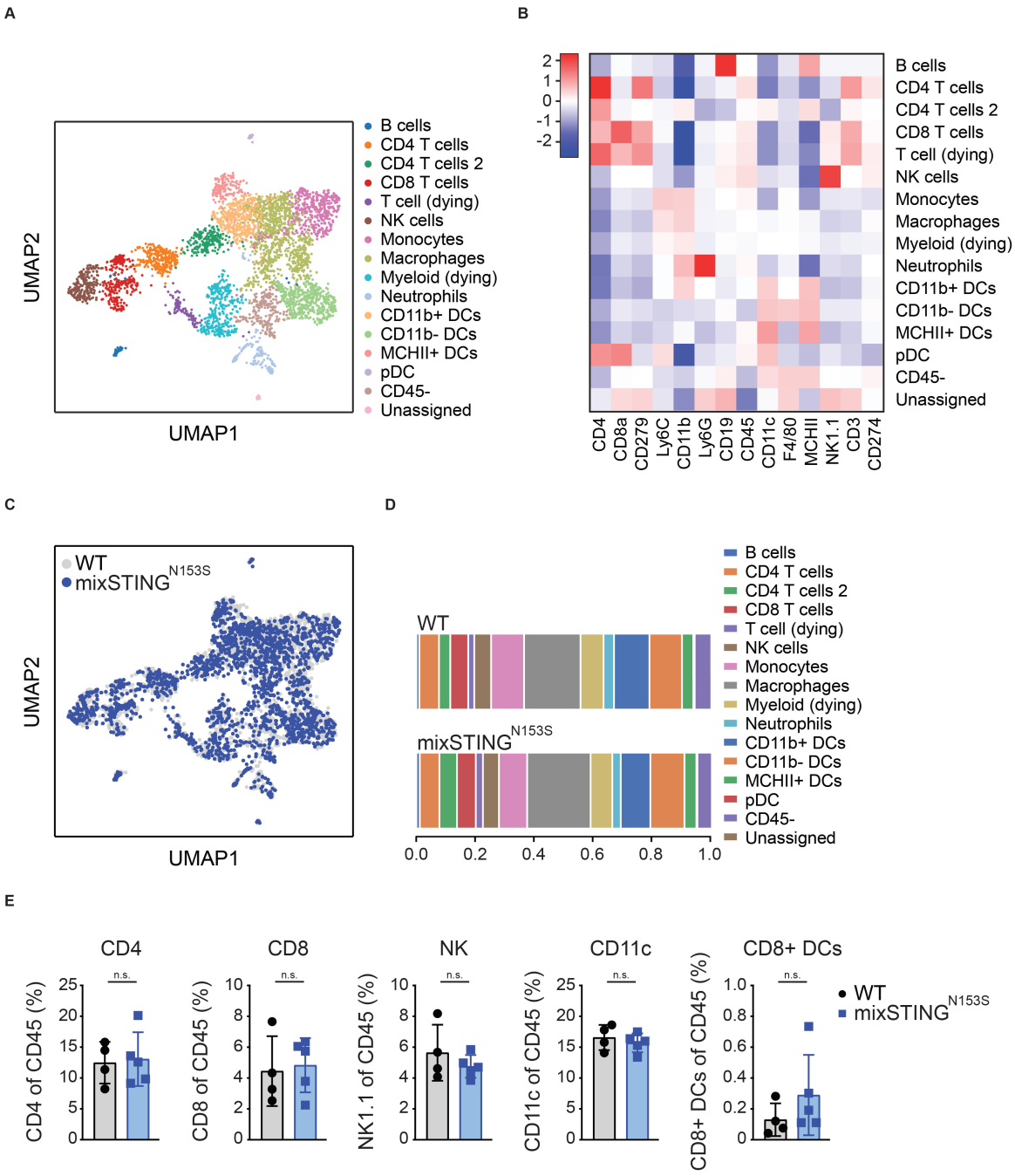

Fig. 15. STING^{N153S} expression in a subset of cancer cells does not alter the TME immune composition.

CITE-seq analyses of subcutaneously grown WT and mixSTING^{N153S} MC38 tumors. (A) UMAP plot of annotated clusters displaying the individual clusters. (B) Heatmap displaying the different cell clusters (y-axis) and the antigen intensity of the antibody-labeled cells (x-axis). (C) UMAP plot displaying the annotated clusters comparing the WT (gray) vs. mixSTING^{N153S} (blue) conditions. (D) Cellular composition of cell clusters in WT and mixSTING^{N153S} tumors. E) WT or mixSTING^{N153S} MC38 tumor cells were subcutaneously inoculated into syngeneic C57BL/6 mice, and the percentages (CD4, CD8, NK, CD11c, CD8+ DCs) of live/CD45+ cells in the tumor were quantified by FACS analysis (n=4-5). Student`s *t*-test was used to determine significance (E).

However, when we performed differential gene expression analysis on the tumor-infiltrating cells using diffxpy and gene set enrichment using g:profiler on the GO:BP database, we found enrichment of key antigen processing and presentation pathways, such as “processing and presentation of endogenous peptide antigens via major histocompatibility complex class I (MHCI),” as well as IFN signaling signatures like “response to IFN-β” and “response to IFN-γ,” specifically in the mixSTING^{N153S} tumors (**Fig. 16A**). To identify the cellular clusters contributing to these differential expression signatures, we next applied an eigengene score approach. Among the strongest contributors to the enhanced activation of antigen presentation and IFN signaling in the TMEs of mixSTING^{N153S} tumors were several types of APCs, including macrophages and subsets of DCs, such as MHC II+ DCs, CD11b+ DCs and pDCs, along with the CD45- nonimmune cells (**Fig. 16B**). Notably, the two DC clusters “MHC II+ DCs” and “CD11b+ DCs” exhibited particularly strong enrichment for antigen processing and presentation as well as IFN signaling (**Fig. 16C**). These cells represent APCs populations that are critical for the initiation of antitumor immunity. In conclusion, synthetic enforcement of STING^{N153S} signaling in a fraction of tumor cells is sufficient to reprogram the TME of originally “cold” tumors and sensitize these to ICI therapy.

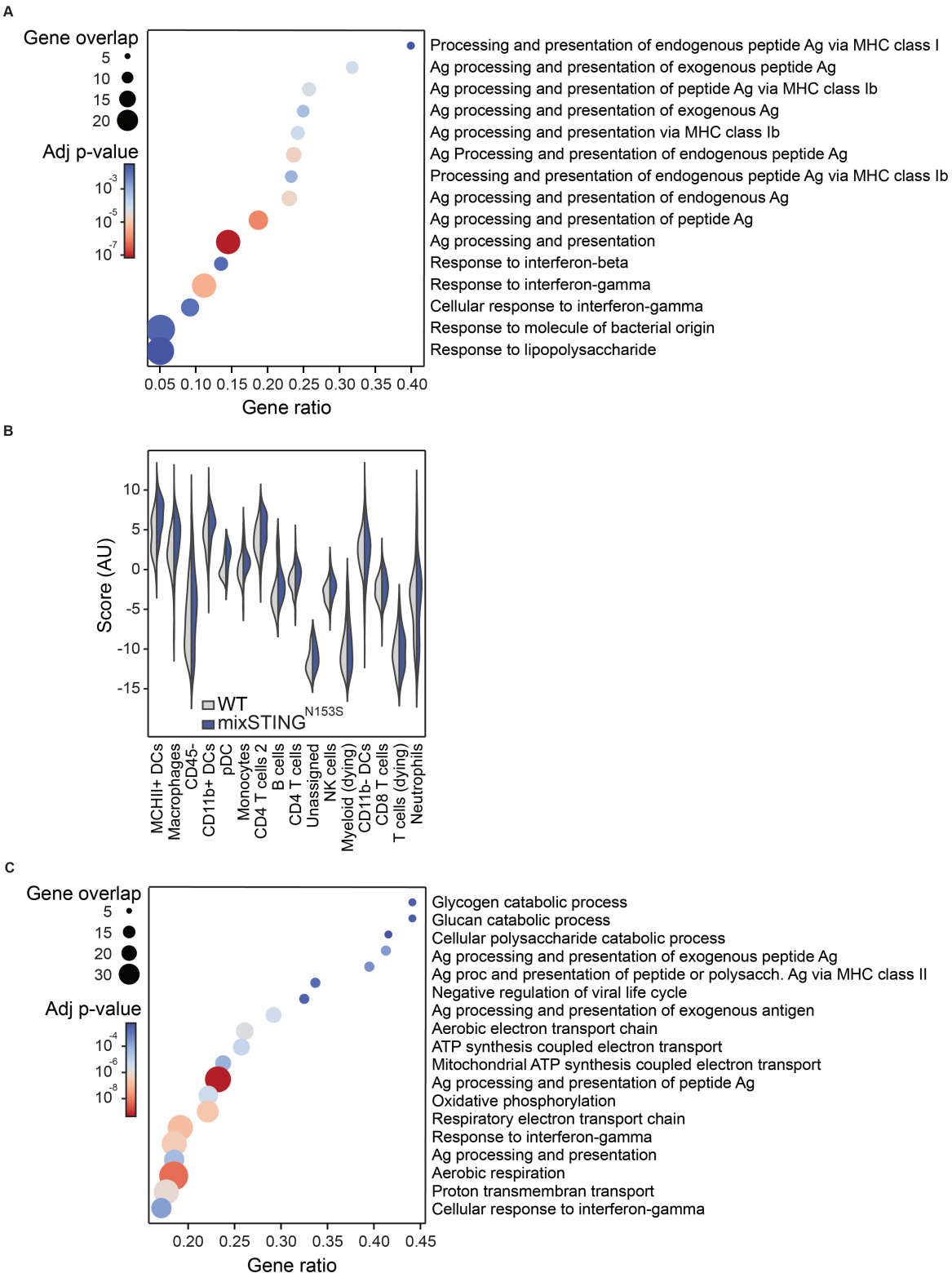

Fig. 16. STING^{N153S} expression in a subset of cancer cells induces inflammatory TME remodeling.

CITE-seq analyses of subcutaneously grown WT and mixSTING^{N153S} MC38 tumors. (A) Differentially expressed gene sets determined by GSEA by using g:profiler for all GO:BP terms enriched for fewer than 400 genes considering all clusters. (B) Violin plot displaying how strongly the different clusters

contribute to the differentially expressed genes observed in Fig. 16A. (C) Differentially expressed gene sets obtained by GSEA by using g:profiler on all GO:BP terms enriched for fewer than 400 genes considering only the DC clusters “MHCII+ DCs” and “CD11b+ DCs”.

2.8 STING^{N153S} sensitizes tumors to ICI therapy beyond CRC

Checkpoint inhibitors were initially approved by the FDA for melanoma (Hodi et al., 2010; Hoos et al., 2010). Although the response rates compared to standard chemotherapeutic regimens have greatly improved the therapy response rates, resistance or non-responsiveness remains a key challenge (Dhanyamraju and Patel, 2022). To test our novel strategy to sensitize tumors to ICI therapy beyond CRC, we next investigated the effects of synthetically enforced STING^{N153S} signaling on the ICI therapy responsiveness in melanoma. For this, we generated STING^{N153S}-expressing B16ova tumor cells (as done for MC38 tumor cells) (**Fig. 17A**). Similarly, we detected increased *Isg15* expression, which indicates that constitutively active STING drives IFN signaling in murine melanoma cells (**Fig. 17B**). Next, we used our well-established subcutaneous tumor model to monitor tumor growth of WT and STING^{N153S}-expressing tumor cells (**Fig 17C**). Without additional treatment, the two tumor conditions displayed equal growth, which indicates that the expression of STING^{N153S} was not sufficient to reject the tumors (**Fig. 17D**). Interestingly, however, when these tumors were treated with anti-PD-1 and anti-CTLA-4-blocking antibodies, those tumors that contained STING^{N153S}-expressing cells displayed significantly better responsiveness to ICI therapy (**Fig. 17E**) and improved survival of the animals (**Fig. 17F**) compared to animals bearing WT tumors. In conclusion, synthetically enforced STING^{N153S} signaling also enhances ICI therapy responsiveness in melanoma.

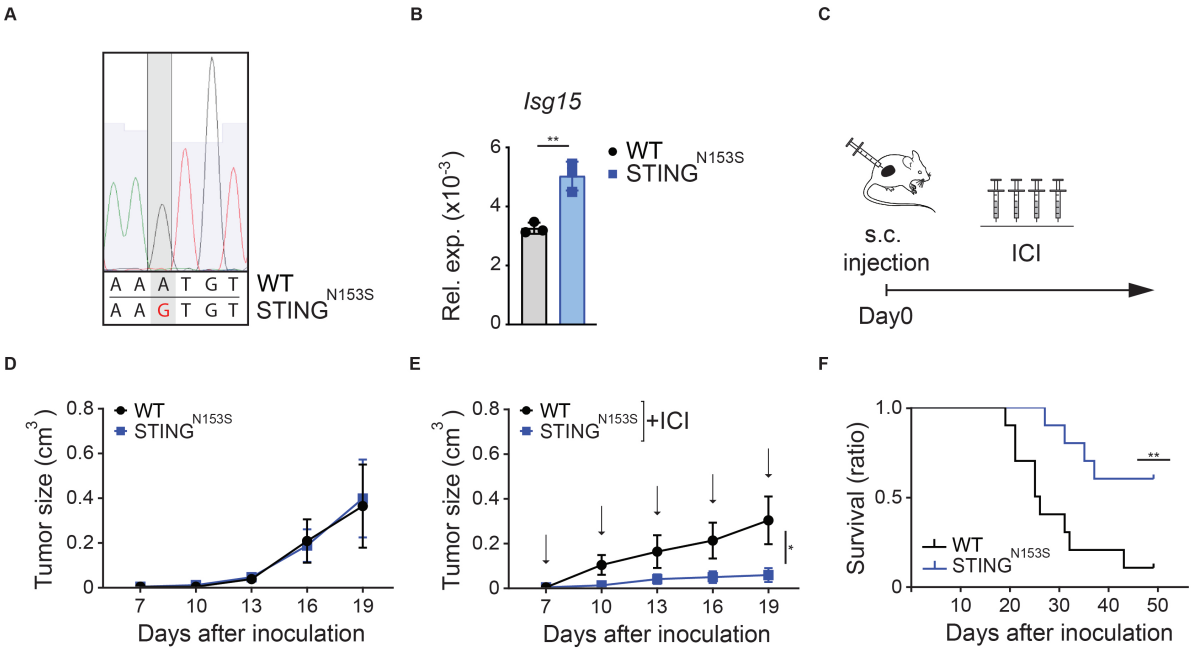

Fig. 17. Synthetically enforced STING^{N153S} signaling promotes ICI therapy responsiveness in melanoma.

(A) Electropherogram displaying the sequencing result of the PCR-amplified transgene STING^{N153S} from genomic DNA of B16ova tumor cells. (E) The relative gene expression of *Isg15* in WT vs. STING^{N153S} B16ova tumor cells was quantified by qPCR. (C) Schematic representation of the experimental setup in vivo. (D, E) Growth of subcutaneously inoculated WT vs. STING^{N153S} B16ova tumors in syngeneic C57BL/6 mice (D) without treatment (n=4) or (E) treated with anti-PD-1/anti-CTLA-4 (=ICI) (n=8-10) every three days (black arrows). (F) Survival of mice bearing WT vs. STING^{N153S} B16ova tumors that were treated with ICI therapy every three days starting on Day 7 after inoculation (n=10). The data represent n=3 independent experiments (B). The data are presented as the mean ± SEM (D, E). Student`s *t*-test (B, E) or Log-rank (Mantel-Cox) test (F) was used to determine significance.

3 Discussion

3.1 STING signaling in dMMR cancer cells

Defective MMR promotes the accumulation of unrepaired replication errors, leading to genome-wide mutations and a high mutational load (Germano et al., 2017; Poulogiannis et al., 2010). Interestingly, recent studies showed that DNA-damage-induced genomic instability can activate the cGAS-STING pathway by releasing DNA-containing micronuclei into the cytosol (Harding et al., 2017b; Mackenzie et al., 2017). By identifying immune-stimulatory pathways in dMMR CRC that could be responsible for their superior susceptibility to ICI, we demonstrate that dMMR tumors of CRC patients exhibit an enrichment in IFN and inflammatory cytokine signaling. Using human primary organoids of dMMR CRC patients, we show that dMMR triggers IFN engagement in an epithelial cell-intrinsic manner. Mechanistically, we provide evidence that defects in the MMR machinery result in an accumulation of DNA in the cancer cell cytosol, which stimulates the cGAS-dependent production of the second messenger cGAMP to trigger STING-mediated IFN signaling in cancer cells (**Fig. 18,** upper left side). These findings are in line with two independent studies that recently reported that dMMR in cancer cells engages STING signaling (Guan et al., 2021; Lu et al., 2021).

The exact mechanism of how defects in MMR couple to cGAS-STING signaling was further elucidated by Guan and colleagues (Guan et al., 2021). During mismatch repair, the MutSα and MutLα complex closely interacts with RPA, EXO1, Polδ, and LIG1 for mismatch recognition, DNA excision, DNA resynthesis, and gap ligation (Jiricny, 2006). Of note, MLH1 is reported to physically interact with EXO1 (Schmutte et al., 1998; Tishkoff et al., 1998; Tran et al., 2001) and to modulate its nuclease activity (Zhang et al., 2005). Guan and colleagues showed that loss of MLH1 results in more abundant and stable EXO1 at the DNA damage site, which leads to excessive DNA digestion (Guan et al., 2021). Under normal conditions, RPA protects the ssDNA generated through nuclease-mediated DNA excision (Bhat and Cortez, 2018; Maréchal and Zou, 2015). When MLH1 is missing, however, the abundance of ssDNA exceeds the capacities of RPA to protect the ssDNA, ultimately leading to the release of nuclear DNA into the cytosol. Taken together, defects in MMR proteins lead to DNA hyperexcision by EXO1 and RPA exhaustion, which collectively promotes the release

of DNA into the cytosol that triggers a cGAS-STING-dependent inflammatory response in cancer cells.

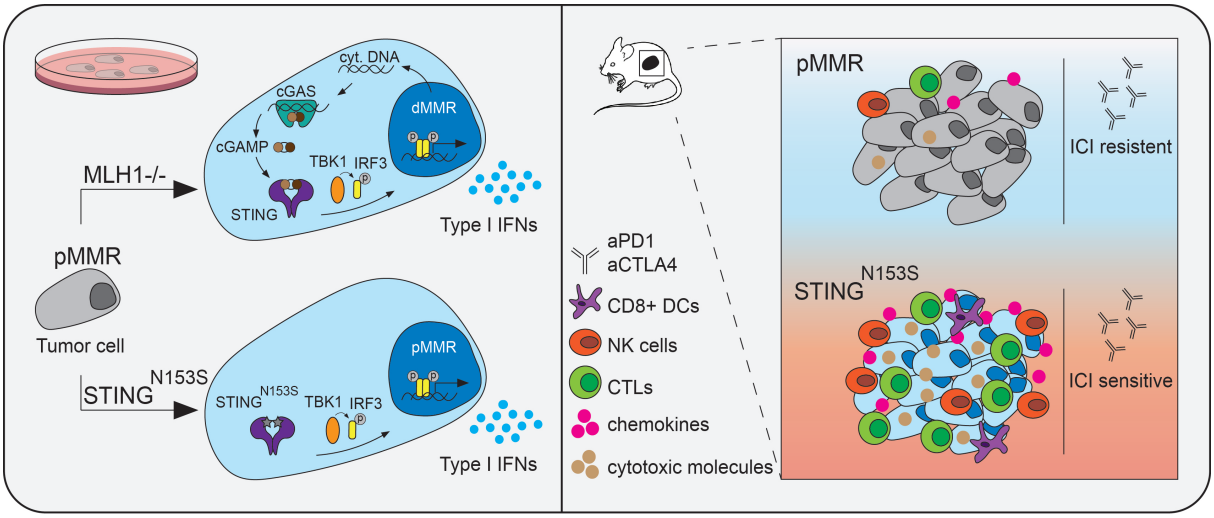

Fig. 18. Proposed model: Tumor cell-intrinsic STING signaling controls antitumor immunity and susceptibility to ICI therapy.

MMR deficiency leads to an accumulation of DNA in the cytosol (cyt. DNA), which is sensed by cGAS to activate STING-IFN signaling (left, upper arrow). Genetic enforcement of constitutively active $STING^{N153S}$ signaling in pMMR tumor cells leads to enhanced IFN expression even in the absence of cytosolic DNA danger signals (left, lower arrow). Synthetic enforcement of $STING^{N153S}$ signaling in tumor cells results in inflammatory remodeling of the TME and increased ICI therapy responsiveness (right).

3.2 STING shapes antitumor immunity and ICI therapy responsiveness in dMMR tumors

The activation of innate immune pathways is essential for mounting a coordinated antitumor immune response (Corrales et al., 2017). The presence of TILs in the tumor bed, the recognition of tumor antigens, and the tumoricidal activity of effector cells are prerequisites for successful tumor control. Until recently, it was suggested that dMMR controls the immunogenic potential of the tumor through genomic instability-driven neoantigen generation (Germano et al., 2017). Here, we report that tumor cell-intrinsic STING signaling is critical for controlling tumor growth and shaping an inflamed “hot” TME with productive antitumor activity, as loss of the cGAS-STING signaling axis

abolishes the anti-dMMR tumor immune responses. More specifically, MMR deficiency leads to increased expression of IFNs, cytokines, and chemokines in the TME. Moreover, cytotoxic effector cells such as CD8+ T cells and NK cells are not only more abundant but also show greater cytotoxic activity in dMMR tumors. Thus, loss of genomic integrity in cancer cells induces an antitumorigenic inflammatory TME via tumor cell-intrinsic STING activation. These findings are in line with a study from Lu and colleagues that recently also reported that MLH1-mutated CRC cells engage STING signaling to mediate antitumor immunity (Lu et al., 2021).

Immune cell trafficking toward the tumor environment is orchestrated by many messenger molecules, such as chemokines (Nagarsheth et al., 2017; Zumwalt et al., 2015). We found that the presence of STING in tumor cells of dMMR tumors was strictly necessary for the expression of TIL-attracting chemokines such as CCL5, CXCL9, CXCL10, and CXCL11. Moreover, blocking CXCR3 (receptor for CXCL9, CXCL10, and CXCL11) with anti-CXCR3 antibodies in dMMR tumor-bearing animals resulted in accelerated tumor growth, which supports the critical role of chemokine signaling in dMMR antitumor immunity. Interestingly, this finding is substantiated by another study that highlighted the importance of CCL5 and CXCL10 in controlling antitumor immunity in dMMR tumors (Mowat et al., 2020). Using dMMR tumor cells in an orthotopic tumor model, Mowat and colleagues showed that the recruitment and activation of CD8+ T cells into the dMMR tumors depends on the expression of *Ccl5* and *Cxcl10* (Mowat et al., 2020). Although not shown with a genetic model, these effects were suggested to be mediated by cGAS-STING-IFN signaling. Together, these data indicate that STING promotes the expression of key TIL-recruiting chemokines in the TME of dMMR tumors.

In line with the TIL-attracting chemokines, we found higher frequencies of CD8+ DCs in dMMR tumors, which was dependent on STING. CD8+ DCs are essential for tumor antigen cross-presentation, priming of T cells, and production of TIL-recruiting chemokines. Notably, IFNs are crucial for activating APCs and their antigen cross-presentation capacity towards CD8+ T cells (Fenton et al., 2021). In line with the effects of IFNs on APCs, Lu and colleagues showed that STING-IFN signaling in dMMR tumor cells controlled APCs-mediated cross-priming (Lu et al., 2021). More specifically, STING in dMMR tumor cells was relevant for optimal epitope-specific T cell

proliferation and cytokine production *in vitro*. Using mice that were conditionally deficient for the type I IFN receptor IFNAR1 in DCs (CD11c-Cre), they furthermore showed that the anti-dMMR tumor immunity *in vivo* was dependent on type I IFN signaling in APCs such as DCs. In line with these data, we also found that blocking IFNAR1 signaling with anti-IFNAR1 antibodies in dMMR tumor-bearing mice accelerated tumor growth, which implies a critical role for IFN signaling in dMMR antitumor immunity. With regard to the interaction of immune with tumor cells, we found higher frequencies of the tumor-killing CD8+ T cells and NK cells in the TME of dMMR tumors, which was dependent on STING. IFNs are also crucial for enhancing the cytotoxic activity of effector cells such as NK cells or CTLs (Fenton et al., 2021). Indeed, besides being more abundant, we also found that the CTLs and NK cells in the TME of dMMR tumors were more activated, as shown by the increased expression of the cytotoxic effector molecules GZMB, PRF1, IFN-γ, and TNF. This antitumor immune activity was dependent on tumor cell-intrinsic STING. Together, this demonstrates that STING-mediated IFN signaling is essential for recruiting effector cells into the TME of dMMR tumors and promoting antitumor activity by shaping APCs and T cell functionality.

Clinically, tumors with “hot” TMEs respond better to ICI therapy (Galon and Bruni, 2019; Herbst et al., 2014; Ochoa de Olza et al., 2020; Ribas et al., 2017). We demonstrate that tumor cell-intrinsic STING signaling is critical for creating immune-inflamed “hot” TMEs and promoting T cell-mediated cytotoxicity in dMMR tumors. Ultimately, this could modulate the success of immune checkpoint blockade in dMMR cancers. Indeed, the study by Lu and colleagues showed that STING controls the responsiveness toward ICIs in dMMR tumors (Lu et al., 2021). Interestingly, whereas the data from Germano and colleagues suggest that the enhanced immunogenicity and ICI responsiveness of dMMR tumors is due to increased generation of neoantigens (Germano et al., 2017), Lu and colleagues provided evidence for neoantigen independence by testing the ICI therapy responsiveness of dMMR tumors in an antigen-controlled system in which they equipped tumor cells with the ova peptide and used OVA-specific OT-I T cells that are only able to recognize the ova peptide on tumor cells (Lu et al., 2021). Taken together, the loss of genomic integrity in dMMR cancer cells induces an antitumorigenic inflammatory TME and promotes ICI therapy responsiveness via tumor cell-intrinsic STING activation.

3.3 Synthetically enforced STING signaling enhances ICI therapy responsiveness

Based on these insights that STING signaling in dMMR tumors controls ICI therapy responsiveness, we envisioned that synthetically enforced STING signaling within tumor cells might be sufficient to create “hot” TME niches in originally “cold” pMMR tumor tissues. Our strategy to genetically enforce STING signaling in MMR-competent cancer cells was guided by gain-of-function mutations within the STING molecule that were originally identified in the germline of SAVI patients who suffer from massive systemic inflammatory disorders that can lead to premature death (Liu et al., 2014). These SAVI-STING variants are characterized by point mutations near the STING dimerization site, which puts the molecule into a constitutively active state that induces TBK1 downstream signaling (Liu et al., 2014).

Ectopic expression of gain-of-function $STING^{N153S}$ was sufficient to induce cell-autonomous STING signaling in both murine colon cancer cells and human CRC organoids, even in the absence of MMR deficiency (**Fig. 18,** lower left side). Furthermore, $STING^{N153S}$-expressing cancer cells created “hot” TMEs *in vivo* that are characterized by excessive expression of ISGs such as *Isg15* and genes encoding TIL-recruiting chemokines such as *Ccl5, Cxcl9, Cxcl10,* and *Cxcl11,* as well as strong infiltration of activated CTLs and NK cells with expression of activation markers such PD-1 and cytotoxic effector molecules such as Gzmb, Prf1, Ifn-γ, and Tnf. Thus, synthetically enforced $STING^{N153S}$ signaling in cancer cells is sufficient to induce the inflammatory cues needed to recruit and prime CTLs in the tumor tissue, even without a hypermutator phenotype (**Fig. 18,** right side). Consistently, $STING^{N153S}$-expressing tumors are rejected in immunocompetent but not in immunodeficient mice. In light of the differential activation of the downstream pathways IFN, autophagy, cell death, or NF-κB signaling of STING by different cell types (e.g., myeloid vs. lymphoid cells) (Wu et al., 2020; Yamashiro et al., 2020), we furthermore equipped tumor cells with the IFN-inactive $STING^{N153S/S365A}$ mutant and thereby showed that $STING^{N153S}$ specifically triggered STING-IFN mediated antitumor immunity.

Characterization of the TME by single-cell analysis demonstrated that introducing constitutively active $STING^{N153S}$ into only a subset of cancer cells already induces inflammatory remodeling of the TME. This remodeling includes changes in gene

expression signatures within defined immune cell subpopulations that indicate upregulated APCs functionality and antigen processing in DCs. These are critical for tumor antigen cross-presentation and coupling innate to adaptive immunity. Consistently, tumors containing STING^{N153S}-expressing cancer cells were sensitized to ICI therapy and displayed superior antitumor immune responses upon anti-PD-1 and anti-CTLA-4 treatment. The TME of these tumors showed increased frequencies of DCs and enhanced expression of *Il12, Ccl5, Cxcl9*, and *Cxcl10*, increased CTLs, and increased expression of *Ifng*. Since effective ICI responses require a productive DC:T cell interaction (Garris et al., 2018), our data provide proof of concept that synthetically enforced STING^{N153S} signaling in tumor cells promotes APCs:CTL crosstalk in the TME. This crosstalk is characterized by IFN-induced APCs activation, the production of TILs-attracting chemokines and cytokines, and CTL priming. Collectively, this indicates that this strategy could be further explored as a therapeutic concept to sensitize tumor tissue to ICI. While our study was triggered by the observation that STING signaling in dMMR CRC promotes antitumor immunity, it is conceivable that genetically enforced STING^{N153S} signaling could also sensitize cancer tissues beyond CRC, such as melanoma or lung cancer.

Interestingly, genomic instability correlates with ICI therapy benefits in lung cancer and melanoma (Rizvi et al., 2015; Snyder et al., 2014). Compared to standard chemotherapeutic regimens, ICI therapies have greatly improved the response rates in these tumor entities (Ma et al., 2023). However, low immunogenicity, lack of pre-existing CD8+ T cells in the TME, or loss of STING in the tumor cells still critically impedes ICI therapy responsiveness (as discussed above). To test our novel strategy to sensitize ICI non-responsive tumors, we synthetically enforced STING^{N153S} signaling in the melanoma cell line B16ova. Indeed, ectopic expression of the constitutively active STING^{N153S} variant induced IFN signaling *in vitro* and significantly increased the ICI therapy responsiveness of animals harboring STING^{N153S} tumors, ultimately improving survival. The critical role of tumor STING in ICI therapy responsiveness is supported by another study in which radiation-induced STING signaling in melanoma cells was essential for mediating maximal ICI therapy-driven abscopal antitumor immune responses (Harding et al., 2017b). This suggests that tumor cell-intrinsic STING-mediated inflammatory signals are essential in promoting sensitivity towards

ICI therapy (**Fig. 18**). Together, these findings provide a rationale for harnessing STING activity as a therapeutic ICI sensitizer.

3.4 Synthetically enforced STING signaling: a therapeutic strategy to sensitize tumors to ICI

DNA-damaging tumor therapies such as radiation, cisplatin chemotherapy, topoisomerase II inhibitor (e.g., etoposide), or PARP inhibitor (PARPI) treatments generate cytosolic DNA, which creates inflammatory milieus and promotes antitumor immunity via the cGAS-STING pathway (Kwon and Bakhoum, 2020; Le Naour et al., 2020). Given the immune stimulatory capacity of STING, much effort has been put into developing clinically usable STING agonists (Flood et al., 2019; Motedayen Aval et al., 2020; Su et al., 2019a). Although various preclinical, phase I, and phase II clinical studies are testing new and ever more refined STING agonist designs and formulations, no candidate agent has made it to phase III clinical trials yet (Le Naour et al., 2020; Motedayen Aval et al., 2020). Some shortcomings are systemically uncontrolled inflammation and cytokine storm, T cell toxicity, or targetability due to STING downregulation or different STING haplotypes (Motedayen Aval et al., 2020).

Our strategy of TME reprogramming via synthetically enforced STING signaling in cancer cells could offer several advantages over current TME-modulating approaches that inject small-molecule STING agonists *in vivo* (Flood et al., 2019; Motedayen Aval et al., 2020; Su et al., 2019b). On the one hand, systemic injections of STING agonists frequently have nonnegligible side effects due to rapid dissemination in the bloodstream, resulting in a massive induction of inflammatory cytokines with cytokine storm syndromes (Barber, 2015; Motedayen Aval et al., 2020). Furthermore, small-molecule STING activators exert unwanted side effects on immune effector cells, including CD8+ T cells, in which STING signaling blocks proliferation and induces apoptosis, which disables CTL function (Cerboni et al., 2017; Gulen et al., 2017; Larkin et al., 2017; Wu et al., 2020) or results in the recruitment of suppressor cells and upregulation of inhibitory molecules such as PD-L1 that impedes the antitumor immune response (Ahn et al., 2014; Lemos et al., 2016; Liang et al., 2017). On the other hand, endogenous STING in tumor cells is frequently downregulated or inhibited (Konno et

al., 2018; Song et al., 2017; Xia et al., 2016b, 2016a), resulting in inadequate pharmacological targetability by small molecules. These mentioned difficulties are exemplary reasons illustrating that although there are constantly new small-molecule STING agonist formulations being developed and tested, their success is limited to early-phase clinical trials since there are no Phase III trials that have been launched yet (Le Naour et al., 2020; Motedayen Aval et al., 2020). Our concept of synthetically enforcing STING signaling selectively in tumor cells could, in principle, overcome these hurdles.

For clinical translation, several key points need to be addressed. The most important next step is the development of an effective protocol for STING gene transfer encoding a constitutively active variant into the tumor cells of patients. One possibility is the isolation of cancer cells from tumor biopsies, *ex vivo* manipulation, and reinjection of engineered STING-expressing cells into the tumor tissues. Alternatively, gene transfer protocols based on viral vectors such as oncolytic viruses (OVs) (Lawler et al., 2017), mRNA (Hotz et al., 2021; Tse et al., 2021), or cell-directed lipid nanoparticles (LNPs) (Miao et al., 2019; Rurik et al., 2022) could be used to express constitutively active STING variants in tumor cells *in vivo*. OVs are promising immunotherapeutic agents that induce selective tumor cell killing and trigger antitumor immunity (Lawler et al., 2017). OVs enter tumor cells via receptor-mediated mechanisms and replicate well in the rapidly dividing tumor cells. In 2015, the OV talimogene laherparepvec (T-VEC), which is an attenuated oncolytic HSV-1 that encodes human granulocyte-macrophage colony-stimulating factor (GM-CSF), gained FDA approval for use in melanoma (Ott and Hodi, 2016). Besides herpesviruses, several other virus stains (e.g., adenoviruses, Vaccinia viruses) are currently tested for immunotherapeutic applications (Lawler et al., 2017). Thus, OVs could be used to deliver the STING^{N153S} transgene into tumor cells. When it comes to mRNA vaccines, they are non-infectious, there is no anti-vector immunity, and they can be administered repeatedly (Pardi et al., 2018). Based on the potent immune responses triggered by mRNA vaccines, there have been efforts to deliver cytokine-encoding mRNA as a treatment for cancer (Hotz et al., 2021) or using mRNA-encoded signaling molecules as genetic adjuvant (Tse et al., 2021). Thus, STING^{N153S} could be encoded as mRNA. Finally, LNPs are nanoparticles composed of lipids and have evolved as competent vehicles for the delivery of a variety of agents, such as chemotherapeutics, small molecules, and nucleic acid therapeutics (Han et

al., 2023). Most recently, LNPs have become particularly interesting for their use in combination with mRNA as LNP-based mRNA vaccines. In the context of boosting antitumor immunity, LNPs are used to deliver mRNA encoding tumor antigens, antigen receptors, adjuvant factors, or therapeutic cytokines and antibodies (Han et al., 2023). Thus, LNPs could be used as a vehicle to deliver STING^{N153S}, for example, encoded as mRNA. Taken together, because selective activation of STING signaling in cancer cells is sufficient to reprogram the TME and enhance ICI responsiveness, the delivery of constitutively active STING variants is a promising TME-modulating strategy to combine with ICI therapy and hopefully provides additional clinical benefits for cancer patients.

3.5 Conclusion and Outlook

The development of ICIs revolutionized cancer therapy and brought survival benefits to patients. In particular, dMMR CRC patients exhibit much better responsiveness to ICI therapy than pMMR CRC patients (Le et al., 2015). By exploring mechanisms that promote superior antitumor immunity in dMMR CRC, we mechanistically found that defects in the MMR machinery lead to tumor cell-intrinsic cGAS-STING mediated IFN responses *in vitro*. Furthermore, STING signaling was strictly necessary for shaping an inflamed “hot” TME with productive antitumor immunity in dMMR tumors *in vivo*.

Aiming to develop strategies to selectively enhance these STING-mediated antitumor immune responses, which could enhance the susceptibility of immunologically “cold” and ICI-insensitive tumors to ICI therapy, we equipped pMMR tumor cells with a constitutively active $STING^{N153S}$ variant. We showed that genetically enforced $STING^{N153S}$ signaling in pMMR tumor cells was sufficient to induce potent IFN signaling *in vitro*, even without a genome instability-driven ligand. Furthermore, $STING^{N153S}$ expression was sufficient to create an inflammatory and immunological “hot” TME and to sensitize the tumor to ICI therapy. More specifically, we provide proof of principle evidence that synthetically enforced STING signaling in tumor cells potently shapes APCs and T cell functionality in the TME by IFN-induced APCs activation, production of TILs-attracting chemokines and cytokines, and CTL priming.

Collectively, these findings provide a rationale for modulating tumor cell-intrinsic pathways by synthetically enforcing STING signaling as a therapeutic concept to sensitize tumors to ICI therapy. For clinical translation, several aspects, such as developing an effective protocol for STING gene transfer encoding a constitutively active variant into the tumor cells of patients, need to be addressed. This, however, remains the subject of further scientific investigation.

4 Methods

4.1 Human COADREAD samples (TCGA)

Clinical and mutation analysis data for the Colorectal Adenocarcinoma TCGA PanCancer Atlas dataset (https://pubmed.ncbi.nlm.nih.gov/29596782/) were downloaded via the cBioPortal for Cancer Genomics (https://pubmed.ncbi.nlm.nih.gov/22588877). In total, 524 tumor samples with complete clinical and mutation calling information were available (as of February 2020). Mutation calls for the four genes *MLH1, MSH2, POLE,* and *POLD1* were used to assign each tumor sample to one of two categories: mismatch repair-proficient (pMMR), with WT *MLH1, MSH2, POLE,* and *POLD1,* and mismatch repair-deficient (dMMR), with at least one mutation in *MLH1, MSH2, POLE,* or *POLD1* (Vornholz et al., 2023). The mutations considered were missense, nonsense (premature stop codon), frameshift insertion or deletion, in-frame deletion, and splice-site mutations. The tumor sample mutation counts reported by TCGA were normalized to a human whole-exome size of 30 Mbp and reported as the mutation count per Mbp. For the same 524 tumor samples, the gene expression values for 20,531 genes obtained by RNA-seq were downloaded via cBioPortal. The siggenes R package (version 1.72.0) was used to identify genes differentially expressed between dMMR and pMMR tumors. The differentially expressed genes were ranked by their fold change, and the ranked gene list was used as input for a pre-ranked GSEA using the fgsea R package (version 1.18.0) against the Reactome gene sets of the MSigDB database (version 7.4) as available in the msigdbr R package (version 7.5.1). Reactome gene sets with an adjusted $p \leq 0.05$ were plotted in a bubble chart, with one bubble representing one gene set. The bubble color depicts the normalized enrichment score (NES), while the bubble size depicts the fraction (Perc) of the number of leading-edge genes as reported by fgsea over the number of total genes in the gene set.

4.2 Mice

All animal work was conducted in accordance with German Federal Animal Protection Laws and approved by the government of Upper Bavaria (Regierung von Oberbayern, Munich, Germany). For murine tumor transplantation experiments, C57BL/6 mice were purchased from Charles River (CR), and NOD-SCID mice were purchased from the

Jackson Laboratory (JAX stock #001303). Female 6- to 8-week-old mice were used for experiments. Tumor size was measured with an electronic caliper every three days and calculated by the following formula: $V= (W^2*L)/2$, where W is the width (minor tumor axis), and L is the length (major tumor axis). Mice were assessed by their general behavior, outer appearance, body condition (BC) parameters, and body weight.

4.3 Cell culture

The mouse colon adenocarcinoma cell line MC38 was kindly gifted by Bavarian Nordic and cultured in DMEM (Gibco: 41966-029) containing 10% FCS, 1% penicillin/streptomycin (P/S), 1% sodium pyruvate (SP), 1% nonessential amino acids (NEAA), 2% HEPES and 0.05 mM b-mercaptoethanol (bME). The colon carcinoma cell line CT26 (CRL-2638) was purchased from ATCC and cultured in RPMI-1640 glutamax medium (Gibco: 61870-010) containing 10% FCS, 1% P/S, 1% SP, 1% HEPES, 4.5g/L glucose. The ova-expressing mouse melanoma cell line B16ova (Rosenbaum et al., 2019) was cultured in RPMI-1640 glutamax medium containing 10% FCS and 1% P/S. Phoenix-Eco cells and HEK-293T cells were cultured in DMEM (Gibco: 41966-029) containing 10% FCS, 1% P/S, 1% NEAA, and 1% SP. Organoid lines (Farin et al., 2023) were maintained in complete tumor expansion medium as described previously (Schnalzger et al., 2020). All cells were cultured under standard cell culture conditions at 37 °C in 5% CO_2 and 95% humidity. Cells were routinely tested for mycoplasma contamination.

4.4 Tumor experiments and treatments

MC38 ($0.5x10^6$) and B16ova ($0.5x10^5$) tumor cells (mixed 1:1 in PBS:Matrigel (Corning)) were injected subcutaneously into the flanks of the recipient mice. For MC38 tumors, tumor-bearing mice were treated with 250 µg anti-PD-1 (clone RPM1-14)/200 µg anti-CTLA-4 (clone 9H10) (both BioXCell) and for B16ova tumors with 100µg anti-PD-1/100 µg anti-CTLA-4 or equal quantities of the respective isotype controls rat IgG2a (clone 2A3)/polyclonal syrian hamster IgG (both BioXCell) by intraperitoneal administration. The mice were treated every three days. For anti-IFNAR1 and anti-CXCR3 inhibitor experiments, tumor-bearing mice were treated without or with 200 µg/mouse anti-IFNAR1 (clone: MAR1-5A3; BioXCell) or 200

µg/mouse anti-CXCR3 (clone: CXCR3-173; BioXCell) every three days starting on Day 0 after inoculation.

4.5 Gene editing

To generate KO cell lines, single guide RNA sequences were designed using the CRISPR tool (http://crispr.mit.edu), cloned into the CRISPR/Cas9 system plasmids pSpCas9(BB)-2A-Puro (PX459) (gift from Feng Zhang, Addgene plasmid #62988) or pSpCas9(BB)-2A-Neo (gift from Ken-Ichi Takemaru, Addgene plasmid #127762) and transfected into MC38 tumor cells with Lipofectamine™ 3000 (Thermo Fisher Scientific). After 24 h, transfected cells were selected with the respective antibiotic for 3-5 days and subsequently seeded in 96-well plates at one cell per well. Expanded cells were then harvested, and KO was validated by western blotting.

Target	**sgRNA sequence**
MLH1	GATGGTCCGTACGGACTCCC
cGAS	CGAGGCGCGGAAAGTCGTAA
STING	GTACCCAATGTAGTATGACC

4.6 Retroviral modification of murine tumor cells and human organoids

Mouse STING^{N153S}, STING$^{N153S/S365A}$, and STING^{WT} cDNA variants were cloned into the MSCV-puro vector (a gift from Tyler Jacks, Addgene plasmid #68469), and the pMSCV-blasticidin vector (a gift from David Mu, Addgene plasmid #75085) using standard cloning techniques. MC38 and B16ova tumor cells were transduced with STING cDNA variant-containing vectors. Retroviral particles were produced with the Phoenix-Eco packaging cell line. Supernatants were collected 48 h after transfection, filtered through a 0.45 µm filter, and used fresh or frozen at -80 °C. Cells were infected with the virus in the presence of protaminsulfat (Sigma–Aldrich). Thereafter, cells with stable expression were selected by the addition of 5 µg/ml puromycin (Invivogen) or 25 µg/ml blasticidin (Invivogen) to the culture medium. The organoid lines (Farin et al., 2023) were transduced with MSCV-puro-STING^{N153S} or as a control with pMSCV-FLIP-puro-dsRed-GFP-miRNA (gift from Bon-Kyoung Koo, Addgene Plasmid # 32704).

Retroviral vectors were packaged in HEK-293T cells using pcDNA3.MLVgp (Schambach et al., 2006) and pCMV-VSV-G (gift from Bob Weinberg, Addgene plasmid # 8454) following the procedure described in Schnalzger et al. 2019 (Schnalzger et al., 2019). Cells with stable expression were selected by the addition of 1 µg/ml puromycin to the culture medium for two passages.

4.7 *In vitro* proliferation assay

MC38 tumor cells ($5x10^3$) were seeded in a flat-bottom 96-well plate. At each time point, absorbance was measured by using the CellTiter96® AQ_{ueuous} One Solution Cell Proliferation Assay kit (Promega) according to the manufacturer`s instructions.

4.8 qPCR

From MC38, CT26, or B16ova tumor cells, RNA was isolated from 10^5 cells 24 h after seeding by using the RNeasy Plus Micro Kit (QIAGEN) according to the manufacturer`s instructions. For organoid lines (Farin et al., 2023), organoids were seeded in triplicate wells and cultured for 3 days in tumor expansion medium without puromycin before the medium change and an additional 16 h of culture. Total RNA was collected using the NucleoSpin-RNA kit (Macherey-Nagel) according to the manufacturer's instructions. Tumor tissue was homogenized in gentleMACS M Tubes (Miltenyi) using a gentleMACS Dissociator (Miltenyi), and then RNA was isolated using the RNeasy Mini Kit (QIAGEN) according to the manufacturer`s instructions. The concentration of RNA was measured with a NanoDrop. RNA was then reverse transcribed into cDNA using qScript reagent (Quantabio), and real-time PCR was performed using Takyon™ No ROX SYBR mix (Eurogentec). The gene expression levels were calculated by the ΔΔCt method and normalized to those of *Gapdh*.

Target	**Forward primer (5`->3`)**	**Reverse primer (5`->3`)**
Murine primer sequences		
Gapdh	AACAGCAACTCCCACTCTTC	CCTGTTGCTGTAGCCGTATT
Isg15	GGTGTCCGTGACTAACTCCAT	CTGTACCACTAGCATCACTGTG
Ccl5	GCTGCTTTGCCTACCTCTCC	TCGAGTGACAAACACGACTGC
Cxcl9	TCCTTTTGGGCATCATCTTCC	TTTGTAGTGGATCGTGCCTCG

Cxcl10	CCAAGTGCTGCCGTCATTTTC	GGCTCGCAGGGATGATTTCAA
Cxcl11	GGCTTCCTTATGTTCAAACAGGG	GCCGTTACTCGGGTAAATTACA
Gzmb	CCACTCTCGACCCTACATGG	GGCCCCCAAAGTGACATTTATT
Ifng	CAGCTCCAAGAAAGGACGAAC	GGCAGTGTAACTCTTCTGCAT
Prf1	AGCACAAGTTCGTGCCAGG	GCGTCTCTCATTAGGGAGTTTTT
Tnf	ATGAGCACAGAAAGCATGATC	TACAGGCTTGTCACTCGAATT
Il12	TGGTTTGCCATCGTTTTGCTG	ACAGGTGAGGTTCACTGTTTCT
Murine primer sequences for cytosolic DNA quantification		
Gapdh	CAACTGCTTAGCCCCCCTGG	GCAGGGTAAGATAAGAAATG
Human primer sequences		
GAPDH	AGCCACATCGCTCAGACAC	GCCCAATACGACCAAATCC
ISG15	GCGAACTCATCTTTGCCAGTA	CCAGCATCTTCACCGTCAG

4.9 Inhibitor treatment

A total of 10^5 MC38 cells were seeded in a flat-bottom 96-well plate. The cells were treated with 10 µM TBK1 inhibitor (Invivogen) or control medium for 16 h. Total RNA was collected using an RNeasy Plus Micro Kit (QIAGEN) according to the manufacturer`s instructions. Organoid fragments were generated by dissociation and seeding in Growth Factor Reduced Matrigel® (Corning) and cultured for three days before the medium change and addition of 10 µM TBK1 inhibitor or control complete tumor expansion medium for an additional 16 h. The experiments were performed in triplicate wells, and RNA was collected using a NucleoSpin-RNA kit (Macherey-Nagel) according to the manufacturer's instructions. For anti-IFNAR1 inhibitor experiments, RNA was isolated from MC38 tumor cells 24 h after treatment with 30 µg/ml anti-IFNAR1 (clone: MAR1-5A3; BioXCell) by using the RNeasy Plus Micro Kit (QIAGEN) according to the manufacturer`s instructions. qPCR was performed as described in the "qPCR" section.

4.10 Isolation of cytosolic DNA

After 48 h of culture, the cytosolic fraction of $5x10^6$ MC38 tumor cells was isolated by using a mitochondrial isolation kit (Thermo Fisher Scientific) as reported (Lu et al., 2021). The manufacturer's protocol was followed until the cytosolic fraction was

obtained. Then, DNA from the cytosolic fraction was isolated using a QIAGEN DNeasy blood and tissue kit (QIAGEN) according to the manufacturer`s instructions. The DNA amount was measured with a QubitTM 4 using a Qubit 1x dsDNA HS assay kit following the manufacturer's instructions. To quantify the relative amount of DNA in the cytosolic fraction, qPCR with primers specific for genomic DNA was performed as described in the "qPCR" section. The relative DNA amount was calculated by normalization to the DNA amount of the WT condition.

4.11 Enzyme-linked immunosorbent assay (ELISA)

After 24 h of culture, $2.5x10^5$ MC38 tumor cells were washed with ice-cold PBS and harvested in M-PER Buffer (Thermo Scientific), and lysates were clarified by centrifugation at 20,000 x g/4 °C for 10 min, stored at -80 °C or used freshly. cGAMP ELISA was then performed according to the manufacturer`s instructions (Cayman Chemical). To measure IFN-β in the cell culture medium, MC38 tumor cells were cultured for 48 h, and the supernatants were harvested and stored at -80 °C or used fresh. Then, mouse IFN-β ELISA was performed according to the manufacturer`s instructions (PBL Assay Science).

4.12 Immunoblotting

Cells were washed with ice-cold PBS and harvested in RIPA buffer (Sigma–Aldrich) supplemented with protease inhibitors, 10 mM NaF, and 4 mM Na_3VO_4 (Calbiochem). The lysates were clarified by centrifugation at 20,000 x g at 4 °C, and the protein concentration was determined with the Pierce™ BCA Protein Assay Kit (Thermo Fisher Scientific). Fifteen micrograms of sample was denatured with NuPAGE™ LDS Sample Buffer (Thermo Fisher Scientific) for 10 min at 70 °C, subsequently separated on a 10% polyacrylamide gel, transferred onto a nitrocellulose membrane (Cytiva), blocked with 5% nonfat dry milk in TBST buffer (0.1% Tween 20) for 1 hour and probed with the following primary and secondary antibodies:

Target	**Company**
MLH1	Abcam (ab92312)
cGAS	Cell Signaling (#31659)

STING	Cell Signaling (#13647)
STING	Cell Signaling (#50494)
Phospho-STAT1	Cell Signaling (#8826)
Phospho-STAT1	Cell Signaling (#9167)
STAT1	Cell Signaling (#9172)
HSP60	BD Biosciences
Anti-mouse IgG-HRP	Cell Signaling
Anti-rabbit IgG-HRP	Cell Signaling

Visualization was performed by using Pierce™ ECL Western blotting substrates (Thermo Fisher Scientific).

4.13 Sample preparation – flow cytometry

For FACS analysis, MC38 mouse tumors were cut into small pieces, dissociated using a mouse tumor dissociation kit (Miltenyi) with a gentleMACS™ Octo Dissociator (Miltenyi), and filtered through 100 µm and 30 µm strainers. Then, immune cells were isolated from the resulting single-cell suspension using the mouse CD45 (TIL) MicroBeads (Miltenyi) with a MACS Separator (Miltenyi). For intracellular cytokine staining, cells were incubated with 100 nM phorbol 12-myristate 13-acetate (PMA), 1 µM ionomycin (both Sigma–Aldrich), and brefeldin A (Biolegend) for 4 h at 37 °C. The cells were then stained with a fixable viability dye (eBioscience). After blocking with anti-CD16/32 and anti-CD16.2 (both Biolegend), the following fluorochrome-coupled antibodies were used for flow cytometric analysis:

Marker	**Fluorophore**	**Clone**
CD45	PerCP-Cy5.5	30F-11
TCRb	APC-Cy7	H57-597
CD4	PE-Cy7	GK1.5
CD8	FITC	53-6.7
IFN-γ	PE	XMG1.2
PD-1	BV421 – ef450	29F.1A12
NK1.1	APC	PK136

CD11c	BV785	N418
CD11b	AF700	M1/70
CD19	BUV395	1D3

Data were collected with an LSRFortessa (BD Bioscience) and analyzed using FlowJo (BD Bioscience).

4.14 RNA-seq

After 24 h of culture, RNA was isolated from 10^5 MC38 tumor cells by using an RNeasy Mini Kit (QIAGEN) according to the manufacturer`s instructions. Next, library preparation for bulk sequencing of poly(A)-RNA was performed as described previously (Parekh et al., 2016). Briefly, the barcoded cDNA of each sample was generated with Maxima RT polymerase (Thermo Fisher) using oligo-dT primers containing barcodes, unique molecular identifiers (UMIs), and an adaptor. The ends of the cDNAs were extended by a template switch oligo (TSO), and full-length cDNA was amplified with primers binding to the TSO site and the adaptor. An NEB UltraII FS kit was used to fragment cDNA. After end repair and A-tailing, a TruSeq adapter was ligated, and 3'-end fragments were finally amplified using primers with Illumina P5 and P7 overhangs. In comparison to the method of Parekh et al. (2016) (Parekh et al., 2016), the P5 and P7 sites were exchanged to allow sequencing of the cDNA in read1 and barcodes and UMIs in read2 to achieve better cluster recognition. The library was sequenced on a NextSeq 500 (Illumina) sequencer with 63 cycles for the cDNA in read1 and 16 cycles for the barcodes and UMIs in read2. The data were processed using the published Drop-seq pipeline (v1.0) to generate sample- and genewise UMI tables (Macosko et al., 2015). The reference genome (GRCm38) was used for alignment. Transcript and gene definitions were used according to GENCODE Version M25. Differential gene expression was assessed with the DESeq2 package (Love et al., 2014) in R (version 3.6.2). Pre-ranked GSEA was performed with the gseapy python package (version 0.10.1) (Fang et al., 2022) by using the Reactome pathway database.

4.15 CITE-seq

4.15.1 Sample and library preparation

For both the pure WT MC38 and mixSTING^{N153S} conditions, three subcutaneously grown tumors (see “Tumor experiments and treatments” section) were harvested, and the isolated cells were pooled into one sample; labeled with CITE-seq antibodies against CD45 (clone 30-F11), CD3 (clone 17A2), CD4 (clone RM4-5), CD8a (clone 53-6.7), CD11b (clone M1/70), CD11c (clone N418), NK1.1 (clone PK136), CD19 (clone 6D5), Ly6C (clone HK1.4), Ly6G (clone 1A8), F4/80 (clone BM8), I-A/E-I (MHC II) (clone M5/114.15.2), CD279 (PD-1) (clone RMP1-30), and CD274 (PD-L1) (clone MIH6), and enriched for live/CD45+ cells by sorting (BD FACSAria™ Fusion). For each genotype, CD45^{+} and CD45^{-} cells were pooled in a 1:1 ratio. Sorted cells were then washed once with PBS + 2% FCS and subsequently counted to determine the exact cell number. The fraction of dead cells was estimated by trypan blue staining. The pooled cell suspensions were immediately used for single-cell RNA-seq with feature barcoding library preparation with a target recovery of 10,000 cells. Libraries were prepared using the Chromium Single Cell 3' Reagent Kit v3.1 (10X Genomics, PN-1000269) and the 3’ Feature Barcode Kit (10X Genomics, PN-1000262) according to the manufacturer’s instructions. All libraries from gene expression and feature barcoding were pooled and sequenced according to 10X Genomics’ recommendations on an Illumina NovaSeq6000 system with a target read depth of 50,000 reads/cell gene expression libraries and 5,000 reads/cell for feature barcoding libraries.

4.15.2 Raw data processing

The raw read data were mapped to version GRCm38 release 101 with Cellranger.

4.15.3 Quality control and preprocessing

Count data tables were loaded into and analyzed in Scanpy (Wolf et al., 2018) (version 1.7.2) according to a recently published best-practices pipeline (Luecken and Theis, 2019). Quality control of the mapped data was performed separately for ADT and for RNA data based on the joint distribution of count depth and the number of genes expressed. The ADT data were filtered to a minimum of 800 and a maximum of 15,000 counts, and the RNA data were filtered to a minimum of 200 and a maximum of 10,000

genes. Only cells passing both thresholds were retained for downstream analysis, leaving a dataset of 4,086 cells that passed this filtering. To make the cellular profiles comparable and remove the effects of sequencing depth, we normalized the RNA and ADT data. The RNA data were normalized using the scran pooling method (Lun et al., 2016) via the computeSumFactors() function implemented in the Scran package (version 1.14.1) and subsequently log+1 transformed. ADT data were normalized using the Seurat implementation (Hao et al., 2021) (version 3.0.2) of centered log ratio transform, clr:

$$clr(x)\left[ln\frac{x_i}{g(x)};\ldots;ln\ \frac{x_D}{g(x)}\right]$$

where g(x) is the geometric mean of the vector, x represents the cells and i to D represent all ADT features.

4.15.4 Clustering and annotation

To generate the joint embedding of the protein and the RNA data, TotalVI (as implemented in scvi-tools version 0.13.1) (Gayoso et al., 2021) was used with the parameters n_layers=2 and latent_distribution='normal'. A k-nearest neighbor graph was computed on the latent space generated by TotalVI using the Euclidean norm to compute the k=15 nearest neighbors via the Scanpy function sc.pp.neighbors. To visualize the data, a UMAP (McInnes et al., 2020) representation (package: umap-learn, version 0.5.1) was computed on this neighborhood graph. Cells were clustered with the Leiden algorithm (package: leidenalg, version 0.8.7) (Traag et al., 2019) on that neighborhood graph, using resolution=1. The clusters were then annotated jointly using the protein and the RNA data. To make the results of this analysis comparable to the results from FACS data, the clusters were annotated predominantly on the basis of the protein abundance levels.

4.15.5 Differential expression analysis

Due to the small number of cells per cell type and the small total expression changes, we first tested differential expression over all cell types. Differential expression between the WT and the SAVI mutant was tested with Diffxpy (version 0.7.4+18.gb8c6ae0) ("theislab/diffxpy," 2022). Diffxpy fits a negative binomial model to

the raw count data and allows the addition of covariates into the model. Here, we fit the model:

$Y \sim 1 + condition,$

where the condition is either a WT or STING^{N153S} mutant in a one-hot encoded covariate. Furthermore, we add the size factors from Scran as an offset to the model. The differential test was performed via a Wald test over the *condition* covariate per gene for all genes expressed in at least 50 cells in the tested cluster. Multiple testing correction was performed via the Benjamini–Hochberg method (Benjamini and Hochberg, 1995). Differentially expressed genes were filtered to a corrected p value below 0.05.

4.15.6 Gene set scoring

As described, per cell type, differential expression tests did not have enough power. To still identify the population from which the differential expression signature comes from, singular value decomposition (SVD)-based scoring was used by computing a PCA on the significantly upregulated genes and using the first component of the PCA as the score (Langfelder and Horvath, 2007), according to the equation:

$X = U\Sigma V^T$

Here, X represents the gene expression matrix size $n \times m$, where n are the signature genes and m are the cells. U and V are $m \times m$ and $n \times n$ orthogonal matrices and Σ is a rectangular diagonal matrix. We then use the first column of U as a signature score. We then ranked the cell populations based on the difference of the mean score between the WT and the SAVI mutant. Gene set enrichment was done with g:profiler (package gprofiler-offical, version 1.0.0) (Raudvere et al., 2019) on all GO:BP (releases/2021-05-01) terms that are larger than 400 genes. Filtering on gene set size was performed to exclude too general terms. All genes expressed in the dataset were used as the background.

4.16 Statistical analyses

Statistical analyses were performed using GraphPad PRISM. The statistical tests are described in the respective figure legends. In short, unpaired two-tailed Student`s *t*-test (comparison of two groups), ordinary one-way ANOVA combined with Dunnett`s multiple comparison test (comparison of more than two groups), and log-rank (Mantel–Cox) test were used. The data are presented as the mean ± SD if not stated otherwise. $P < 0.05$ was considered to indicate statistical significance (* $p < 0.05$; ** $p < 0.01$; *** $p < 0.001$; **** $p < 0.0001$).

5 References

Agalioti, T., Lomvardas, S., Parekh, B., Yie, J., Maniatis, T., Thanos, D., 2000. Ordered recruitment of chromatin modifying and general transcription factors to the IFN-beta promoter. Cell 103, 667–678. https://doi.org/10.1016/s0092-8674(00)00169-0

Ahn, J., Xia, T., Konno, H., Konno, K., Ruiz, P., Barber, G.N., 2014. Inflammation-driven carcinogenesis is mediated through STING. Nat Commun 5, 5166. https://doi.org/10.1038/ncomms6166

Akira, S., Uematsu, S., Takeuchi, O., 2006. Pathogen Recognition and Innate Immunity. Cell 124, 783–801. https://doi.org/10.1016/j.cell.2006.02.015

Alatise, O.I., Knapp, G.C., Sharma, A., Chatila, W.K., Arowolo, O.A., Olasehinde, O., Famurewa, O.C., Omisore, A.D., Komolafe, A.O., Olaofe, O.O., Katung, A.I., Ibikunle, D.E., Egberongbe, A.A., Olatoke, S.A., Agodirin, S.O., Adesiyun, O.A., Adeyeye, A., Kolawole, O.A., Olakanmi, A.O., Arora, K., Constable, J., Shah, R., Basunia, A., Sylvester, B., Wu, C., Weiser, M.R., Seier, K., Gonen, M., Stadler, Z.K., Kemel, Y., Vakiani, E., Berger, M.F., Chan, T.A., Solit, D.B., Shia, J., Sanchez-Vega, F., Schultz, N., Brennan, M., Smith, J.J., Kingham, T.P., 2021. Molecular and phenotypic profiling of colorectal cancer patients in West Africa reveals biological insights. Nat Commun 12, 6821. https://doi.org/10.1038/s41467-021-27106-w

Alex, A.K., Siqueira, S., Coudry, R., Santos, J., Alves, M., Hoff, P.M., Riechelmann, R.P., 2017. Response to Chemotherapy and Prognosis in Metastatic Colorectal Cancer With DNA Deficient Mismatch Repair. Clinical Colorectal Cancer 16, 228–239. https://doi.org/10.1016/j.clcc.2016.11.001

Alzahrani, S.M., Al Doghaither, H.A., Al-Ghafari, A.B., 2021. General insight into cancer: An overview of colorectal cancer (Review). Molecular and Clinical Oncology 15, 1–8. https://doi.org/10.3892/mco.2021.2433

Arasanz, H., Gato-Cañas, M., Zuazo, M., Ibañez-Vea, M., Breckpot, K., Kochan, G., Escors, D., 2017. PD1 signal transduction pathways in T cells. Oncotarget 8, 51936–51945. https://doi.org/10.18632/oncotarget.17232

Bai, L., Li, W., Zheng, W., Xu, D., Chen, N., Cui, J., 2020. Promising targets based on pattern recognition receptors for cancer immunotherapy. Pharmacological Research 159, 105017. https://doi.org/10.1016/j.phrs.2020.105017

Barber, G.N., 2015. STING: infection, inflammation and cancer. Nature Reviews Immunology 15, 760–770. https://doi.org/10.1038/nri3921

Bardelli, A., Cahill, D.P., Lederer, G., Speicher, M.R., Kinzler, K.W., Vogelstein, B., Lengauer, C., 2001. Carcinogen-specific induction of genetic instability. Proceedings of the National Academy of Sciences 98, 5770–5775. https://doi.org/10.1073/pnas.081082898

Batlle, E., Massagué, J., 2019. Transforming Grown Factor-β Signaling in Immunity and Cancer. Immunity 50, 924–940. https://doi.org/10.1016/j.immuni.2019.03.024

Belli, C., Trapani, D., Viale, G., D'Amico, P., Duso, B.A., Della Vigna, P., Orsi, F., Curigliano, G., 2018. Targeting the microenvironment in solid tumors. Cancer Treatment Reviews 65, 22–32. https://doi.org/10.1016/j.ctrv.2018.02.004

Benjamini, Y., Hochberg, Y., 1995. Controlling the False Discovery Rate: A Practical and Powerful Approach to Multiple Testing. Journal of the Royal Statistical Society. Series B (Methodological) 57, 289–300.

Bhat, K.P., Cortez, D., 2018. RPA and RAD51: fork reversal, fork protection, and genome stability. Nat Struct Mol Biol 25, 446–453. https://doi.org/10.1038/s41594-018-0075-z

Blank, C.U., Haanen, J.B., Ribas, A., Schumacher, T.N., 2016. The "cancer immunogram." Science 352, 658–660. https://doi.org/10.1126/science.aaf2834

Boland, C.R., Goel, A., 2010. Microsatellite Instability in Colorectal Cancer. Gastroenterology, Colon Cancer: An Update and Future Directions 138, 2073-2087.e3. https://doi.org/10.1053/j.gastro.2009.12.064

Brault, M., Olsen, T.M., Martinez, J., Stetson, D.B., Oberst, A., 2018. Intracellular Nucleic Acid Sensing Triggers Necroptosis through Synergistic Type I IFN and TNF Signaling. J Immunol 200, 2748–2756. https://doi.org/10.4049/jimmunol.1701492

Bridgeman, A., Maelfait, J., Davenne, T., Partridge, T., Peng, Y., Mayer, A., Dong, T., Kaever, V., Borrow, P., Rehwinkel, J., 2015. Viruses transfer the antiviral second messenger cGAMP between cells. Science 349, 1228–1232. https://doi.org/10.1126/science.aab3632

Bronger, H., Singer, J., Windmüller, C., Reuning, U., Zech, D., Delbridge, C., Dorn, J., Kiechle, M., Schmalfeldt, B., Schmitt, M., Avril, S., 2016. CXCL9 and CXCL10 predict survival and are regulated by cyclooxygenase inhibition in advanced serous ovarian cancer. Br J Cancer 115, 553–563. https://doi.org/10.1038/bjc.2016.172

Bronner, C.E., Baker, S.M., Morrison, P.T., Warren, G., Smith, L.G., Lescoe, M.K., Kane, M., Earabino, C., Lipford, J., Lindblom, A., 1994. Mutation in the DNA mismatch repair gene homologue hMLH1 is associated with hereditary non-polyposis colon cancer. Nature 368, 258–261. https://doi.org/10.1038/368258a0

Bruni, D., Angell, H.K., Galon, J., 2020. The immune contexture and Immunoscore in cancer prognosis and therapeutic efficacy. Nat Rev Cancer 20, 662–680. https://doi.org/10.1038/s41568-020-0285-7

Burdette, D.L., Monroe, K.M., Sotelo-Troha, K., Iwig, J.S., Eckert, B., Hyodo, M., Hayakawa, Y., Vance, R.E., 2011. STING is a direct innate immune sensor of cyclic di-GMP. Nature 478, 515–518. https://doi.org/10.1038/nature10429

Cao, Y., Jiao, N., Sun, T., Ma, Y., Zhang, X., Chen, H., Hong, J., Zhang, Y., 2021. CXCL11 Correlates With Antitumor Immunity and an Improved Prognosis in Colon Cancer. Frontiers in Cell and Developmental Biology 9.

Cerboni, S., Jeremiah, N., Gentili, M., Gehrmann, U., Conrad, C., Stolzenberg, M.-C., Picard, C., Neven, B., Fischer, A., Amigorena, S., Rieux-Laucat, F., Manel, N., 2017. Intrinsic antiproliferative activity of the innate sensor STING in T lymphocytes. J Exp Med 214, 1769–1785. https://doi.org/10.1084/jem.20161674

Cercek, A., Dos Santos Fernandes, G., Roxburgh, C.S., Ganesh, K., Ng, S., Sanchez-Vega, F., Yaeger, R., Segal, N.H., Reidy-Lagunes, D.L., Varghese, A.M., Markowitz, A., Wu, C., Szeglin, B., Sauvé, C.-E.G., Salo-Mullen, E., Tran, C., Patel, Z., Krishnan, A., Tkachuk, K., Nash, G.M., Guillem, J., Paty, P.B., Shia, J., Schultz, N., Garcia-Aguilar, J., Diaz, L.A., Goodman, K., Saltz, L.B., Weiser, M.R., Smith, J.J., Stadler, Z.K., 2020. Mismatch Repair–Deficient Rectal Cancer and Resistance to Neoadjuvant Chemotherapy. Clin Cancer Res 26, 3271–3279. https://doi.org/10.1158/1078-0432.CCR-19-3728

Cercek, A., Lumish, M., Sinopoli, J., Weiss, J., Shia, J., Lamendola-Essel, M., El Dika, I.H., Segal, N., Shcherba, M., Sugarman, R., Stadler, Z., Yaeger, R., Smith, J.J., Rousseau, B., Argiles, G., Patel, M., Desai, A., Saltz, L.B., Widmar, M., Iyer, K., Zhang, J., Gianino, N., Crane, C., Romesser, P.B., Pappou, E.P., Paty, P., Garcia-Aguilar, J., Gonen, M., Gollub, M., Weiser, M.R., Schalper, K.A., Diaz, L.A., 2022. PD-1 Blockade in Mismatch Repair–Deficient, Locally Advanced Rectal Cancer. N Engl J Med 386, 2363–2376. https://doi.org/10.1056/NEJMoa2201445

Chatterjee, N., Walker, G.C., 2017. Mechanisms of DNA damage, repair and mutagenesis. Environ Mol Mutagen 58, 235–263. https://doi.org/10.1002/em.22087

Chen, D.S., Mellman, I., 2017. Elements of cancer immunity and the cancer–immune set point. Nature 541, 321–330. https://doi.org/10.1038/nature21349

Chen, D.S., Mellman, I., 2013. Oncology Meets Immunology: The Cancer-Immunity Cycle. Immunity 39, 1–10. https://doi.org/10.1016/j.immuni.2013.07.012

Chen, L., Han, X., 2015. Anti-PD-1/PD-L1 therapy of human cancer: past, present, and future. J Clin Invest 125, 3384–3391. https://doi.org/10.1172/JCI80011

Chen, Q., Boire, A., Jin, X., Valiente, M., Er, E.E., Lopez-Soto, A., Jacob, L., Patwa, R., Shah, H., Xu, K., Cross, J.R., Massagué, J., 2016. Carcinoma-astrocyte gap junctions promote brain metastasis by cGAMP transfer. Nature 533, 493–498. https://doi.org/10.1038/nature18268

Corrales, L., Glickman, L.H., McWhirter, S.M., Kanne, D.B., Sivick, K.E., Katibah, G.E., Woo, S.-R., Lemmens, E., Banda, T., Leong, J.J., Metchette, K., Dubensky, T.W., Gajewski, T.F., 2015. Direct Activation of STING in the Tumor Microenvironment Leads to Potent and Systemic Tumor Regression and Immunity. Cell Reports 11, 1018–1030. https://doi.org/10.1016/j.celrep.2015.04.031

Corrales, L., Matson, V., Flood, B., Spranger, S., Gajewski, T.F., 2017. Innate immune signaling and regulation in cancer immunotherapy. Cell Res 27, 96–108. https://doi.org/10.1038/cr.2016.149

Cullen, S.P., Brunet, M., Martin, S.J., 2010. Granzymes in cancer and immunity. Cell Death Differ 17, 616–623. https://doi.org/10.1038/cdd.2009.206

de Oliveira Mann, C.C., Orzalli, M.H., King, D.S., Kagan, J.C., Lee, A.S.Y., Kranzusch, P.J., 2019. Modular Architecture of the STING C-Terminal Tail Allows Interferon and NF-κB Signaling Adaptation. Cell Reports 27, 1165-1175.e5. https://doi.org/10.1016/j.celrep.2019.03.098

Demaria, O., De Gassart, A., Coso, S., Gestermann, N., Di Domizio, J., Flatz, L., Gaide, O., Michielin, O., Hwu, P., Petrova, T.V., Martinon, F., Modlin, R.L., Speiser, D.E., Gilliet, M., 2015. STING activation of tumor endothelial cells initiates spontaneous and therapeutic antitumor immunity. Proc Natl Acad Sci U S A 112, 15408–15413. https://doi.org/10.1073/pnas.1512832112

Deng, L., Liang, H., Xu, M., Yang, X., Burnette, B., Arina, A., Li, X.-D., Mauceri, H., Beckett, M., Darga, T., Huang, X., Gajewski, T.F., Chen, Z.J., Fu, Y.-X., Weichselbaum, R.R., 2014. STING-Dependent Cytosolic DNA Sensing Promotes Radiation-Induced Type I Interferon-Dependent Antitumor Immunity in Immunogenic Tumors. Immunity 41, 843–852. https://doi.org/10.1016/j.immuni.2014.10.019

Dhanyamraju, P.K., Patel, T.N., 2022. Melanoma therapeutics: a literature review. J Biomed Res 36, 77–97. https://doi.org/10.7555/JBR.36.20210163

Diamond, J.M., Vanpouille-Box, C., Spada, S., Rudqvist, N.-P., Chapman, J.R., Ueberheide, B.M., Pilones, K.A., Sarfraz, Y., Formenti, S.C., Demaria, S., 2018. Exosomes Shuttle TREX1-Sensitive IFN-Stimulatory dsDNA from Irradiated Cancer Cells to DCs. Cancer Immunol Res 6, 910–920. https://doi.org/10.1158/2326-6066.CIR-17-0581

Droeser, R.A., Hirt, C., Viehl, C.T., Frey, D.M., Nebiker, C., Huber, X., Zlobec, I., Eppenberger-Castori, S., Tzankov, A., Rosso, R., Zuber, M., Muraro, M.G., Amicarella, F., Cremonesi, E., Heberer, M., Iezzi, G., Lugli, A., Terracciano, L., Sconocchia, G., Oertli, D., Spagnoli, G.C., Tornillo, L., 2013. Clinical impact of programmed cell death ligand 1 expression in colorectal cancer. Eur J Cancer 49, 2233–2242. https://doi.org/10.1016/j.ejca.2013.02.015

Du, W., Frankel, T.L., Green, M., Zou, W., 2021. IFNγ signaling integrity in colorectal cancer immunity and immunotherapy. Cell Mol Immunol 1–10. https://doi.org/10.1038/s41423-021-00735-3

Duraturo, F., Liccardo, R., Izzo, P., 2016. Coexistence of MLH3 germline variants in colon cancer patients belonging to families with Lynch syndrome-associated brain tumors. J Neurooncol 129, 577–578. https://doi.org/10.1007/s11060-016-2203-0

Ergun, S.L., Fernandez, D., Weiss, T.M., Li, L., 2019. STING Polymer Structure Reveals Mechanisms for Activation, Hyperactivation, and Inhibition. Cell 178, 290-301.e10. https://doi.org/10.1016/j.cell.2019.05.036

Fang, Z., Liu, X., Peltz, G., 2022. GSEApy: a comprehensive package for performing gene set enrichment analysis in Python. Bioinformatics btac757. https://doi.org/10.1093/bioinformatics/btac757

Farin, H.F., Mosa, M.H., Ndreshkjana, B., Grebbin, B.M., Ritter, B., Menche, C., Kennel, K.B., Ziegler, P.K., Szabó, L., Bollrath, J., Rieder, D., Michels, B.E., Kress, A., Bozlar, M., Darvishi, T., Stier, S., Kur, I.-M., Bankov, K., Kesselring, R., Fichtner-Feigl, S., Brüne, B., Goetze, T.O., Al-Batran, S.-E., Brandts, C.H., Bechstein, W.O., Wild, P.J., Weigert, A., Müller, S., Knapp, S., Trajanoski, Z., Greten, F.R., 2023. Colorectal Cancer Organoid–Stroma Biobank Allows Subtype-Specific Assessment of Individualized Therapy Responses. Cancer Discovery OF1–OF20. https://doi.org/10.1158/2159-8290.CD-23-0050

Fenton, S.E., Saleiro, D., Platanias, L.C., 2021. Type I and II Interferons in the Anti-Tumor Immune Response. Cancers (Basel) 13, 1037. https://doi.org/10.3390/cancers13051037

Fink, D., Aebi, S., Howell, S.B., 1998. The role of DNA mismatch repair in drug resistance. Clin Cancer Res 4, 1–6.

Fishel, R., Lescoe, M.K., Rao, M.R., Copeland, N.G., Jenkins, N.A., Garber, J., Kane, M., Kolodner, R., 1993. The human mutator gene homolog MSH2 and its association with hereditary nonpolyposis colon cancer. Cell 75, 1027–1038. https://doi.org/10.1016/0092-8674(93)90546-3

Flood, B.A., Higgs, E.F., Li, S., Luke, J.J., Gajewski, T.F., 2019. STING pathway agonism as a cancer therapeutic. Immunological Reviews 290, 24–38. https://doi.org/10.1111/imr.12765

Fuertes, M.B., Kacha, A.K., Kline, J., Woo, S.-R., Kranz, D.M., Murphy, K.M., Gajewski, T.F., 2011. Host type I IFN signals are required for antitumor CD8+ T cell responses through CD8{alpha}+ dendritic cells. J Exp Med 208, 2005–2016. https://doi.org/10.1084/jem.20101159

Galon, J., Bruni, D., 2019. Approaches to treat immune hot, altered and cold tumours with combination immunotherapies. Nat Rev Drug Discov 18, 197–218. https://doi.org/10.1038/s41573-018-0007-y

Garris, C.S., Arlauckas, S.P., Kohler, R.H., Trefny, M.P., Garren, S., Piot, C., Engblom, C., Pfirschke, C., Siwicki, M., Gungabeesoon, J., Freeman, G.J., Warren, S.E., Ong, S., Browning, E., Twitty, C.G., Pierce, R.H., Le, M.H., Algazi, A.P., Daud, A.I., Pai, S.I., Zippelius, A., Weissleder, R., Pittet, M.J., 2018. Successful Anti-PD-1 Cancer Immunotherapy Requires T Cell-Dendritic Cell Crosstalk Involving the Cytokines IFN-γ and IL-12. Immunity 49, 1148-1161.e7. https://doi.org/10.1016/j.immuni.2018.09.024

Gayoso, A., Steier, Z., Lopez, R., Regier, J., Nazor, K.L., Streets, A., Yosef, N., 2021. Joint probabilistic modeling of single-cell multi-omic data with totalVI. Nat Methods 18, 272–282. https://doi.org/10.1038/s41592-020-01050-x

Gentili, M., Kowal, J., Tkach, M., Satoh, T., Lahaye, X., Conrad, C., Boyron, M., Lombard, B., Durand, S., Kroemer, G., Loew, D., Dalod, M., Théry, C., Manel, N., 2015. Transmission of innate immune signaling by packaging of cGAMP in viral particles. Science 349, 1232–1236. https://doi.org/10.1126/science.aab3628

Germano, G., Lamba, S., Rospo, G., Barault, L., Magrì, A., Maione, F., Russo, M., Crisafulli, G., Bartolini, A., Lerda, G., Siravegna, G., Mussolin, B., Frapolli, R., Montone, M., Morano, F., de Braud, F., Amirouchene-Angelozzi, N., Marsoni, S., D'Incalci, M., Orlandi, A., Giraudo, E., Sartore-Bianchi, A., Siena, S., Pietrantonio, F., Di Nicolantonio, F., Bardelli, A., 2017. Inactivation of DNA repair triggers neoantigen generation and impairs tumour growth. Nature 552, 116–120. https://doi.org/10.1038/nature24673

Gibney, G.T., Weiner, L.M., Atkins, M.B., 2016. Predictive biomarkers for checkpoint inhibitor-based immunotherapy. Lancet Oncol 17, e542–e551. https://doi.org/10.1016/S1470-2045(16)30406-5

Goto, A., Okado, K., Martins, N., Cai, H., Barbier, V., Lamiable, O., Troxler, L., Santiago, E., Kuhn, L., Paik, D., Silverman, N., Holleufer, A., Hartmann, R., Liu, J., Peng, T., Hoffmann, J.A., Meignin, C., Daeffler, L., Imler, J.-L., 2018. The Kinase IKKβ Regulates a STING- and NF-κB-Dependent Antiviral Response Pathway in Drosophila. Immunity 49, 225-234.e4. https://doi.org/10.1016/j.immuni.2018.07.013

Grady, W.M., Carethers, J.M., 2008. Genomic and Epigenetic Instability in Colorectal Cancer Pathogenesis. Gastroenterology 135, 1079–1099. https://doi.org/10.1053/j.gastro.2008.07.076

Greenwald, R.J., Freeman, G.J., Sharpe, A.H., 2005. The B7 family revisited. Annu Rev Immunol 23, 515–548. https://doi.org/10.1146/annurev.immunol.23.021704.115611

Guan, J., Lu, C., Jin, Q., Lu, H., Chen, X., Tian, L., Zhang, Y., Ortega, J., Zhang, J., Siteni, S., Chen, M., Gu, L., Shay, J.W., Davis, A.J., Chen, Z.J., Fu, Y.-X., Li, G.-M., 2021. MLH1 Deficiency-Triggered DNA Hyperexcision by Exonuclease 1 Activates the cGAS-STING Pathway. Cancer Cell 39, 109-121.e5. https://doi.org/10.1016/j.ccell.2020.11.004

Gulen, M.F., Koch, U., Haag, S.M., Schuler, F., Apetoh, L., Villunger, A., Radtke, F., Ablasser, A., 2017. Signalling strength determines proapoptotic functions of STING. Nature Communications 8, 427. https://doi.org/10.1038/s41467-017-00573-w

Han, J., Lim, J., Wang, C.-P.J., Han, J.-H., Shin, H.E., Kim, S.-N., Jeong, D., Lee, S.H., Chun, B.-H., Park, C.G., Park, W., 2023. Lipid nanoparticle-based mRNA delivery systems for cancer immunotherapy. Nano Convergence 10, 36. https://doi.org/10.1186/s40580-023-00385-3

Hanahan, D., Weinberg, R.A., 2011. Hallmarks of cancer: the next generation. Cell 144, 646–674. https://doi.org/10.1016/j.cell.2011.02.013

Hanahan, D., Weinberg, R.A., 2000. The Hallmarks of Cancer. Cell 100, 57–70. https://doi.org/10.1016/S0092-8674(00)81683-9

Hanna, G.J., Lizotte, P., Cavanaugh, M., Kuo, F.C., Shivdasani, P., Frieden, A., Chau, N.G., Schoenfeld, J.D., Lorch, J.H., Uppaluri, R., MacConaill, L.E., Haddad, R.I., 2018. Frameshift events predict anti-PD-1/L1 response in head and neck cancer. JCI Insight 3, 98811. https://doi.org/10.1172/jci.insight.98811

Hao, Y., Hao, S., Andersen-Nissen, E., Mauck, W.M., Zheng, S., Butler, A., Lee, M.J., Wilk, A.J., Darby, C., Zager, M., Hoffman, P., Stoeckius, M., Papalexi, E., Mimitou, E.P., Jain, J., Srivastava, A., Stuart, T., Fleming, L.M., Yeung, B., Rogers, A.J., McElrath, J.M., Blish, C.A., Gottardo, R., Smibert, P., Satija, R., 2021. Integrated analysis of multimodal single-cell data. Cell 184, 3573-3587.e29. https://doi.org/10.1016/j.cell.2021.04.048

Harding, S.M., Benci, J.L., Irianto, J., Discher, D.E., Minn, A.J., Greenberg, R.A., 2017a. Mitotic progression following DNA damage enables pattern recognition within micronuclei. Nature 548, 466–470. https://doi.org/10.1038/nature23470

Harding, S.M., Benci, J.L., Irianto, J., Discher, D.E., Minn, A.J., Greenberg, R.A., 2017b. Mitotic progression following DNA damage enables pattern recognition within micronuclei. Nature 548, 466–470. https://doi.org/10.1038/nature23470

Harlin, H., Meng, Y., Peterson, A.C., Zha, Y., Tretiakova, M., Slingluff, C., McKee, M., Gajewski, T.F., 2009. Chemokine expression in melanoma metastases associated with CD8+ T-cell recruitment. Cancer Res 69, 3077–3085. https://doi.org/10.1158/0008-5472.CAN-08-2281

Hegde, P.S., Chen, D.S., 2020. Top 10 Challenges in Cancer Immunotherapy. Immunity 52, 17–35. https://doi.org/10.1016/j.immuni.2019.12.011

Hegde, P.S., Karanikas, V., Evers, S., 2016. The Where, the When, and the How of Immune Monitoring for Cancer Immunotherapies in the Era of Checkpoint Inhibition. Clin Cancer Res 22, 1865–1874. https://doi.org/10.1158/1078-0432.CCR-15-1507

Herbst, R.S., Baas, P., Kim, D.-W., Felip, E., Pérez-Gracia, J.L., Han, J.-Y., Molina, J., Kim, J.-H., Arvis, C.D., Ahn, M.-J., Majem, M., Fidler, M.J., de Castro, G., Garrido, M., Lubiniecki, G.M., Shentu, Y., Im, E., Dolled-Filhart, M., Garon, E.B., 2016. Pembrolizumab versus docetaxel for previously treated, PD-L1-positive, advanced non-small-cell lung cancer (KEYNOTE-010): a randomised controlled trial. Lancet 387, 1540–1550. https://doi.org/10.1016/S0140-6736(15)01281-7

Herbst, R.S., Giaccone, G., de Marinis, F., Reinmuth, N., Vergnenegre, A., Barrios, C.H., Morise, M., Felip, E., Andric, Z., Geater, S., Özgüroğlu, M., Zou, W., Sandler, A., Enquist, I., Komatsubara, K., Deng, Y., Kuriki, H., Wen, X., McCleland, M., Mocci, S., Jassem, J., Spigel, D.R., 2020. Atezolizumab for First-Line Treatment of PD-L1–Selected Patients

with NSCLC. New England Journal of Medicine 383, 1328–1339. https://doi.org/10.1056/NEJMoa1917346

Herbst, R.S., Soria, J.-C., Kowanetz, M., Fine, G.D., Hamid, O., Gordon, M.S., Sosman, J.A., McDermott, D.F., Powderly, J.D., Gettinger, S.N., Kohrt, H.E.K., Horn, L., Lawrence, D.P., Rost, S., Leabman, M., Xiao, Y., Mokatrin, A., Koeppen, H., Hegde, P.S., Mellman, I., Chen, D.S., Hodi, F.S., 2014. Predictive correlates of response to the anti-PD-L1 antibody MPDL3280A in cancer patients. Nature 515, 563–567. https://doi.org/10.1038/nature14011

Hodi, F.S., O'Day, S.J., McDermott, D.F., Weber, R.W., Sosman, J.A., Haanen, J.B., Gonzalez, R., Robert, C., Schadendorf, D., Hassel, J.C., Akerley, W., van den Eertwegh, A.J.M., Lutzky, J., Lorigan, P., Vaubel, J.M., Linette, G.P., Hogg, D., Ottensmeier, C.H., Lebbé, C., Peschel, C., Quirt, I., Clark, J.I., Wolchok, J.D., Weber, J.S., Tian, J., Yellin, M.J., Nichol, G.M., Hoos, A., Urba, W.J., 2010. Improved survival with ipilimumab in patients with metastatic melanoma. N Engl J Med 363, 711–723. https://doi.org/10.1056/NEJMoa1003466

Holm, C.K., Jensen, S.B., Jakobsen, M.R., Cheshenko, N., Horan, K.A., Moeller, H.B., Gonzalez-Dosal, R., Rasmussen, S.B., Christensen, M.H., Yarovinsky, T.O., Rixon, F.J., Herold, B.C., Fitzgerald, K.A., Paludan, S.R., 2012. Virus-cell fusion as a trigger of innate immunity dependent on the adaptor STING. Nat Immunol 13, 737–743. https://doi.org/10.1038/ni.2350

Hoos, A., Ibrahim, R., Korman, A., Abdallah, K., Berman, D., Shahabi, V., Chin, K., Canetta, R., Humphrey, R., 2010. Development of ipilimumab: contribution to a new paradigm for cancer immunotherapy. Semin Oncol 37, 533–546. https://doi.org/10.1053/j.seminoncol.2010.09.015

Hopfner, K.-P., Hornung, V., 2020. Molecular mechanisms and cellular functions of cGAS–STING signalling. Nature Reviews Molecular Cell Biology 1–21. https://doi.org/10.1038/s41580-020-0244-x

Horn, L., Mansfield, A.S., Szczęsna, A., Havel, L., Krzakowski, M., Hochmair, M.J., Huemer, F., Losonczy, G., Johnson, M.L., Nishio, M., Reck, M., Mok, T., Lam, S., Shames, D.S., Liu, J., Ding, B., Lopez-Chavez, A., Kabbinavar, F., Lin, W., Sandler, A., Liu, S.V., 2018. First-Line Atezolizumab plus Chemotherapy in Extensive-Stage Small-Cell Lung Cancer. New England Journal of Medicine 379, 2220–2229. https://doi.org/10.1056/NEJMoa1809064

Hotz, C., Wagenaar, T.R., Gieseke, F., Bangari, D.S., Callahan, M., Cao, H., Diekmann, J., Diken, M., Grunwitz, C., Hebert, A., Hsu, K., Bernardo, M., Karikó, K., Kreiter, S., Kuhn, A.N., Levit, M., Malkova, N., Masciari, S., Pollard, J., Qu, H., Ryan, S., Selmi, A., Schlereth, J., Singh, K., Sun, F., Tillmann, B., Tolstykh, T., Weber, W., Wicke, L., Witzel, S., Yu, Q., Zhang, Y.-A., Zheng, G., Lager, J., Nabel, G.J., Sahin, U., Wiederschain, D., 2021. Local delivery of mRNA-encoded cytokines promotes antitumor immunity and tumor eradication across multiple preclinical tumor models. Science Translational Medicine. https://doi.org/10.1126/scitranslmed.abc7804

Hsieh, P., Zhang, Y., 2017. The Devil is in the details for DNA mismatch repair. Proceedings of the National Academy of Sciences 114, 3552–3554. https://doi.org/10.1073/pnas.1702747114

Huang, Y., Li, G.-M., 2018. DNA mismatch repair preferentially safeguards actively transcribed genes. DNA Repair, Cutting-edge Perspectives in Genomic Maintenance V 71, 82–86. https://doi.org/10.1016/j.dnarep.2018.08.010

Hudson, W.A., Li, Q., Le, C., Kersey, J.H., 1998. Xenotransplantation of human lymphoid malignancies is optimized in mice with multiple immunologic defects. Leukemia 12, 2029–2033. https://doi.org/10.1038/sj.leu.2401236

Ishikawa, H., Barber, G.N., 2008. STING is an endoplasmic reticulum adaptor that facilitates innate immune signalling. Nature 455, 674–678. https://doi.org/10.1038/nature07317

Ishikawa, H., Ma, Z., Barber, G.N., 2009. STING regulates intracellular DNA-mediated, type I interferon-dependent innate immunity. Nature 461, 788–792. https://doi.org/10.1038/nature08476

Jiricny, J., 2013. Postreplicative Mismatch Repair. Cold Spring Harb Perspect Biol 5, a012633. https://doi.org/10.1101/cshperspect.a012633

Jiricny, J., 2006. The multifaceted mismatch-repair system. Nat Rev Mol Cell Biol 7, 335–346. https://doi.org/10.1038/nrm1907

Kawai, T., Akira, S., 2010. The role of pattern-recognition receptors in innate immunity: update on Toll-like receptors. Nat Immunol 11, 373–384. https://doi.org/10.1038/ni.1863

Kawakami, T., Shiina, H., Igawa, M., Deguchi, M., Nakajima, K., Ogishima, T., Tokizane, T., Urakami, S., Enokida, H., Miura, K., Ishii, N., Kane, C.J., Carroll, P.R., Dahiya, R., 2004. Inactivation of the hMSH3 mismatch repair gene in bladder cancer. Biochemical and Biophysical Research Communications 325, 934–942. https://doi.org/10.1016/j.bbrc.2004.10.114

Kitajima, S., Ivanova, E., Guo, S., Yoshida, R., Campisi, M., Sundararaman, S.K., Tange, S., Mitsuishi, Y., Thai, T.C., Masuda, S., Piel, B.P., Sholl, L.M., Kirschmeier, P.T., Paweletz, C.P., Watanabe, H., Yajima, M., Barbie, D.A., 2019. Suppression of STING Associated with LKB1 Loss in KRAS-Driven Lung Cancer. Cancer Discov 9, 34–45. https://doi.org/10.1158/2159-8290.CD-18-0689

Konno, H., Yamauchi, S., Berglund, A., Putney, R.M., Mulé, J.J., Barber, G.N., 2018. Suppression of STING signaling through epigenetic silencing and missense mutation impedes DNA damage mediated cytokine production. Oncogene 37, 2037–2051. https://doi.org/10.1038/s41388-017-0120-0

Kubli, S.P., Berger, T., Araujo, D.V., Siu, L.L., Mak, T.W., 2021. Beyond immune checkpoint blockade: emerging immunological strategies. Nature Reviews Drug Discovery 1–21. https://doi.org/10.1038/s41573-021-00155-y

Kwon, J., Bakhoum, S.F., 2020. The Cytosolic DNA-Sensing cGAS-STING Pathway in Cancer. Cancer Discov 10, 26–39. https://doi.org/10.1158/2159-8290.CD-19-0761

Langfelder, P., Horvath, S., 2007. Eigengene networks for studying the relationships between co-expression modules. BMC Syst Biol 1, 54. https://doi.org/10.1186/1752-0509-1-54

Lao, V.V., Grady, W.M., 2011. Epigenetics and colorectal cancer. Nat Rev Gastroenterol Hepatol 8, 686–700. https://doi.org/10.1038/nrgastro.2011.173

Larkin, B., Ilyukha, V., Sorokin, M., Buzdin, A., Vannier, E., Poltorak, A., 2017. Cutting Edge: Activation of STING in T Cells Induces Type I IFN Responses and Cell Death. J Immunol 199, 397–402. https://doi.org/10.4049/jimmunol.1601999

Larkin, J., Chiarion-Sileni, V., Gonzalez, R., Grob, J.-J., Rutkowski, P., Lao, C.D., Cowey, C.L., Schadendorf, D., Wagstaff, J., Dummer, R., Ferrucci, P.F., Smylie, M., Hogg, D., Hill, A., Márquez-Rodas, I., Haanen, J., Guidoboni, M., Maio, M., Schöffski, P., Carlino, M.S., Lebbé, C., McArthur, G., Ascierto, P.A., Daniels, G.A., Long, G.V., Bastholt, L., Rizzo, J.I., Balogh, A., Moshyk, A., Hodi, F.S., Wolchok, J.D., 2019. Five-Year Survival with Combined Nivolumab and Ipilimumab in Advanced Melanoma. N Engl J Med 381, 1535–1546. https://doi.org/10.1056/NEJMoa1910836

Lawler, S.E., Speranza, M.-C., Cho, C.-F., Chiocca, E.A., 2017. Oncolytic Viruses in Cancer Treatment: A Review. JAMA Oncol 3, 841–849. https://doi.org/10.1001/jamaoncol.2016.2064

Le, D.T., Durham, J.N., Smith, K.N., Wang, H., Bartlett, B.R., Aulakh, L.K., Lu, S., Kemberling, H., Wilt, C., Luber, B.S., Wong, F., Azad, N.S., Rucki, A.A., Laheru, D., Donehower, R., Zaheer, A., Fisher, G.A., Crocenzi, T.S., Lee, J.J., Greten, T.F., Duffy, A.G., Ciombor, K.K., Eyring, A.D., Lam, B.H., Joe, A., Kang, S.P., Holdhoff, M., Danilova, L., Cope, L., Meyer, C., Zhou, S., Goldberg, R.M., Armstrong, D.K., Bever, K.M., Fader, A.N., Taube, J., Housseau, F., Spetzler, D., Xiao, N., Pardoll, D.M., Papadopoulos, N., Kinzler, K.W., Eshleman, J.R., Vogelstein, B., Anders, R.A., Diaz, L.A., 2017. Mismatch repair deficiency predicts response of solid tumors to PD-1 blockade. Science 357, 409–413. https://doi.org/10.1126/science.aan6733

Le, D.T., Kavan, P., Kim, T.W., Burge, M.E., Van Cutsem, E., Hara, H., Boland, P.M., Van Laethem, J.-L., Geva, R., Taniguchi, H., Crocenzi, T.S., Sharma, M., Atreya, C.E., Diaz, L.A., Liang, L.W., Marinello, P., Dai, T., O'Neil, B.H., 2018. KEYNOTE-164: Pembrolizumab for patients with advanced microsatellite instability high (MSI-H) colorectal cancer. JCO 36, 3514–3514. https://doi.org/10.1200/JCO.2018.36.15_suppl.3514

Le, D.T., Kim, T.W., Van Cutsem, E., Geva, R., Jäger, D., Hara, H., Burge, M., O'Neil, B., Kavan, P., Yoshino, T., Guimbaud, R., Taniguchi, H., Elez, E., Al-Batran, S.-E., Boland, P.M., Crocenzi, T., Atreya, C.E., Cui, Y., Dai, T., Marinello, P., Diaz, L.A., André, T., 2020. Phase II Open-Label Study of Pembrolizumab in Treatment-Refractory, Microsatellite Instability-High/Mismatch Repair-Deficient Metastatic Colorectal Cancer: KEYNOTE-164. J Clin Oncol 38, 11–19. https://doi.org/10.1200/JCO.19.02107

Le, D.T., Uram, J.N., Wang, H., Bartlett, B.R., Kemberling, H., Eyring, A.D., Skora, A.D., Luber, B.S., Azad, N.S., Laheru, D., Biedrzycki, B., Donehower, R.C., Zaheer, A., Fisher, G.A., Crocenzi, T.S., Lee, J.J., Duffy, S.M., Goldberg, R.M., de la Chapelle, A., Koshiji, M., Bhaijee, F., Huebner, T., Hruban, R.H., Wood, L.D., Cuka, N., Pardoll, D.M., Papadopoulos, N., Kinzler, K.W., Zhou, S., Cornish, T.C., Taube, J.M., Anders, R.A., Eshleman, J.R., Vogelstein, B., Diaz, L.A., 2015. PD-1 Blockade in Tumors with Mismatch-Repair Deficiency. N Engl J Med 372, 2509–2520. https://doi.org/10.1056/NEJMoa1500596

Le Naour, J., Zitvogel, L., Galluzzi, L., Vacchelli, E., Kroemer, G., 2020. Trial watch: STING agonists in cancer therapy. Oncoimmunology 9, 1777624. https://doi.org/10.1080/2162402X.2020.1777624

Leach, F.S., Nicolaides, N.C., Papadopoulos, N., Liu, B., Jen, J., Parsons, R., Peltomäki, P., Sistonen, P., Aaltonen, L.A., Nyström-Lahti, M., 1993. Mutations of a mutS homolog in hereditary nonpolyposis colorectal cancer. Cell 75, 1215–1225. https://doi.org/10.1016/0092-8674(93)90330-s

Lemery, S., Keegan, P., Pazdur, R., 2017. First FDA Approval Agnostic of Cancer Site — When a Biomarker Defines the Indication. N Engl J Med 377, 1409–1412. https://doi.org/10.1056/NEJMp1709968

Lemos, H., Mohamed, E., Huang, L., Ou, R., Pacholczyk, G., Arbab, A.S., Munn, D., Mellor, A.L., 2016. STING Promotes the Growth of Tumors Characterized by Low Antigenicity via IDO Activation. Cancer Res 76, 2076–2081. https://doi.org/10.1158/0008-5472.CAN-15-1456

Lenz, H.-J.J., Cutsem, E.V., Limon, M.L., Wong, K.Y., Hendlisz, A., Aglietta, M., Garcia-Alfonso, P., Neyns, B., Luppi, G., Cardin, D., Dragovich, T., Shah, U., Atasoy, A., Postema, R., Boyd, Z., Ledeine, J.-M., Overman, M., Lonardi, S., 2018. Durable clinical benefit with nivolumab (NIVO) plus low-dose ipilimumab (IPI) as first-line therapy in microsatellite instability-high/mismatch repair deficient (MSI-H/dMMR) metastatic colorectal cancer (mCRC). Annals of Oncology 29, viii714. https://doi.org/10.1093/annonc/mdy424.019

Li, G.-M., 2008. Mechanisms and functions of DNA mismatch repair. Cell Res 18, 85–98. https://doi.org/10.1038/cr.2007.115

Li, L., Guan, Y., Chen, X., Yang, J., Cheng, Y., 2021. DNA Repair Pathways in Cancer Therapy and Resistance. Frontiers in Pharmacology 11.

Li, L., Yin, Q., Kuss, P., Maliga, Z., Millán, J.L., Wu, H., Mitchison, T.J., 2014. Hydrolysis of 2’3’-cGAMP by ENPP1 and design of nonhydrolyzable analogs. Nat Chem Biol 10, 1043–1048. https://doi.org/10.1038/nchembio.1661

Li, W., Lu, L., Lu, J., Wang, X., Yang, C., Jin, J., Wu, L., Hong, X., Li, F., Cao, D., Yang, Y., Wu, M., Su, B., Cheng, J., Yang, X., Di, W., Deng, L., 2020. cGAS-STING-mediated DNA sensing maintains CD8+ T cell stemness and promotes antitumor T cell therapy. Sci Transl Med 12, eaay9013. https://doi.org/10.1126/scitranslmed.aay9013

Li, X., Shu, C., Yi, G., Chaton, C.T., Shelton, C.L., Diao, J., Zuo, X., Kao, C.C., Herr, A.B., Li, P., 2013. Cyclic GMP-AMP synthase is activated by double-stranded DNA-induced oligomerization. Immunity 39, 1019–1031. https://doi.org/10.1016/j.immuni.2013.10.019

Liang, H., Deng, L., Hou, Y., Meng, X., Huang, X., Rao, E., Zheng, W., Mauceri, H., Mack, M., Xu, M., Fu, Y.-X., Weichselbaum, R.R., 2017. Host STING-dependent MDSC mobilization drives extrinsic radiation resistance. Nat Commun 8, 1736. https://doi.org/10.1038/s41467-017-01566-5

Liu, D., Keijzers, G., Rasmussen, L.J., 2017. DNA mismatch repair and its many roles in eukaryotic cells. Mutation Research/Reviews in Mutation Research 773, 174–187. https://doi.org/10.1016/j.mrrev.2017.07.001

Liu, S., Cai, X., Wu, J., Cong, Q., Chen, X., Li, T., Du, F., Ren, J., Wu, Y.-T., Grishin, N.V., Chen, Z.J., 2015. Phosphorylation of innate immune adaptor proteins MAVS, STING, and TRIF induces IRF3 activation. Science 347, aaa2630. https://doi.org/10.1126/science.aaa2630

Liu, Y., Jesus, A.A., Marrero, B., Yang, D., Ramsey, S.E., Montealegre Sanchez, G.A., Tenbrock, K., Wittkowski, H., Jones, O.Y., Kuehn, H.S., Lee, C.-C.R., DiMattia, M.A., Cowen, E.W., Gonzalez, B., Palmer, I., DiGiovanna, J.J., Biancotto, A., Kim, H., Tsai, W.L., Trier, A.M., Huang, Y., Stone, D.L., Hill, S., Kim, H.J., St. Hilaire, C., Gurprasad, S., Plass, N., Chapelle, D., Horkayne-Szakaly, I., Foell, D., Barysenka, A., Candotti, F., Holland, S.M., Hughes, J.D., Mehmet, H., Issekutz, A.C., Raffeld, M., McElwee, J., Fontana, J.R., Minniti, C.P., Moir, S., Kastner, D.L., Gadina, M., Steven, A.C., Wingfield, P.T., Brooks, S.R., Rosenzweig, S.D., Fleisher, T.A., Deng, Z., Boehm, M., Paller, A.S., Goldbach-Mansky, R., 2014. Activated STING in a Vascular and Pulmonary Syndrome. New England Journal of Medicine 371, 507–518. https://doi.org/10.1056/NEJMoa1312625

Liu, Y.-T., Sun, Z.-J., 2021. Turning cold tumors into hot tumors by improving T-cell infiltration. Theranostics 11, 5365–5386. https://doi.org/10.7150/thno.58390

Love, M.I., Huber, W., Anders, S., 2014. Moderated estimation of fold change and dispersion for RNA-seq data with DESeq2. Genome Biology 15, 550. https://doi.org/10.1186/s13059-014-0550-8

Lu, C., Guan, J., Lu, S., Jin, Q., Rousseau, B., Lu, T., Stephens, D., Zhang, H., Zhu, J., Yang, M., Ren, Z., Liang, Y., Liu, Z., Han, C., Liu, L., Cao, X., Zhang, A., Qiao, J., Batten, K., Chen, M., Castrillon, D.H., Wang, T., Li, B., Diaz, L.A., Li, G.-M., Fu, Y.-X., 2021. DNA Sensing in Mismatch Repair-Deficient Tumor Cells Is Essential for Anti-tumor Immunity. Cancer Cell 39, 96-108.e6. https://doi.org/10.1016/j.ccell.2020.11.006

Luecken, M.D., Theis, F.J., 2019. Current best practices in single-cell RNA-seq analysis: a tutorial. Mol Syst Biol 15, e8746. https://doi.org/10.15252/msb.20188746

Luksch, H., Stinson, W.A., Platt, D.J., Qian, W., Kalugotla, G., Miner, C.A., Bennion, B.G., Gerbaulet, A., Rösen-Wolff, A., Miner, J.J., 2019. STING-associated lung disease in mice

relies on T cells but not type I interferon. Journal of Allergy and Clinical Immunology S0091674919302088. https://doi.org/10.1016/j.jaci.2019.01.044

Lun, A.T.L., McCarthy, D.J., Marioni, J.C., 2016. A step-by-step workflow for low-level analysis of single-cell RNA-seq data with Bioconductor. https://doi.org/10.12688/f1000research.9501.2

Luteijn, R.D., Zaver, S.A., Gowen, B.G., Wyman, S.K., Garelis, N.E., Onia, L., McWhirter, S.M., Katibah, G.E., Corn, J.E., Woodward, J.J., Raulet, D.H., 2019. SLC19A1 transports immunoreactive cyclic dinucleotides. Nature 573, 434–438. https://doi.org/10.1038/s41586-019-1553-0

Lyu, G.-Y., Yeh, Y.-H., Yeh, Y.-C., Wang, Y.-C., 2018. Mutation load estimation model as a predictor of the response to cancer immunotherapy. NPJ Genom Med 3, 12. https://doi.org/10.1038/s41525-018-0051-x

Ma, W., Xue, R., Zhu, Z., Farrukh, H., Song, W., Li, T., Zheng, L., Pan, C., 2023. Increasing cure rates of solid tumors by immune checkpoint inhibitors. Experimental Hematology & Oncology 12, 10. https://doi.org/10.1186/s40164-023-00372-8

Mackenzie, K.J., Carroll, P., Martin, C.-A., Murina, O., Fluteau, A., Simpson, D.J., Olova, N., Sutcliffe, H., Rainger, J.K., Leitch, A., Osborn, R.T., Wheeler, A.P., Nowotny, M., Gilbert, N., Chandra, T., Reijns, M.A.M., Jackson, A.P., 2017. cGAS surveillance of micronuclei links genome instability to innate immunity. Nature 548, 461–465. https://doi.org/10.1038/nature23449

Macosko, E.Z., Basu, A., Satija, R., Nemesh, J., Shekhar, K., Goldman, M., Tirosh, I., Bialas, A.R., Kamitaki, N., Martersteck, E.M., Trombetta, J.J., Weitz, D.A., Sanes, J.R., Shalek, A.K., Regev, A., McCarroll, S.A., 2015. Highly Parallel Genome-wide Expression Profiling of Individual Cells Using Nanoliter Droplets. Cell 161, 1202–1214. https://doi.org/10.1016/j.cell.2015.05.002

Mandal, R., Samstein, R.M., Lee, K.-W., Havel, J.J., Wang, H., Krishna, C., Sabio, E.Y., Makarov, V., Kuo, F., Blecua, P., Ramaswamy, A.T., Durham, J.N., Bartlett, B., Ma, X., Srivastava, R., Middha, S., Zehir, A., Hechtman, J.F., Morris, L.G., Weinhold, N., Riaz, N., Le, D.T., Diaz, L.A., Chan, T.A., 2019. Genetic diversity of tumors with mismatch repair deficiency influences anti–PD-1 immunotherapy response. Science 364, 485–491. https://doi.org/10.1126/science.aau0447

Marabelle, A., Le, D.T., Ascierto, P.A., Di Giacomo, A.M., De Jesus-Acosta, A., Delord, J.-P., Geva, R., Gottfried, M., Penel, N., Hansen, A.R., Piha-Paul, S.A., Doi, T., Gao, B., Chung, H.C., Lopez-Martin, J., Bang, Y.-J., Frommer, R.S., Shah, M., Ghori, R., Joe, A.K., Pruitt, S.K., Diaz, L.A., 2020. Efficacy of Pembrolizumab in Patients With Noncolorectal High Microsatellite Instability/Mismatch Repair-Deficient Cancer: Results From the Phase II KEYNOTE-158 Study. J Clin Oncol 38, 1–10. https://doi.org/10.1200/JCO.19.02105

Marcus, A., Mao, A.J., Lensink-Vasan, M., Wang, L., Vance, R.E., Raulet, D.H., 2018. Tumor-Derived cGAMP Triggers a STING-Mediated Interferon Response in Non-tumor Cells to

Activate the NK Cell Response. Immunity 49, 754-763.e4. https://doi.org/10.1016/j.immuni.2018.09.016

Maréchal, A., Zou, L., 2015. RPA-coated single-stranded DNA as a platform for post-translational modifications in the DNA damage response. Cell Res 25, 9–23. https://doi.org/10.1038/cr.2014.147

Mármol, I., Sánchez-de-Diego, C., Pradilla Dieste, A., Cerrada, E., Rodriguez Yoldi, M., 2017. Colorectal Carcinoma: A General Overview and Future Perspectives in Colorectal Cancer. IJMS 18, 197. https://doi.org/10.3390/ijms18010197

Martin, M., Hiroyasu, A., Guzman, R.M., Roberts, S.A., Goodman, A.G., 2018. Analysis of Drosophila STING Reveals an Evolutionarily Conserved Antimicrobial Function. Cell Rep 23, 3537-3550.e6. https://doi.org/10.1016/j.celrep.2018.05.029

Mathieu, L., Shah, S., Pai-Scherf, L., Larkins, E., Vallejo, J., Li, X., Rodriguez, L., Mishra-Kalyani, P., Goldberg, K.B., Kluetz, P.G., Theoret, M.R., Beaver, J.A., Pazdur, R., Singh, H., 2021. FDA Approval Summary: Atezolizumab and Durvalumab in Combination with Platinum-Based Chemotherapy in Extensive Stage Small Cell Lung Cancer. The Oncologist 26, 433–438. https://doi.org/10.1002/onco.13752

McInnes, L., Healy, J., Melville, J., 2020. UMAP: Uniform Manifold Approximation and Projection for Dimension Reduction (No. arXiv:1802.03426). arXiv. https://doi.org/10.48550/arXiv.1802.03426

Meng, X., Huang, Z., Teng, F., Xing, L., Yu, J., 2015. Predictive biomarkers in PD-1/PD-L1 checkpoint blockade immunotherapy. Cancer Treat Rev 41, 868–876. https://doi.org/10.1016/j.ctrv.2015.11.001

Miao, D., Margolis, C.A., Gao, W., Voss, M.H., Li, W., Martini, D.J., Norton, C., Bossé, D., Wankowicz, S.M., Cullen, D., Horak, C., Wind-Rotolo, M., Tracy, A., Giannakis, M., Hodi, F.S., Drake, C.G., Ball, M.W., Allaf, M.E., Snyder, A., Hellmann, M.D., Ho, T., Motzer, R.J., Signoretti, S., Kaelin, W.G., Choueiri, T.K., Van Allen, E.M., 2018. Genomic correlates of response to immune checkpoint therapies in clear cell renal cell carcinoma. Science 359, 801–806. https://doi.org/10.1126/science.aan5951

Miao, L., Li, L., Huang, Y., Delcassian, D., Chahal, J., Han, J., Shi, Y., Sadtler, K., Gao, W., Lin, J., Doloff, J.C., Langer, R., Anderson, D.G., 2019. Delivery of mRNA vaccines with heterocyclic lipids increases anti-tumor efficacy by STING-mediated immune cell activation. Nature Biotechnology 37, 1174–1185. https://doi.org/10.1038/s41587-019-0247-3

Mlecnik, B., Tosolini, M., Kirilovsky, A., Berger, A., Bindea, G., Meatchi, T., Bruneval, P., Trajanoski, Z., Fridman, W.-H., Pagès, F., Galon, J., 2011. Histopathologic-based prognostic factors of colorectal cancers are associated with the state of the local immune reaction. J Clin Oncol 29, 610–618. https://doi.org/10.1200/JCO.2010.30.5425

Moretti, J., Roy, S., Bozec, D., Martinez, J., Chapman, J.R., Ueberheide, B., Lamming, D.W., Chen, Z.J., Horng, T., Yeretssian, G., Green, D.R., Blander, J.M., 2017. STING Senses Microbial Viability to Orchestrate Stress-Mediated Autophagy of the Endoplasmic Reticulum. Cell 171, 809-823.e13. https://doi.org/10.1016/j.cell.2017.09.034

Morse, M.A., Overman, M.J., Hartman, L., Khoukaz, T., Brutcher, E., Lenz, H.-J., Atasoy, A., Shangguan, T., Zhao, H., El-Rayes, B., 2019. Safety of Nivolumab plus Low-Dose Ipilimumab in Previously Treated Microsatellite Instability-High/Mismatch Repair-Deficient Metastatic Colorectal Cancer. Oncologist 24, 1453–1461. https://doi.org/10.1634/theoncologist.2019-0129

Motedayen Aval, L., Pease, J.E., Sharma, R., Pinato, D.J., 2020. Challenges and Opportunities in the Clinical Development of STING Agonists for Cancer Immunotherapy. J Clin Med 9. https://doi.org/10.3390/jcm9103323

Motzer, R.J., Tannir, N.M., McDermott, D.F., Arén Frontera, O., Melichar, B., Choueiri, T.K., Plimack, E.R., Barthélémy, P., Porta, C., George, S., Powles, T., Donskov, F., Neiman, V., Kollmannsberger, C.K., Salman, P., Gurney, H., Hawkins, R., Ravaud, A., Grimm, M.-O., Bracarda, S., Barrios, C.H., Tomita, Y., Castellano, D., Rini, B.I., Chen, A.C., Mekan, S., McHenry, M.B., Wind-Rotolo, M., Doan, J., Sharma, P., Hammers, H.J., Escudier, B., CheckMate 214 Investigators, 2018. Nivolumab plus Ipilimumab versus Sunitinib in Advanced Renal-Cell Carcinoma. N Engl J Med 378, 1277–1290. https://doi.org/10.1056/NEJMoa1712126

Mowat, C., Mosley, S.R., Namdar, A., Schiller, D., Baker, K., 2020. Antitumor immunity in dMMR colorectal cancers requires interferon-induced CCL5 and CXCL10. bioRxiv 2020.09.15.291765. https://doi.org/10.1101/2020.09.15.291765

Mur, P., García-Mulero, S., del Valle, J., Magraner-Pardo, L., Vidal, A., Pineda, M., Cinnirella, G., Martín-Ramos, E., Pons, T., López-Doriga, A., Belhadj, S., Feliubadaló, L., Munoz-Torres, P.M., Navarro, M., Grau, E., Darder, E., Llort, G., Sanz, J., Ramón y Cajal, T., Balmana, J., Brunet, J., Moreno, V., Piulats, J.M., Matías-Guiu, X., Sanz-Pamplona, R., Aligué, R., Capellá, G., Lázaro, C., Valle, L., 2020. Role of POLE and POLD1 in familial cancer. Genet Med 22, 2089–2100. https://doi.org/10.1038/s41436-020-0922-2

Nagarsheth, N., Wicha, M.S., Zou, W., 2017. Chemokines in the cancer microenvironment and their relevance in cancer immunotherapy. Nat Rev Immunol 17, 559–572. https://doi.org/10.1038/nri.2017.49

Nassour, J., Radford, R., Correia, A., Fusté, J.M., Schoell, B., Jauch, A., Shaw, R.J., Karlseder, J., 2019. Autophagic cell death restricts chromosomal instability during replicative crisis. Nature 565, 659–663. https://doi.org/10.1038/s41586-019-0885-0

Nicolaides, N.C., Papadopoulos, N., Liu, B., Wei, Y.F., Carter, K.C., Ruben, S.M., Rosen, C.A., Haseltine, W.A., Fleischmann, R.D., Fraser, C.M., 1994. Mutations of two PMS homologues in hereditary nonpolyposis colon cancer. Nature 371, 75–80. https://doi.org/10.1038/371075a0

Ning, Y., Suzman, D., Maher, V.E., Zhang, L., Tang, S., Ricks, T., Palmby, T., Fu, W., Liu, Q., Goldberg, K.B., Kim, G., Pazdur, R., 2017. FDA Approval Summary: Atezolizumab for the Treatment of Patients with Progressive Advanced Urothelial Carcinoma after Platinum-Containing Chemotherapy. Oncologist 22, 743–749. https://doi.org/10.1634/theoncologist.2017-0087

Nishimura, H., Nose, M., Hiai, H., Minato, N., Honjo, T., 1999. Development of lupus-like autoimmune diseases by disruption of the PD-1 gene encoding an ITIM motif-carrying immunoreceptor. Immunity 11, 141–151. https://doi.org/10.1016/s1074-7613(00)80089-8

Noubade, R., Majri-Morrison, S., Tarbell, K.V., 2019. Beyond cDC1: Emerging Roles of DC Crosstalk in Cancer Immunity. Frontiers in Immunology 10.

Ochoa de Olza, M., Navarro Rodrigo, B., Zimmermann, S., Coukos, G., 2020. Turning up the heat on non-immunoreactive tumours: opportunities for clinical development. The Lancet Oncology 21, e419–e430. https://doi.org/10.1016/S1470-2045(20)30234-5

O'Neil, B.H., Wallmark, J.M., Lorente, D., Elez, E., Raimbourg, J., Gomez-Roca, C., Ejadi, S., Piha-Paul, S.A., Stein, M.N., Abdul Razak, A.R., Dotti, K., Santoro, A., Cohen, R.B., Gould, M., Saraf, S., Stein, K., Han, S.-W., 2017. Safety and antitumor activity of the anti-PD-1 antibody pembrolizumab in patients with advanced colorectal carcinoma. PLoS One 12, e0189848. https://doi.org/10.1371/journal.pone.0189848

Ott, P.A., Hodi, F.S., 2016. Talimogene Laherparepvec for the Treatment of Advanced Melanoma. Clin Cancer Res 22, 3127–3131. https://doi.org/10.1158/1078-0432.CCR-15-2709

Overman, M.J., Lonardi, S., Wong, K.Y.M., Lenz, H.-J., Gelsomino, F., Aglietta, M., Morse, M.A., Van Cutsem, E., McDermott, R., Hill, A., Sawyer, M.B., Hendlisz, A., Neyns, B., Svrcek, M., Moss, R.A., Ledeine, J.-M., Cao, Z.A., Kamble, S., Kopetz, S., André, T., 2018. Durable Clinical Benefit With Nivolumab Plus Ipilimumab in DNA Mismatch Repair-Deficient/Microsatellite Instability-High Metastatic Colorectal Cancer. J. Clin. Oncol. 36, 773–779. https://doi.org/10.1200/JCO.2017.76.9901

Overman, M.J., McDermott, R., Leach, J.L., Lonardi, S., Lenz, H.-J., Morse, M.A., Desai, J., Hill, A., Axelson, M., Moss, R.A., Goldberg, M.V., Cao, Z.A., Ledeine, J.-M., Maglinte, G.A., Kopetz, S., André, T., 2017. Nivolumab in patients with metastatic DNA mismatch repair-deficient or microsatellite instability-high colorectal cancer (CheckMate 142): an open-label, multicentre, phase 2 study. Lancet Oncol. 18, 1182–1191. https://doi.org/10.1016/S1470-2045(17)30422-9

Ozga, A.J., Chow, M.T., Luster, A.D., 2021. Chemokines and the immune response to cancer. Immunity 54, 859–874. https://doi.org/10.1016/j.immuni.2021.01.012

Pagès, F., Mlecnik, B., Marliot, F., Bindea, G., Ou, F.-S., Bifulco, C., Lugli, A., Zlobec, I., Rau, T.T., Berger, M.D., Nagtegaal, I.D., Vink-Börger, E., Hartmann, A., Geppert, C., Kolwelter, J., Merkel, S., Grützmann, R., Van den Eynde, M., Jouret-Mourin, A., Kartheuser, A.,

Léonard, D., Remue, C., Wang, J.Y., Bavi, P., Roehrl, M.H.A., Ohashi, P.S., Nguyen, L.T., Han, S., MacGregor, H.L., Hafezi-Bakhtiari, S., Wouters, B.G., Masucci, G.V., Andersson, E.K., Zavadova, E., Vocka, M., Spacek, J., Petruzelka, L., Konopasek, B., Dundr, P., Skalova, H., Nemejcova, K., Botti, G., Tatangelo, F., Delrio, P., Ciliberto, G., Maio, M., Laghi, L., Grizzi, F., Fredriksen, T., Buttard, B., Angelova, M., Vasaturo, A., Maby, P., Church, S.E., Angell, H.K., Lafontaine, L., Bruni, D., El Sissy, C., Haicheur, N., Kirilovsky, A., Berger, A., Lagorce, C., Meyers, J.P., Paustian, C., Feng, Z., Ballesteros-Merino, C., Dijkstra, J., van de Water, C., van Lent-van Vliet, S., Knijn, N., Mușină, A.-M., Scripcariu, D.-V., Popivanova, B., Xu, M., Fujita, T., Hazama, S., Suzuki, N., Nagano, H., Okuno, K., Torigoe, T., Sato, N., Furuhata, T., Takemasa, I., Itoh, K., Patel, P.S., Vora, H.H., Shah, B., Patel, J.B., Rajvik, K.N., Pandya, S.J., Shukla, S.N., Wang, Y., Zhang, G., Kawakami, Y., Marincola, F.M., Ascierto, P.A., Sargent, D.J., Fox, B.A., Galon, J., 2018. International validation of the consensus Immunoscore for the classification of colon cancer: a prognostic and accuracy study. Lancet 391, 2128–2139. https://doi.org/10.1016/S0140-6736(18)30789-X

Pardi, N., Hogan, M.J., Porter, F.W., Weissman, D., 2018. mRNA vaccines — a new era in vaccinology. Nat Rev Drug Discov 17, 261–279. https://doi.org/10.1038/nrd.2017.243

Parekh, S., Ziegenhain, C., Vieth, B., Enard, W., Hellmann, I., 2016. The impact of amplification on differential expression analyses by RNA-seq. Sci Rep 6, 25533. https://doi.org/10.1038/srep25533

Patsoukis, N., Wang, Q., Strauss, L., Boussiotis, V.A., 2020. Revisiting the PD-1 pathway. Science Advances 6, eabd2712. https://doi.org/10.1126/sciadv.abd2712

Pauken, K.E., Wherry, E.J., 2015. Overcoming T cell exhaustion in infection and cancer. Trends in Immunology 36, 265–276. https://doi.org/10.1016/j.it.2015.02.008

Paz-Ares, L., Dvorkin, M., Chen, Yuanbin, Reinmuth, N., Hotta, K., Trukhin, D., Statsenko, G., Hochmair, M.J., Özgüroğlu, M., Ji, J.H., Voitko, O., Poltoratskiy, A., Ponce, S., Verderame, F., Havel, L., Bondarenko, I., Kazarnowicz, A., Losonczy, G., Conev, N.V., Armstrong, J., Byrne, N., Shire, N., Jiang, H., Goldman, J.W., Batagelj, E., Casarini, I., Pastor, A.V., Sena, S.N., Zarba, J.J., Burghuber, O., Hartl, S., Hochmair, M.J., Lamprecht, B., Studnicka, M., Schlittler, L.A., Oliveira, F.A.M. de, Calabrich, A., Girotto, G.C., Reis, P.D., Gorini, C.F.N., Marchi, P.R.M.D., Baldotto, C.S. da R., Sette, C., Zukin, M., Conev, N.V., Dudov, A., Ilieva, R., Koynov, K., Krasteva, R., Tonev, I., Valev, S., Venkova, V., Bi, M., Chen, C., Chen, Yuan, Chen, Z., Fang, J., Feng, J., Han, Z., Hu, J., Hu, Y., Li, W., Liang, Z., Lin, Z., Ma, R., Ma, S., Nan, K., Shu, Y., Wang, K., Wang, M., Wu, G., Yang, N., Yang, Z., Zhang, H., Zhang, W., Zhao, J., Zhao, Y., Zhou, C., Zhou, J., Zhou, X., Havel, L., Kolek, V., Koubkova, L., Roubec, J., Skrickova, J., Zemanova, M., Chouaid, C., Hilgers, W., Lena, H., Moro-Sibilot, D., Robinet, G., Souquet, P.-J., Alt, J., Bischoff, H., Grohe, C., Laack, E., Lang, S., Panse, J., Reinmuth, N., Schulz, C., Bogos, K., Csánky, E., Fülöp, A., Horváth, Z., Kósa, J., Laczó, I., Losonczy, G., Pajkos, G., Pápai, Z., Székely, Z.P., Sárosi, V., Somfay, A., Ezer, É.S., Telekes, A., Bar, J., Gottfried, M., Heching, N.I., Kuch, A.Z., Bartolucci, R., Bettini, A.C., Delmonte, A., Garassino, M.C., Minelli, M., Roila, F., Verderame, F., Atagi, S., Azuma, K., Goto, H., Goto, K., Hara, Y., Hayashi, H., Hida, T., Hotta, K., Kanazawa, K., Kanda, S., Kim, Y.H., Kuyama, S., Maeda, T., Morise, M., Nakahara, Y., Nishio, M.,

Nogami, N., Okamoto, I., Saito, H., Shinoda, M., Umemura, S., Yoshida, T., Claessens, N., Cornelissen, R., Heniks, L., Hiltermann, J., Smit, E., Brekel, A.S. van den, Kazarnowicz, A., Kowalski, D., Mańdziuk, S., Mróz, R., Wojtukiewicz, M., Ciuleanu, T., Ganea, D., Ungureanu, A., Dvorkin, M., Luft, A., Moiseenko, V., Poltoratskiy, A., Sakaeva, D., Smolin, A., Statsenko, G., Vasilyev, A., Vladimirova, L., Anasina, I., Chovanec, J., Demo, P., Godal, R., Kasan, P., Stresko, M., Urda, M., Cho, E.K., Ji, J.H., Kim, J.-H., Kim, S.-W., Lee, G.-W., Lee, J.-S., Lee, Ki Hyeong, Lee, Kyung Hee, Lee, Y.G., Molla, M.A.I., Gomez, M.D., Mingorance, J.I.D., Casado, D.I., Brea, M.L., Tarruella, M.M., Bueno, T.M., Mendivil, A.N., Rodríguez, L.P.-A., Aix, S.P., Campelo, M.R.G., Chang, G.-C., Chen, Y.-H., Chiu, C.-H., Hsia, T.-C., Lee, K.-Y., Li, C.-T., Wang, C.-C., Wei, Y.-F., Wu, S.-Y., Alacacıoğlu, A., Çiçin, I., Demirkazik, A., Erman, M., Göksel, T., Özgüroğlu, M., Adamchuk, H., Bondarenko, I., Kolesnik, O., Kryzhanivska, A., Ostapenko, Y., Shevnia, S., Shparyk, Y., Trukhin, D., Ursol, G., Voitko, N., Voitko, O., Vynnychenko, I., Babu, S., Chen, Yuanbin, Chiang, A., Chua, W., Dakhil, S., Dowlati, A., Goldman, J.W., Haque, B., Jamil, R., Knoble, J., Lakhanpal, S., Mi, K., Nikolinakos, P., Powell, S., Ross, H., Schaefer, E., Schneider, J., Spahr, J., Spigel, D., Stilwill, J., Sumey, C., Williamson, M., 2019. Durvalumab plus platinum–etoposide versus platinum–etoposide in first-line treatment of extensive-stage small-cell lung cancer (CASPIAN): a randomised, controlled, open-label, phase 3 trial. The Lancet 394, 1929–1939. https://doi.org/10.1016/S0140-6736(19)32222-6

Pećina-Šlaus, N., Kafka, A., Salamon, I., Bukovac, A., 2020. Mismatch Repair Pathway, Genome Stability and Cancer. Frontiers in Molecular Biosciences 7.

Perng, Y.-C., Lenschow, D.J., 2018. ISG15 in antiviral immunity and beyond. Nat Rev Microbiol 16, 423–439. https://doi.org/10.1038/s41579-018-0020-5

Petrasek, J., Iracheta-Vellve, A., Csak, T., Satishchandran, A., Kodys, K., Kurt-Jones, E.A., Fitzgerald, K.A., Szabo, G., 2013. STING-IRF3 pathway links endoplasmic reticulum stress with hepatocyte apoptosis in early alcoholic liver disease. Proc Natl Acad Sci U S A 110, 16544–16549. https://doi.org/10.1073/pnas.1308331110

Pino, M.S., Chung, D.C., 2010. The chromosomal instability pathway in colon cancer. Gastroenterology 138, 2059–2072. https://doi.org/10.1053/j.gastro.2009.12.065

Poulogiannis, G., Frayling, I.M., Arends, M.J., 2010. DNA mismatch repair deficiency in sporadic colorectal cancer and Lynch syndrome. Histopathology 56, 167–179. https://doi.org/10.1111/j.1365-2559.2009.03392.x

Prall, F., Dührkop, T., Weirich, V., Ostwald, C., Lenz, P., Nizze, H., Barten, M., 2004. Prognostic role of CD8+ tumor-infiltrating lymphocytes in stage III colorectal cancer with and without microsatellite instability. Hum Pathol 35, 808–816. https://doi.org/10.1016/j.humpath.2004.01.022

Qureshi, O.S., Zheng, Y., Nakamura, K., Attridge, K., Manzotti, C., Schmidt, E.M., Baker, J., Jeffery, L.E., Kaur, S., Briggs, Z., Hou, T.Z., Futter, C.E., Anderson, G., Walker, L.S.K., Sansom, D.M., 2011. Trans-endocytosis of CD80 and CD86: a molecular basis for the

cell-extrinsic function of CTLA-4. Science 332, 600–603. https://doi.org/10.1126/science.1202947

Raudvere, U., Kolberg, L., Kuzmin, I., Arak, T., Adler, P., Peterson, H., Vilo, J., 2019. g:Profiler: a web server for functional enrichment analysis and conversions of gene lists (2019 update). Nucleic Acids Research 47, W191–W198. https://doi.org/10.1093/nar/gkz369

Ready, N., Hellmann, M.D., Awad, M.M., Otterson, G.A., Gutierrez, M., Gainor, J.F., Borghaei, H., Jolivet, J., Horn, L., Mates, M., Brahmer, J., Rabinowitz, I., Reddy, P.S., Chesney, J., Orcutt, J., Spigel, D.R., Reck, M., O'Byrne, K.J., Paz-Ares, L., Hu, W., Zerba, K., Li, X., Lestini, B., Geese, W.J., Szustakowski, J.D., Green, G., Chang, H., Ramalingam, S.S., 2019. First-Line Nivolumab Plus Ipilimumab in Advanced Non-Small-Cell Lung Cancer (CheckMate 568): Outcomes by Programmed Death Ligand 1 and Tumor Mutational Burden as Biomarkers. J Clin Oncol 37, 992–1000. https://doi.org/10.1200/JCO.18.01042

Riaz, N., Havel, J.J., Makarov, V., Desrichard, A., Urba, W.J., Sims, J.S., Hodi, F.S., Martín-Algarra, S., Mandal, R., Sharfman, W.H., Bhatia, S., Hwu, W.-J., Gajewski, T.F., Slingluff, C.L., Chowell, D., Kendall, S.M., Chang, H., Shah, R., Kuo, F., Morris, L.G.T., Sidhom, J.-W., Schneck, J.P., Horak, C.E., Weinhold, N., Chan, T.A., 2017. Tumor and Microenvironment Evolution during Immunotherapy with Nivolumab. Cell 171, 934-949.e16. https://doi.org/10.1016/j.cell.2017.09.028

Ribas, A., Dummer, R., Puzanov, I., VanderWalde, A., Andtbacka, R.H.I., Michielin, O., Olszanski, A.J., Malvehy, J., Cebon, J., Fernandez, E., Kirkwood, J.M., Gajewski, T.F., Chen, L., Gorski, K.S., Anderson, A.A., Diede, S.J., Lassman, M.E., Gansert, J., Hodi, F.S., Long, G.V., 2017. Oncolytic Virotherapy Promotes Intratumoral T Cell Infiltration and Improves Anti-PD-1 Immunotherapy. Cell 170, 1109-1119.e10. https://doi.org/10.1016/j.cell.2017.08.027

Rizvi, N.A., Hellmann, M.D., Snyder, A., Kvistborg, P., Makarov, V., Havel, J.J., Lee, W., Yuan, J., Wong, P., Ho, T.S., Miller, M.L., Rekhtman, N., Moreira, A.L., Ibrahim, F., Bruggeman, C., Gasmi, B., Zappasodi, R., Maeda, Y., Sander, C., Garon, E.B., Merghoub, T., Wolchok, J.D., Schumacher, T.N., Chan, T.A., 2015. Mutational landscape determines sensitivity to PD-1 blockade in non–small cell lung cancer. Science 348, 124–128. https://doi.org/10.1126/science.aaa1348

Robert, C., 2020. A decade of immune-checkpoint inhibitors in cancer therapy. Nat Commun 11, 3801. https://doi.org/10.1038/s41467-020-17670-y

Robert, C., Long, G.V., Brady, B., Dutriaux, C., Maio, M., Mortier, L., Hassel, J.C., Rutkowski, P., McNeil, C., Kalinka-Warzocha, E., Savage, K.J., Hernberg, M.M., Lebbé, C., Charles, J., Mihalcioiu, C., Chiarion-Sileni, V., Mauch, C., Cognetti, F., Arance, A., Schmidt, H., Schadendorf, D., Gogas, H., Lundgren-Eriksson, L., Horak, C., Sharkey, B., Waxman, I.M., Atkinson, V., Ascierto, P.A., 2015a. Nivolumab in previously untreated melanoma without BRAF mutation. N Engl J Med 372, 320–330. https://doi.org/10.1056/NEJMoa1412082

Robert, C., Schachter, J., Long, G.V., Arance, A., Grob, J.J., Mortier, L., Daud, A., Carlino, M.S., McNeil, C., Lotem, M., Larkin, J., Lorigan, P., Neyns, B., Blank, C.U., Hamid, O., Mateus, C., Shapira-Frommer, R., Kosh, M., Zhou, H., Ibrahim, N., Ebbinghaus, S., Ribas, A., KEYNOTE-006 investigators, 2015b. Pembrolizumab versus Ipilimumab in Advanced Melanoma. N Engl J Med 372, 2521–2532. https://doi.org/10.1056/NEJMoa1503093

Rosenbaum, M., Gewies, A., Pechloff, K., Heuser, C., Engleitner, T., Gehring, T., Hartjes, L., Krebs, S., Krappmann, D., Kriegsmann, M., Weichert, W., Rad, R., Kurts, C., Ruland, J., 2019. Bcl10-controlled Malt1 paracaspase activity is key for the immune suppressive function of regulatory T cells. Nat Commun 10, 1–15. https://doi.org/10.1038/s41467-019-10203-2

Rosenthal, S.H., Sun, W., Zhang, K., Liu, Y., Nguyen, Q., Gerasimova, A., Nery, C., Cheng, L., Castonguay, C., Hiller, E., Li, J., Elzinga, C., Wolfson, D., Smolgovsky, A., Chen, R., Buller-Burckle, A., Catanese, J., Grupe, A., Lacbawan, F., Owen, R., 2020. Development and Validation of a 34-Gene Inherited Cancer Predisposition Panel Using Next-Generation Sequencing. BioMed Research International 2020, e3289023. https://doi.org/10.1155/2020/3289023

Rowshanravan, B., Halliday, N., Sansom, D.M., 2018. CTLA-4: a moving target in immunotherapy. Blood 131, 58–67. https://doi.org/10.1182/blood-2017-06-741033

Rurik, J.G., Tombácz, I., Yadegari, A., Méndez Fernández, P.O., Shewale, S.V., Li, L., Kimura, T., Soliman, O.Y., Papp, T.E., Tam, Y.K., Mui, B.L., Albelda, S.M., Puré, E., June, C.H., Aghajanian, H., Weissman, D., Parhiz, H., Epstein, J.A., 2022. CAR T cells produced in vivo to treat cardiac injury. Science 375, 91–96. https://doi.org/10.1126/science.abm0594

Safiri, S., Sepanlou, S.G., Ikuta, K.S., Bisignano, C., Salimzadeh, H., Delavari, A., Ansari, R., Roshandel, G., Merat, S., Fitzmaurice, C., Force, L.M., Nixon, M.R., Abbastabar, H., Abegaz, K.H., Afarideh, M., Ahmadi, A., Ahmed, M.B., Akinyemiju, T., Alahdab, F., Ali, R., Alikhani, M., Alipour, V., Aljunid, S.M., Almadi, M.A.H., Almasi-Hashiani, A., Al-Raddadi, R.M., Alvis-Guzman, N., Amini, S., Anber, N.H., Ansari-Moghaddam, A., Arabloo, J., Arefi, Z., Asghari Jafarabadi, M., Azadmehr, A., Badawi, A., Baheiraei, N., Bärnighausen, T.W., Basaleem, H., Behzadifar, Masoud, Behzadifar, Meysam, Belayneh, Y.M., Berhe, K., Bhattacharyya, K., Biadgo, B., Bijani, A., Biondi, A., Bjørge, T., Borzì, A.M., Bosetti, C., Bou-Orm, I.R., Brenner, H., Briko, A.N., Briko, N.I., Carreras, G., Carvalho, F., Castañeda-Orjuela, C.A., Cerin, E., Chiang, P.P.-C., Chido-Amajuoyi, O.G., Daryani, A., Davitoiu, D.V., Demoz, G.T., Desai, R., Dianati nasab, M., Eftekhari, A., El Sayed, I., Elbarazi, I., Emamian, M.H., Endries, A.Y., Esmaeilzadeh, F., Esteghamati, A., Etemadi, A., Farzadfar, F., Fernandes, E., Fernandes, J.C., Filip, I., Fischer, F., Foroutan, M., Gad, M.M., Gallus, S., Ghaseni-Kebria, F., Ghashghaee, A., Gorini, G., Hafezi-Nejad, N., Haj-Mirzaian, Arvin, Haj-Mirzaian, Arya, Hasanpour-Heidari, S., Hasanzadeh, A., Hassanipour, S., Hay, S.I., Hoang, C.L., Hostiuc, M., Househ, M., Ilesanmi, O.S., Ilic, M.D., Innos, K., Irvani, S.S.N., Islami, F., Jaca, A., Jafari Balalami, N., Jafari delouei, N., Jafarinia, M., Jahani, M.A., Jakovljevic, M., James, S.L., Javanbakht, M., Jenabi, E., Jha, R.P., Joukar, F., Kasaeian, A., Kassa, T.D., Kassaw, M.W., Kengne, A.P., Khader, Y.S., Khaksarian, M., Khalilov, R., Khan, E.A., Khayamzadeh, M.,

Khazaee-Pool, M., Khazaei, S., Khosravi Shadmani, F., Khubchandani, J., Kim, D., Kisa, A., Kisa, S., Kocarnik, J.M., Komaki, H., Kopec, J.A., Koyanagi, A., Kuipers, E.J., Kumar, V., La Vecchia, C., Lami, F.H., Lopez, A.D., Lopukhov, P.D., Lunevicius, R., Majeed, A., Majidinia, M., Manafi, A., Manafi, N., Manda, A.-L., Mansour-Ghanaei, F., Mantovani, L.G., Mehta, D., Meier, T., Meles, H.G., Mendoza, W., Mestrovic, T., Miazgowski, B., Miazgowski, T., Mir, S.M., Mirzaei, H., Mohammad, K.A., Mohammad Gholi Mezerji, N., Mohammadian-Hafshejani, A., Mohammadoo-Khorasani, M., Mohammed, S., Mohebi, F., Mokdad, A.H., Monasta, L., Moossavi, M., Moradi, G., Moradpour, F., Moradzadeh, R., Nahvijou, A., Naik, G., Najafi, F., Nazari, J., Negoi, I., Nguyen, C.T., Nguyen, T.H., Ningrum, D.N.A., Ogbo, F.A., Olagunju, A.T., Olagunju, T.O., Pana, A., Pereira, D.M., Pirestani, M., Pourshams, A., Poustchi, H., Qorbani, M., Rabiee, M., Rabiee, N., Radfar, A., Rahmati, M., Rajati, F., Rawaf, D.L., Rawaf, S., Reiner, R.C., Renzaho, A.M.N., Rezaei, N., Rezapour, A., Saad, A.M., Saadatagah, S., Saddik, B., Salehi, F., Salehi Zahabi, S., Salz, I., Samy, A.M., Sanabria, J., Santric Milicevic, M.M., Sarveazad, A., Satpathy, M., Schneider, I.J.C., Sekerija, M., Shaahmadi, F., Shabaninejad, H., Shamsizadeh, M., Sharafi, Z., Sharif, M., Sharifi, A., Sheikhbahaei, S., Shirkoohi, R., Siddappa Malleshappa, S.K., Silva, D.A.S., Sisay, M., Smarandache, C.-G., Soofi, M., Soreide, K., Soshnikov, S., Starodubov, V.I., Subart, M.L., Sullman, M.J., Tabarés-Seisdedos, R., Taherkhani, A., Tesfay, B. etsay, Topor-Madry, R., Traini, E., Tran, B.X., Tran, K.B., Ullah, I., Uthman, O.A., Vacante, M., Vahedian-Azimi, A., Valli, A., Varavikova, E., Vujcic, I.S., Westerman, R., Yazdi-Feyzabadi, V., Yisma, E., Yu, C., Zadnik, V., Zahirian Moghadam, T., Zaki, L., Zandian, H., Zhang, Z.-J., Murray, C.J.L., Naghavi, M., Malekzadeh, R., 2019. The global, regional, and national burden of colorectal cancer and its attributable risk factors in 195 countries and territories, 1990–2017: a systematic analysis for the Global Burden of Disease Study 2017. The Lancet Gastroenterology & Hepatology 4, 913–933. https://doi.org/10.1016/S2468-1253(19)30345-0

Sahin, I.H., Akce, M., Alese, O., Shaib, W., Lesinski, G.B., El-Rayes, B., Wu, C., 2019. Immune checkpoint inhibitors for the treatment of MSI-H/MMR-D colorectal cancer and a perspective on resistance mechanisms. Br J Cancer 121, 809–818. https://doi.org/10.1038/s41416-019-0599-y

Sawicki, T., Ruszkowska, M., Danielewicz, A., Niedźwiedzka, E., Arłukowicz, T., Przybyłowicz, K.E., 2021. A Review of Colorectal Cancer in Terms of Epidemiology, Risk Factors, Development, Symptoms and Diagnosis. Cancers (Basel) 13, 2025. https://doi.org/10.3390/cancers13092025

Schadt, L., Sparano, C., Schweiger, N.A., Silina, K., Cecconi, V., Lucchiari, G., Yagita, H., Guggisberg, E., Saba, S., Nascakova, Z., Barchet, W., Broek, M. van den, 2019. Cancer-Cell-Intrinsic cGAS Expression Mediates Tumor Immunogenicity. Cell Reports 29, 1236-1248.e7. https://doi.org/10.1016/j.celrep.2019.09.065

Schambach, A., Bohne, J., Chandra, S., Will, E., Margison, G.P., Williams, D.A., Baum, C., 2006. Equal potency of gammaretroviral and lentiviral SIN vectors for expression of O6-methylguanine–DNA methyltransferase in hematopoietic cells. Molecular Therapy 13, 391–400. https://doi.org/10.1016/j.ymthe.2005.08.012

Schlee, M., Hartmann, G., 2016. Discriminating self from non-self in nucleic acid sensing. Nat Rev Immunol 16, 566–580. https://doi.org/10.1038/nri.2016.78

Schmutte, C., Marinescu, R.C., Sadoff, M.M., Guerrette, S., Overhauser, J., Fishel, R., 1998. Human exonuclease I interacts with the mismatch repair protein hMSH2. Cancer Res 58, 4537–4542.

Schnalzger, T.E., de Groot, M.H., Zhang, C., Mosa, M.H., Michels, B.E., Röder, J., Darvishi, T., Wels, W.S., Farin, H.F., 2019. 3D model for CAR-mediated cytotoxicity using patient-derived colorectal cancer organoids. EMBO J 38, e100928. https://doi.org/10.15252/embj.2018100928

Schneider, W.M., Chevillotte, M.D., Rice, C.M., 2014. Interferon-Stimulated Genes: A Complex Web of Host Defenses. Annu. Rev. Immunol. 32, 513–545. https://doi.org/10.1146/annurev-immunol-032713-120231

Schumacher, T.N., Scheper, W., Kvistborg, P., 2019. Cancer Neoantigens. Annual Review of Immunology 37, 173–200. https://doi.org/10.1146/annurev-immunol-042617-053402

Shang, G., Zhang, C., Chen, Z.J., Bai, X.-C., Zhang, X., 2019. Cryo-EM structures of STING reveal its mechanism of activation by cyclic GMP-AMP. Nature 567, 389–393. https://doi.org/10.1038/s41586-019-0998-5

Sharpe, A.H., Pauken, K.E., 2018. The diverse functions of the PD1 inhibitory pathway. Nat Rev Immunol 18, 153–167. https://doi.org/10.1038/nri.2017.108

Siegel, R.L., Miller, K.D., Goding Sauer, A., Fedewa, S.A., Butterly, L.F., Anderson, J.C., Cercek, A., Smith, R.A., Jemal, A., 2020. Colorectal cancer statistics, 2020. CA Cancer J Clin 70, 145–164. https://doi.org/10.3322/caac.21601

Snyder, A., Makarov, V., Merghoub, T., Yuan, J., Zaretsky, J.M., Desrichard, A., Walsh, L.A., Postow, M.A., Wong, P., Ho, T.S., Hollmann, T.J., Bruggeman, C., Kannan, K., Li, Y., Elipenahli, C., Liu, C., Harbison, C.T., Wang, L., Ribas, A., Wolchok, J.D., Chan, T.A., 2014. Genetic Basis for Clinical Response to CTLA-4 Blockade in Melanoma. N Engl J Med 371, 2189–2199. https://doi.org/10.1056/NEJMoa1406498

Song, S., Peng, P., Tang, Z., Zhao, J., Wu, W., Li, H., Shao, M., Li, L., Yang, C., Duan, F., Zhang, M., Zhang, J., Wu, H., Li, C., Wang, X., Wang, H., Ruan, Y., Gu, J., 2017. Decreased expression of STING predicts poor prognosis in patients with gastric cancer. Sci Rep 7. https://doi.org/10.1038/srep39858

Spranger, S., Sivan, A., Corrales, L., Gajewski, T.F., 2016. Tumor and Host Factors Controlling Antitumor Immunity and Efficacy of Cancer Immunotherapy, in: Advances in Immunology. Elsevier, pp. 75–93. https://doi.org/10.1016/bs.ai.2015.12.003

Srikanth, S., Woo, J.S., Wu, B., El-Sherbiny, Y.M., Leung, J., Chupradit, K., Rice, L., Seo, G.J., Calmettes, G., Ramakrishna, C., Cantin, E., An, D.S., Sun, R., Wu, T.-T., Jung, J.U., Savic, S., Gwack, Y., 2019. The Ca2+ sensor STIM1 regulates the type I interferon response by

retaining the signaling adaptor STING at the endoplasmic reticulum. Nat Immunol 20, 152–162. https://doi.org/10.1038/s41590-018-0287-8

Stoeckius, M., Hafemeister, C., Stephenson, W., Houck-Loomis, B., Chattopadhyay, P.K., Swerdlow, H., Satija, R., Smibert, P., 2017. Simultaneous epitope and transcriptome measurement in single cells. Nat Methods 14, 865–868. https://doi.org/10.1038/nmeth.4380

Su, T., Zhang, Y., Valerie, K., Wang, X.-Y., Lin, S., Zhu, G., 2019a. STING activation in cancer immunotherapy. Theranostics 9, 7759–7771. https://doi.org/10.7150/thno.37574

Su, T., Zhang, Y., Valerie, K., Wang, X.-Y., Lin, S., Zhu, G., 2019b. STING activation in cancer immunotherapy. Theranostics 9, 7759–7771. https://doi.org/10.7150/thno.37574

Sun, L., Wu, J., Du, F., Chen, X., Chen, Z.J., 2013. Cyclic GMP-AMP synthase is a cytosolic DNA sensor that activates the type I interferon pathway. Science 339, 786–791. https://doi.org/10.1126/science.1232458

Talens, F., Van Vugt, M.A.T.M., 2019. Inflammatory signaling in genomically instable cancers. Cell Cycle 18, 1830–1848. https://doi.org/10.1080/15384101.2019.1638192

Tanakaya, K., 2019. Current clinical topics of Lynch syndrome. Int J Clin Oncol 24, 1013–1019. https://doi.org/10.1007/s10147-018-1282-7

theislab/diffxpy, 2022.

Tishkoff, D.X., Amin, N.S., Viars, C.S., Arden, K.C., Kolodner, R.D., 1998. Identification of a human gene encoding a homologue of Saccharomyces cerevisiae EXO1, an exonuclease implicated in mismatch repair and recombination. Cancer Res 58, 5027–5031.

Topalian, S.L., Taube, J.M., Anders, R.A., Pardoll, D.M., 2016. Mechanism-driven biomarkers to guide immune checkpoint blockade in cancer therapy. Nat Rev Cancer 16, 275–287. https://doi.org/10.1038/nrc.2016.36

Traag, V.A., Waltman, L., van Eck, N.J., 2019. From Louvain to Leiden: guaranteeing well-connected communities. Sci Rep 9, 5233. https://doi.org/10.1038/s41598-019-41695-z

Tran, P.T., Simon, J.A., Liskay, R.M., 2001. Interactions of Exo1p with components of MutLalpha in Saccharomyces cerevisiae. Proc Natl Acad Sci U S A 98, 9760–9765. https://doi.org/10.1073/pnas.161175998

Tse, S.-W., McKinney, K., Walker, W., Nguyen, M., Iacovelli, J., Small, C., Hopson, K., Zaks, T., Huang, E., 2021. mRNA-encoded, constitutively active STINGV155M is a potent genetic adjuvant of antigen-specific CD8+ T cell response. Molecular Therapy 0. https://doi.org/10.1016/j.ymthe.2021.03.002

Uggenti, C., Lepelley, A., Crow, Y.J., 2019. Self-Awareness: Nucleic Acid-Driven Inflammation and the Type I Interferonopathies. Annu Rev Immunol 37, 247–267. https://doi.org/10.1146/annurev-immunol-042718-041257

Valle, L., de Voer, R.M., Goldberg, Y., Sjursen, W., Försti, A., Ruiz-Ponte, C., Caldés, T., Garré, P., Olsen, M.F., Nordling, M., Castellvi-Bel, S., Hemminki, K., 2019. Update on genetic predisposition to colorectal cancer and polyposis. Molecular Aspects of Medicine, New insights on the molecular aspects of colorectal cancer 69, 10–26. https://doi.org/10.1016/j.mam.2019.03.001

Vornholz, L., Isay, S.E., Kurgyis, Z., Strobl, D.C., Loll, P., Mosa, M.H., Luecken, M.D., Sterr, M., Lickert, H., Winter, C., Greten, F.R., Farin, H.F., Theis, F.J., Ruland, J., 2023. Synthetic enforcement of STING signaling in cancer cells appropriates the immune microenvironment for checkpoint inhibitor therapy. Science Advances 9, eadd8564. https://doi.org/10.1126/sciadv.add8564

Warner, J.D., Irizarry-Caro, R.A., Bennion, B.G., Ai, T.L., Smith, A.M., Miner, C.A., Sakai, T., Gonugunta, V.K., Wu, J., Platt, D.J., Yan, N., Miner, J.J., 2017. STING-associated vasculopathy develops independently of IRF3 in mice. J. Exp. Med. 214, 3279–3292. https://doi.org/10.1084/jem.20171351

Watson, R.O., Manzanillo, P.S., Cox, J.S., 2012. Extracellular M. tuberculosis DNA targets bacteria for autophagy by activating the host DNA-sensing pathway. Cell 150, 803–815. https://doi.org/10.1016/j.cell.2012.06.040

Webster, S.J., Brode, S., Ellis, L., Fitzmaurice, T.J., Elder, M.J., Gekara, N.O., Tourlomousis, P., Bryant, C., Clare, S., Chee, R., Gaston, H.J.S., Goodall, J.C., 2017. Detection of a microbial metabolite by STING regulates inflammasome activation in response to Chlamydia trachomatis infection. PLoS Pathog 13, e1006383. https://doi.org/10.1371/journal.ppat.1006383

Weigelin, B., den Boer, A.T., Wagena, E., Broen, K., Dolstra, H., de Boer, R.J., Figdor, C.G., Textor, J., Friedl, P., 2021. Cytotoxic T cells are able to efficiently eliminate cancer cells by additive cytotoxicity. Nat Commun 12, 5217. https://doi.org/10.1038/s41467-021-25282-3

West, A.P., Khoury-Hanold, W., Staron, M., Tal, M.C., Pineda, C.M., Lang, S.M., Bestwick, M., Duguay, B.A., Raimundo, N., MacDuff, D.A., Kaech, S.M., Smiley, J.R., Means, R.E., Iwasaki, A., Shadel, G.S., 2015. Mitochondrial DNA stress primes the antiviral innate immune response. Nature 520, 553–557. https://doi.org/10.1038/nature14156

Wolchok, J.D., Kluger, H., Callahan, M.K., Postow, M.A., Rizvi, N.A., Lesokhin, A.M., Segal, N.H., Ariyan, C.E., Gordon, R.-A., Reed, K., Burke, M.M., Caldwell, A., Kronenberg, S.A., Agunwamba, B.U., Zhang, X., Lowy, I., Inzunza, H.D., Feely, W., Horak, C.E., Hong, Q., Korman, A.J., Wigginton, J.M., Gupta, A., Sznol, M., 2013. Nivolumab plus ipilimumab in advanced melanoma. N Engl J Med 369, 122–133. https://doi.org/10.1056/NEJMoa1302369

Wolf, F.A., Angerer, P., Theis, F.J., 2018. SCANPY: large-scale single-cell gene expression data analysis. Genome Biology 19, 15. https://doi.org/10.1186/s13059-017-1382-0

Wong, S.K., Beckermann, K.E., Johnson, D.B., Das, S., 2021. Combining anti-cytotoxic T-lymphocyte antigen 4 (CTLA-4) and -programmed cell death protein 1 (PD-1) agents for cancer immunotherapy. Expert Opin Biol Ther 21, 1623–1634. https://doi.org/10.1080/14712598.2021.1921140

Woo, S.-R., Fuertes, M.B., Corrales, L., Spranger, S., Furdyna, M.J., Leung, M.Y.K., Duggan, R., Wang, Y., Barber, G.N., Fitzgerald, K.A., Alegre, M.-L., Gajewski, T.F., 2014. STING-dependent cytosolic DNA sensing mediates innate immune recognition of immunogenic tumors. Immunity 41, 830–842. https://doi.org/10.1016/j.immuni.2014.10.017

Woodward, J.J., Iavarone, A.T., Portnoy, D.A., 2010. c-di-AMP Secreted by Intracellular Listeria monocytogenes Activates a Host Type I Interferon Response. Science 328, 1703–1705. https://doi.org/10.1126/science.1189801

Wu, J., Dobbs, N., Yang, K., Yan, N., 2020. Interferon-Independent Activities of Mammalian STING Mediate Antiviral Response and Tumor Immune Evasion. Immunity 53, 115-126.e5. https://doi.org/10.1016/j.immuni.2020.06.009

Xia, T., Konno, H., Ahn, J., Barber, G.N., 2016a. Deregulation of STING Signaling in Colorectal Carcinoma Constrains DNA-Damage Responses and Correlates With Tumorigenesis. Cell Rep 14, 282–297. https://doi.org/10.1016/j.celrep.2015.12.029

Xia, T., Konno, H., Barber, G.N., 2016b. Recurrent Loss of STING Signaling in Melanoma Correlates with Susceptibility to Viral Oncolysis. Cancer Res 76, 6747–6759. https://doi.org/10.1158/0008-5472.CAN-16-1404

Xie, Y.-H., Chen, Y.-X., Fang, J.-Y., 2020. Comprehensive review of targeted therapy for colorectal cancer. Sig Transduct Target Ther 5, 1–30. https://doi.org/10.1038/s41392-020-0116-z

Xin Yu, J., Hubbard-Lucey, V.M., Tang, J., 2019. Immuno-oncology drug development goes global. Nature Reviews Drug Discovery 18, 899–900. https://doi.org/10.1038/d41573-019-00167-9

Xu, M.M., Pu, Y., Han, D., Shi, Y., Cao, X., Liang, H., Chen, X., Li, X.-D., Deng, L., Chen, Z.J., Weichselbaum, R.R., Fu, Y.-X., 2017. Dendritic Cells but Not Macrophages Sense Tumor Mitochondrial DNA for Cross-priming through Signal Regulatory Protein α Signaling. Immunity 47, 363-373.e5. https://doi.org/10.1016/j.immuni.2017.07.016

Yamamoto, H., Imai, K., 2015. Microsatellite instability: an update. Arch Toxicol 89, 899–921. https://doi.org/10.1007/s00204-015-1474-0

Yamashiro, L.H., Wilson, S.C., Morrison, H.M., Karalis, V., Chung, J.-Y.J., Chen, K.J., Bateup, H.S., Szpara, M.L., Lee, A.Y., Cox, J.S., Vance, R.E., 2020. Interferon-independent STING

signaling promotes resistance to HSV-1 in vivo. Nat Commun 11. https://doi.org/10.1038/s41467-020-17156-x

Yang, H., Lee, W.S., Kong, S.J., Kim, C.G., Kim, J.H., Chang, S.K., Kim, S., Kim, G., Chon, H.J., Kim, C., 2019. STING activation reprograms tumor vasculatures and synergizes with VEGFR2 blockade. J Clin Invest 129, 4350–4364. https://doi.org/10.1172/JCI125413

Yarchoan, M., Albacker, L.A., Hopkins, A.C., Montesion, M., Murugesan, K., Vithayathil, T.T., Zaidi, N., Azad, N.S., Laheru, D.A., Frampton, G.M., Jaffee, E.M., 2019. PD-L1 expression and tumor mutational burden are independent biomarkers in most cancers. JCI Insight 4. https://doi.org/10.1172/jci.insight.126908

Yarchoan, M., Hopkins, A., Jaffee, E.M., 2017. Tumor Mutational Burden and Response Rate to PD-1 Inhibition. N Engl J Med 377, 2500–2501. https://doi.org/10.1056/NEJMc1713444

Yu, H., Chen, Z., Ballman, K.V., Watson, M.A., Govindan, R., Lanc, I., Beer, D.G., Bueno, R., Chirieac, L.R., Chui, M.H., Chen, G., Franklin, W.A., Gandara, D.R., Genova, C., Brovsky, K.A., Joshi, M.-B.M., Merrick, D.T., Richards, W.G., Rivard, C.J., Harpole, D.H., Tsao, M.-S., van Bokhoven, A., Shepherd, F.A., Hirsch, F.R., 2019. Correlation of PD-L1 Expression with Tumor Mutation Burden and Gene Signatures for Prognosis in Early-Stage Squamous Cell Lung Carcinoma. J Thorac Oncol 14, 25–36. https://doi.org/10.1016/j.jtho.2018.09.006

Zhang, C., Shang, G., Gui, X., Zhang, X., Bai, X.-C., Chen, Z.J., 2019. Structural basis of STING binding with and phosphorylation by TBK1. Nature 567, 394–398. https://doi.org/10.1038/s41586-019-1000-2

Zhang, Xu, Wu, J., Du, F., Xu, H., Sun, L., Chen, Z., Brautigam, C.A., Zhang, Xuewu, Chen, Z.J., 2014. The cytosolic DNA sensor cGAS forms an oligomeric complex with DNA and undergoes switch-like conformational changes in the activation loop. Cell Rep 6, 421–430. https://doi.org/10.1016/j.celrep.2014.01.003

Zhang, Y., Yuan, F., Presnell, S.R., Tian, K., Gao, Y., Tomkinson, A.E., Gu, L., Li, G.-M., 2005. Reconstitution of 5'-directed human mismatch repair in a purified system. Cell 122, 693–705. https://doi.org/10.1016/j.cell.2005.06.027

Zhao, B., Du, F., Xu, P., Shu, C., Sankaran, B., Bell, S.L., Liu, M., Lei, Y., Gao, X., Fu, X., Zhu, F., Liu, Y., Laganowsky, A., Zheng, X., Ji, J.-Y., West, A.P., Watson, R.O., Li, P., 2019. A conserved PLPLRT/SD motif of STING mediates the recruitment and activation of TBK1. Nature 569, 718–722. https://doi.org/10.1038/s41586-019-1228-x

Zhao, B., Shu, C., Gao, X., Sankaran, B., Du, F., Shelton, C.L., Herr, A.B., Ji, J.-Y., Li, P., 2016. Structural basis for concerted recruitment and activation of IRF-3 by innate immune adaptor proteins. Proc Natl Acad Sci U S A 113, E3403-3412. https://doi.org/10.1073/pnas.1603269113

Zhao, B., Zhao, H., Zhao, J., 2020. Efficacy of PD-1/PD-L1 blockade monotherapy in clinical trials. Ther Adv Med Oncol 12, 1758835920937612. https://doi.org/10.1177/1758835920937612

Zhao, P., Li, L., Jiang, X., Li, Q., 2019. Mismatch repair deficiency/microsatellite instability-high as a predictor for anti-PD-1/PD-L1 immunotherapy efficacy. Journal of Hematology & Oncology 12, 54. https://doi.org/10.1186/s13045-019-0738-1

Zhou, C., Chen, X., Planells-Cases, R., Chu, J., Wang, L., Cao, L., Li, Z., López-Cayuqueo, K.I., Xie, Y., Ye, S., Wang, X., Ullrich, F., Ma, S., Fang, Y., Zhang, X., Qian, Z., Liang, X., Cai, S.-Q., Jiang, Z., Zhou, D., Leng, Q., Xiao, T.S., Lan, K., Yang, J., Li, H., Peng, C., Qiu, Z., Jentsch, T.J., Xiao, H., 2020. Transfer of cGAMP into Bystander Cells via LRRC8 Volume-Regulated Anion Channels Augments STING-Mediated Interferon Responses and Anti-viral Immunity. Immunity 52, 767-781.e6. https://doi.org/10.1016/j.immuni.2020.03.016

Zhou, Y., Fei, M., Zhang, G., Liang, W.-C., Lin, W., Wu, Y., Piskol, R., Ridgway, J., McNamara, E., Huang, H., Zhang, J., Oh, J., Patel, J.M., Jakubiak, D., Lau, J., Blackwood, B., Bravo, D.D., Shi, Y., Wang, J., Hu, H.-M., Lee, W.P., Jesudason, R., Sangaraju, D., Modrusan, Z., Anderson, K.R., Warming, S., Roose-Girma, M., Yan, M., 2020. Blockade of the Phagocytic Receptor MerTK on Tumor-Associated Macrophages Enhances P2X7R-Dependent STING Activation by Tumor-Derived cGAMP. Immunity 52, 357-373.e9. https://doi.org/10.1016/j.immuni.2020.01.014

Zhu, Y., An, X., Zhang, X., Qiao, Y., Zheng, T., Li, X., 2019. STING: a master regulator in the cancer-immunity cycle. Mol Cancer 18, 152. https://doi.org/10.1186/s12943-019-1087-y

Zumwalt, T.J., Arnold, M., Goel, A., Boland, C.R., 2015. Active secretion of CXCL10 and CCL5 from colorectal cancer microenvironments associates with GranzymeB+ CD8+ T-cell infiltration. Oncotarget 6, 2981–2991. https://doi.org/10.18632/oncotarget.3205

6 Acknowledgments

I was privileged to conduct research in the laboratory of Prof. Ruland. All the work leading to this thesis would not have been possible without the support of many wonderful people.

First, I would like to thank Prof. Dr. Jürgen Ruland for the opportunity to perform my research project in his lab, for providing scientific resources and intellectual input, and for giving me the freedom to explore my curiosity. Also, I would like to thank Prof. Dr. Dirk Haller and Prof. Dr. Andreas Pichlmair for agreeing to be part of my thesis advisory committee and providing project-related feedback.

Second, I would like to thank Dr. Zsuzsanna Kurgyis for her encouraging guidance in the beginning, and the many fruitful scientific discussions throughout the project. Also, I would like to thank Dr. Shawn P. Kubli for his positive attitude and focused advice. I would like to thank all master and medical doctor students, whom I was privileged to mentor, for their trust, dedication, and excellent work. I especially want to thank Sophie E. Isay and Patricia Loll for the fantastic teamwork, unconditional engagement, and many fun moments. Furthermore, I would like to thank Dr. Erik Hameister, Andreas Kratzert, Miriam Schulz, and Theresa Schnalzger for a great time inside and outside the lab. I would like to thank Dr. Konstanze Pechloff for her support in all animal-related matters and Dr. Marc Rosenbaum for his support in safety and genetech-related matters. Also, I would like to thank Valentin Höfl, Nicole Prause, and Kerstin Burmeister for their administrative and technical assistance in the lab, as well as their help in the mouse facilities. Moreover, I would like to thank all members of AG Ruland, AG Buchner, AG Keppler, and AG Jellusova, who took part in my journey, for the intellectual exchange and personal support. I would like to thank the i-Target community for the educational framework and Prof. Dr. Stefan Endres for his enthusiasm and mentoring. Also, I would like to thank the Transregio 237 for the academic opportunities and stimulating environment. I am most grateful to all co-authors for their effort and work to get our joint manuscript published.

Finally, I would like to express my deepest gratitude to Franziska Füchsl, my family, and my friends for their moral support, patience, and understanding.

7 Publications

Vornholz, L., Isay E.S., Kurgyis, Z., Strobl, C.S., Loll, P., Mosa M.H., Luecken, M.D., Sterr, M., Lickert, H., Winter, C., Greten, F.R., Farin, H.F., Theis, J.T., Ruland, J. 2023. *Synthetic enforcement of STING signaling in cancer cells appropriates the immune microenvironment for checkpoint inhibitor therapy*. Sci. Adv. 9, eadd8564. (https://doi.org/10.1126/sciadv.add8564)

Zecha, J., Bayer, F.P., Wiechmann, S., Woortman, J., Berner, N., Müller, J., Schneider, A., Kramer, K., Abril-Gil, M., Hopf, T., Reichart, L., Chen, L., Hansen, F.M., Lechner, S., Samaras, P., Eckert, S., Lautenbacher, L., Reinecke, M., Hamood, F., Prokofeva, P., Vornholz, L., Falcomatà, C., Dorsch, M., Schröder, A., Venhuizen, A., Wilhelm, S., Médard, G., Stoehr, G., Ruland, J., Grüner, B.M., Saur, D., Buchner, M., Ruprecht, B., Hahne, H., The, M., Wilhelm, M., Kuster, B., 2023. *Decrypting drug actions and protein modifications by dose- and time-resolved proteomics*. Science 0, eade3925. (https://doi.org/10.1126/science.ade3925)

Theobald, H., Bejarano, D.A., Katzmarski, N., Haub, J., Schulte-Schrepping, J., Yu, J., Bassler, K., Ćirović, B., Osei-Sarpong, C., Piattini, F., Vornholz, L., Yu, X., Sheoran, S., Jawazneh, A.A., Chakarov, S., Haendler, K., Brown, G.D., Williams, D.L., Bosurgi, L., Ginhoux, F., Ruland, J., Beyer, M., Greter, M., Kopf, M., Schultze, J.L., Schlitzer, A., 2022. Apolipoprotein E controls Dectin-1-dependent development of monocyte-derived alveolar macrophages upon pulmonary β-glucan-induced inflammatory adaptation. bioRxiv. (https://doi.org/10.1101/2022.09.15.505390)

Kurgyis, Z., Vornholz, L., Pechloff, K., Kemény, L.V., Wartewig, T., Muschaweckh, A., Joshi, A., Kranen, K., Hartjes, L., Möckel, S., Steiger, K., Hameister, E., Volz, T., Mellett, M., French, L.E., Biedermann, T., Korn, T., Ruland, J. 2021. *Keratinocyte-intrinsic BCL10/MALT1 activity initiates and amplifies psoriasiform skin inflammation*. Sci. Immunol. 6, eabi4425. (https://doi.org/10.1126/sciimmunol.abi4425)

Vornholz, L., and Ruland, J. 2020. *Physiological and Pathological Functions of CARD9 Signaling in the Innate Immune System*. Curr. Top. Microbiol. Immunol. 429, 177–203. (https://doi.org/10.1007/82_2020_211)

8 Table and Figure list